

University of Colorado
Department of Aerospace Engineering Sciences
Senior Projects - ASEN 4028
Spacial HEO Autonomous Detector & Evaluator (SHADE)
 Project Final Report
 Monday, May 3rd, 2021

Project Customers

Name: Mark Stakhiv Email: mark.stakhiv@aero.org	Name: Jonathan Aziz Email: jonathan.d.aziz@aero.org
--	--

Advisor

Name: Zachary Sunberg Email: zachary.sunberg@colorado.edu
--

Team Members

Name: Robert Redfern, Project Manager Email: robert.redfern@colorado.edu Phone: (720) 884-6148	Name: Quinton Dombrowski, Software Systems Email: quinton.dombrowski@colorado.edu Phone: (720) 545-6007
Name: Benjamin Vidaurre, Systems Email: benjamin.vidaurre@colorado.edu Phone: (303) 919-7671	Name: Elliott Tung, Solar Integration Email: elliot.tung@colorado.edu Phone: (650) 722-7894
Name: Katherine Nyland, Testing & Safety Email: katherine.nyland@sbcglobal.net Phone: (847) 373-2021	Name: Marlin Jacobson, Active Protection Email: marlin.jacobson@colorado.edu Phone: (813) 765-8249
Name: Jacob Weiner, Power Systems Email: jacob.a.weiner@colorado.edu Phone: (330) 949-3521	Name: Davis Peirce, Orbit Analysis Email: davis.peirce@colorado.edu Phone: (303) 847-7400
Name: John Hugo, Manufacturing Email: john.hugo@colorado.edu Phone: (702) 286-1565	Name: Vinay Simlot, Finance Email: vinay.simlot@colorado.edu Phone: (703) 943-6508

Contents

I Project Purpose	1
II Project Objectives and Functional Requirements	3
II.1 What is Project Success	3
II.2 Levels of Success	3
II.3 Concept of Operations	4
II.4 System Block Diagrams	5
II.4.1 Functional Flow Block Diagram	6
II.4.2 Full System Physical Block Diagram	7
II.5 Functional Requirements	7
III Final Design	9
III.1 Full System Overview	9
III.2 Design Requirements Analysis & Allocation	10
III.3 Solar Charging	16
III.3.1 Overview	16
III.3.2 Panel Construction	16
III.3.3 Modeling	18
III.3.4 Charging Simulation	20
III.3.5 Thermal Analysis	21
III.3.6 The Power Module	26
III.3.7 System and Legacy System Integration	27
III.4 Active Protection System	28
III.4.1 Overview	29
III.4.2 Enclosure Design Materials and Geometry	30
III.4.3 Active Protection Element	31
III.4.4 Passive Protection Elements	32
III.5 Software	34
III.5.1 Overall Software FBD	34
III.5.2 Main Computer and Software Dependencies	34
III.5.3 Software Architecture	35
III.5.4 Startup Procedure and Data Handling	36
III.5.5 Scheduler	37
III.5.6 Orbit Propagation	37
III.5.7 Image Processing	39
III.5.8 Automatic Calibration	39
IV Manufacturing	40
IV.1 Power System	40
IV.1.1 The Solar Panels	40
IV.1.2 The Heatsinks and Thermal Epoxy	41

IV.1.3	PV Cell Soldering and Adhesion	41
IV.1.4	Power Module and Integration	41
IV.2	Active Protection Enclosure	42
IV.2.1	Gathering Materials	42
IV.2.2	Machining	42
IV.2.3	Assembly	43
IV.2.4	Modification	43
IV.2.5	Summary	43
V	Verification and Validation	44
V.1	Component Testing	44
V.1.1	Battery Duration	44
V.1.2	Low-Power Shutdown	45
V.1.3	Solar Panel Connection Test	46
V.1.4	Solar Charging Test	46
V.1.5	Thermal Solar Cell Test	47
V.1.6	Thermal	49
V.1.7	Structural	52
V.1.8	Lid Actuation	53
V.1.9	Week-Long Dynamic Scheduling	56
V.1.10	Image Processing	57
V.1.11	Timed Software Setup	58
V.2	Full System Testing - Test Plan (TP)	58
V.2.1	30-Minute Transport & Assembly	58
V.2.2	Single Night Deployment	60
V.2.3	Multi-Night Deployment	61
V.3	Satisfaction of Functional Requirements	61
VI	Risk Assessment and Mitigation	63
VII	Project Planning	66
VII.1	Organization Chart	66
VII.2	Work Breakdown Structure	67
VII.3	Work Plan	68
VII.3.1	Overview	68
VII.3.2	Fall Legacy Testing	68
VII.3.3	Spring Legacy Testing	69
VII.3.4	Spring Work Plan	70
VII.4	Test Plan & Testing Hardware	73
VII.5	Cost Plan	73
VIII	Lessons Learned	74
VIII.1	Appropriate Scoping	74

VIII.2	Proactivity	74
VIII.3	Subsystem Team Tag-Ups	75
VIII.4	Component Design Reviews	75
IX	Individual Report Contributions	76
IX.1	Robert Redfern	76
IX.2	Benjamin Vidaurre	76
IX.3	Quinton Dombrowski	76
IX.4	John Hugo	76
IX.5	Marlin Jacobson	76
IX.6	Jacob Weiner	76
IX.7	Vinay Simlot	77
IX.8	Davis Peirce	77
IX.9	Katherine Nyland	77
IX.10	Elliott Tung	77
X	Appendices	80
X.1	Standard Operating Conditions	80
X.2	Supplemental Solar Panel Dimensions	81
X.3	Software Dependencies	81
X.4	Software Diagrams	83
X.4.1	Setup Script FBD	83
X.4.2	Startup Process	83
X.4.3	Scheduler Flow Chart	84
X.4.4	Image Processor Flow Chart	84
X.4.5	Calibration Flow Chart	85
X.4.6	Wiring Diagram for UDOO Arduino and Braswell Pinouts	85
X.5	Full Risk Accounting	86
X.6	Conceptual Design	89
X.6.1	Power System	89
X.6.2	Modularity	98
X.6.3	Passive Protection	100
X.6.4	Active Protection	107
X.6.5	System Verification: Open Enclosure Force and Moment Models	112
X.6.6	System Verification: Closed Enclosure Force and Moment Models	113
X.7	Full Work Breakdown Structure	115

List of Figures

1	Earth-Orbiting Objects Courtesy of NASA Goddard Space Flight Center	1
2	GHOST (Left) and WRAITH (Right) Hardware	2
3	SHADE Project Logo	2
4	CONOPS	4
5	Overall Functional Flow Block Diagram for SHADE	6
6	Full System Physical Block Diagram for SHADE	7
7	SHADE Design	9
8	Assembled SHADE System	10
9	Dimensioned solar panel	18
10	Estimated Energy Collected By Solar Panels	19
11	Estimated Energy Collected By Solar Panels on Hot Day	19
12	Estimated Energy Collected By Solar Panels on Cold Day	20
13	Estimated Battery Charge Profile on Hot Day	21
14	Estimated Battery Charge Profile on Cold Day	21
15	Thermal Analysis Setup	22
16	Hot Case w/ Heat Sinks	23
17	Hot Case w/o Heat Sinks	23
18	Cold Case w/ Heat Sinks	24
19	Cold Case w/o Heat Sinks	24
20	Solar Irradiance Graph	25
21	Surface Temperature Graph	25
22	Solar Charging Circuit Diagram and Charger	26
23	Power Module Design	27
24	Final Power System	28
25	Active Protection System Design	28
26	Active Protection System Overview	29
27	Active Protection System Opened	29
28	Active Protection System Dimensions	30
29	Active Protection System Liquid Mitigation	31
30	Lid Actuation Stepper Motor	31
31	Active Protection System Thermal Protection	32
32	Active Protection System Edge Protection	33
33	Active Protection System Internal Component Protection	33
34	Active Protection System Umbilical Connections	34
35	Overall software functional block diagram, including (from left to right) required internet services, operator's computer, data transfer USB flash drive, and SHADE main computer. . .	34
36	Flow chart of software runtime architecture. Each large arrow represents a python process. Small arrows show important data passes between these processes as events of queues. . . .	36
37	Angular Error for NOAA-6 Using SGP4	38
38	Solar Panel Fitment Fix	40

39	Broken Heatsink	41
40	Battery Discharge Percentage vs Time	45
41	Energy Collected By Solar Panels Based off 2019 Solar Irradiance Data	47
42	Thermal Test and Simulation Images	48
43	IR images of Heat Sink Effectiveness	49
44	Thermal Test Results	50
45	Thermal Model Setup with Test Inputs	51
46	Thermal Model-Test Comparison	51
47	Thermal Model Hot Case	52
48	Tipping Model	53
49	Tip-Over Test Results	53
50	Roof Velocity vs Time Model	54
51	Lid Actuation Design Point	54
52	Safe Mode Trigger Conditions	55
53	Scheduler Test: Azimuth-Elevation Plot with Meridian 8	56
54	Scheduler Test: Azimuth-Elevation Plot with SDS-F6	57
55	Image Processing Test: Result of streak detection and selection on a suite of synthetic test images	58
56	Time Budget	59
57	Experimental Time Budget	60
58	The full risk matrix for SHADE prior to mitigation	63
59	The full risk matrix for SHADE following mitigation	65
60	Team Organizational Chart	67
61	SHADE Summary WBS	67
62	SHADE WBS - Third Level of Detail, Development Product Work Packages	68
63	Gantt Chart of Fall 2020 Legacy Testing	69
64	Gantt Chart of Remaining Legacy Testing	70
65	Gantt Chart of Power Work Plan	71
66	Gantt Chart of Active Protection Work Plan	71
67	Gantt Chart of Software Work Plan	72
68	Gantt Chart of Full System Work Plan	73
69	SHADE's Cost Plan	74
70	Solar Panel Hinge Location	81
71	Dimensioned Heatsink	81
72	FBD of the setup script	83
73	Flow chart of the on-board computer's startup sequence	83
74	Flow chart of SHADE scheduler	84
75	Flow chart of SHADE image processor	84
76	Flow chart for both the initial (left) and pre-image (right) portions of the calibration process.	85
77	Diagram showing all necessary wiring from the UDOO to weather detection module, power module, limit switches and stepper motor controller.	85

78	Criteria for evaluating risk likelihood	86
79	Criteria for evaluating risk recoverability	86
80	Comparison of technical risks pre and post mitigation	88
81	Comparison of management risks pre and post mitigation	88
82	Comparison of external risks pre and post mitigation	89
83	Power System Functional Block Diagram	89
84	Power Budget	90
85	Duracell 12V SLA	91
86	Power Sonic 12V LiFePO4	91
87	Example of Li-ion Battery Pack	92
88	Lithium King 48V LiPo	92
89	Battery Pro Con Table	92
90	Battery Choice Metrics and Rationale	93
91	Battery Metrics Values	93
92	Battery Trade Study Results	94
93	Monocrystalline vs Polycrystalline cells	96
94	Solar cell technology metrics	96
95	Solar cell technology trade study	97
96	Modularity Options Pros and Cons	99
97	Transport Grouping Modules Design Choice	100
98	Polycase WH-18 Hinged NEMA Enclosure	101
99	Pelican Air Case	101
100	Sterilite Industrial Storage Bin	102
101	Plano Small Sportsman’s Trunk	102
102	Passive Protection Option Pros and Cons	103
103	Passive Protection Metric Rationale and Descriptions	104
104	Passive Protection Metric Values	105
105	Passive Protection Case Study	105
106	WRAITH Weather Protection Box with 6061-T6 Aluminum	108
107	Type 316 Stainless Steel Sheet	108
108	Magnesium Alloy (AZ31) Sheet	108
109	Polycarbonate Plastic Sheet	109
110	Material Options Pros and Cons	109
111	Material Metric Rationale and Descriptions	110
112	Materials Metric Values	110
113	Materials Trade Study Results	111
114	Hardware Failure Prevention Model	113
115	Maximum Distributed Load Model	114
116	Maximum Load at Center Model	115

List of Tables

Table of Acronyms

Acronym	Definition
COTS	Commercial Off-the-Shelf
CU	University of Colorado
DC	Direct Current
DR	Design Requirement
FBD	Functional Block Diagram
FLIR	Forward Looking Infrared
FR	Functional Requirement
FOV	Field of View
GEO	Geostationary Orbit
GHOST	Ground-Based Hardware for Optical Space Tracking
HEO	Highly Elliptical Orbit
LEO	Low Earth Orbit
LiFePO4	Lithium Iron Phosphate
LiPo	Lithium Polymer
Li-Ion	Lithium Ion
MEO	Medium Earth Orbit
MPPT	Maximum Power Point Tracking
OSHA	Occupational Safety and Health Administration
R2R	Return to Research
SHADE	Spacial HEO Autonomous Detector & Evaluator
SLA	Sealed Lead Acid
SSA	Space Situational Awareness
SWBS	Summary Work Breakdown Structure
TLE	Two Line Element
WBS	Work Breakdown Structure
WRAITH	Weather Resistant Autonomous Imaging for Tracking HEOs
FMEA	Failure Modes and Effects Analysis

Nomenclature

α	=	solar absorptance of solar array [%]
α_p	=	temperature coefficient of power [%/°C]
G_T	=	solar radiation striking the solar array [kW/m^2]
$G_{T,NOCT}$	=	solar radiation at which NOCT is defined [$0.8kW/m^2$]
P_{mpp}	=	power at maximum power point [W]
T_c	=	solar cell temperature [°C]
T_a	=	ambient temperature [°C]
$T_{c,NOCT}$	=	nominal operating cell temperature [°C]
$T_{a,NOCT}$	=	ambient temperature at which NOCT is defined [20°C]
$\eta_{mp,STC}$	=	maximum power point efficiency under standard testing conditions [%]
$T_{c,STC}$	=	cell temperature under standard testing conditions [25°C]
τ	=	solar transmittance of cover over solar array [%]
V_{mpp}	=	Voltage at maximum power point [V]

I. Project Purpose

Authors: Robert Redfern, Vinay Simlot

As of April 1, 2020, 2,666 satellites orbit Earth, with the global satellite industry generating almost \$280 billion in revenue. The European Space Agency predicts the "space highways" around Earth will become more congested than ever, threatening orbital conditions. To prevent collisions and assist in the prediction of re-entries, Space Situational Awareness (SSA) systems collect optical and radar data to track and characterize orbital environments. Many existing SSA systems utilize a suite of large radar and imaging sensors, and because of the high cost, can only be operated by those with access to an abundance of technology and finances.



Fig. 1 Earth-Orbiting Objects Courtesy of NASA Goddard Space Flight Center

In 2018, The Aerospace Corporation tasked a senior projects group at the University of Colorado Boulder, to develop a low-cost portable SSA system that could track larger objects such as satellites and certain pieces of debris. By reducing the number of "trivial" tracking request on the larger SSA systems, this would allow them more bandwidth to track smaller objects that require more powerful hardware and software. The 2018 project team was named GHOST and developed foundation systems to optically track and categorize satellites primarily in LEO and MEO. The next year a 2019 projects team known as WRAITH evolved this design by adding the ability to track objects in Highly Elliptical Orbits (HEO). WRAITH also expanded the work of GHOST to allow 12 hour autonomous operation, as well as making the system deployable by two people within 30 minutes. Unfortunately WRAITH's work was abruptly ended in March of 2020 due to the COVID-19 pandemic. This left the project in a non-integrated state with many designs undeveloped. When the project was revitalized in the fall, the new design team known as SHADE estimated just 15% of the legacy GHOST/WRAITH systems were operating as intended. The justification for this figure will be discussed later in this report. While the SHADE team did inherit a large amount of technical debt from previous work, another full year of development would allow for a more compact, reusable, and complete system to be delivered.

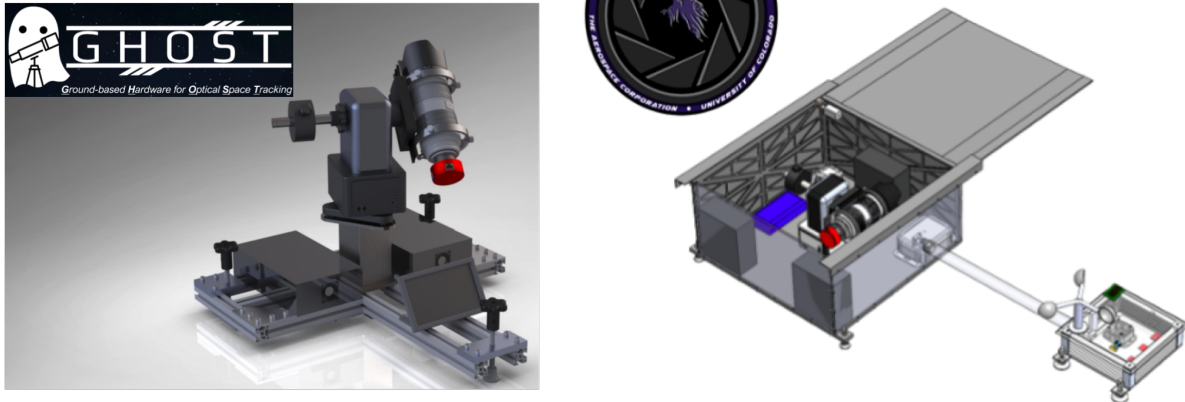


Fig. 2 GHOST (Left) and WRAITH (Right) Hardware

The Spacial HEO Autonomous Detector and Evaluator (SHADE) project will continue and expand the design and development of WRAITH and GHOST. SHADE will demonstrate orbit tracking of objects in HEO, MEO, LEO, and GEO and will improve the systems portability, durability, and ease of use. SHADE's new design will allow a single operator to deploy SHADE within 30 minutes of arrival at the imaging location. A solar-based rechargeable power system uses a unique heat sink design to lower solar cell temperatures and reduce solar power loss. This will enable SHADE's deployment to extend through multiple nights autonomously. Multi-night deployments increase the number of observation windows, as well as lessen the frequency of operator-system interactions. A new image processing system will result in more accurate streak detection with fewer missed targets and false positive tracks. A new polycarbonate-based active protection enclosure will safely house the imaging hardware. This material change, along with a change in batteries, look to increase durability while reducing system mass. SHADE's budget remains under the \$5000 CU Boulder design budget; thus providing an economical solution for the SSA community to accurately determine orbital trajectories including HEOs. All hardware and software additions will build off of and integrate with certain legacy system redesigns in order to provide an exceptional culmination of three years of design work.



Fig. 3 SHADE Project Logo

II. Project Objectives and Functional Requirements

1. What is Project Success

Author: Vinay Simlot

SHADE's success is predicated on the fulfillment of both legacy functional requirements, as well as two new requirements introduced by SHADE. When complete SHADE shall successfully schedule, track, and identify objects in LEO, HEO, GEO, and MEO. SHADE's updates to the previous system should enable one person to carry all of the components to a site, and set them up within thirty minutes, and enable multi-day, autonomous satellite tracking.

2. Levels of Success

Authors: Robert Redfern, Vinay Simlot

Category	Level 1	Level 2	Level 3
Scheduling	Accept list of NORAD satellite IDs and sort based on field of view (FOV), time, and visibility constraints. Capability for up to six objects per hour.	Prioritize objects according to human input or probability of image capture.	Adjust schedule to search for a missing or maneuvered object, and issue an alert when this occurs.
Image Processing	Extract endpoints of streaks at photometric signal-to-noise ratio (SNR) of 30 or less.	Identify missing target object.	The camera will maneuver to find the missing object.
Orbital Determination	Accurate orbit determination using Batch filter.	Level 1.	Predicting possible orbits for missing objects.
Pointing	Tracking HEO orbits near apogee (GEO).	Tracking HEO orbits near perigee (LEO).	Search for missing objects using predicted possible locations.
Environmental Control	Retract environmental protection in accordance with on-board sensors. Safety hardware will protect against light rain, wind, and the safe temperature range.	Level 1.	Retract environmental protection in accordance with remote override from operators. Updates ground station with environmental state and safety hardware status.

Modularity	One operator deploys all modules that each weigh 50 lbs or less. On-site system construction is required after transportation but before deployment.	Level 1.	One operator deploys all modules that each weigh 35 lbs or less. There is minimal required on-site assembly.
Endurance	Demonstrate full, autonomous operation for two nights.	Demonstrate full, autonomous operation for three nights.	Demonstrate full, autonomous operation for five nights.

The above levels of success sought to fulfill the original purpose of both WRAITH and SHADE, while increasing the portability and length of deployment. Therefore, the levels of success for the scheduling, image processing, orbital determination, pointing and environmental control come from the legacy projects. Meeting these levels of success, however, required significant design work. Just 15% of the existing system worked as intended in August 2020.

The levels of success for modularity and endurance are new to SHADE. The SHADE team completed 100% of the design work for these portions of the system.

3. Concept of Operations

Author: Katherine Nyland

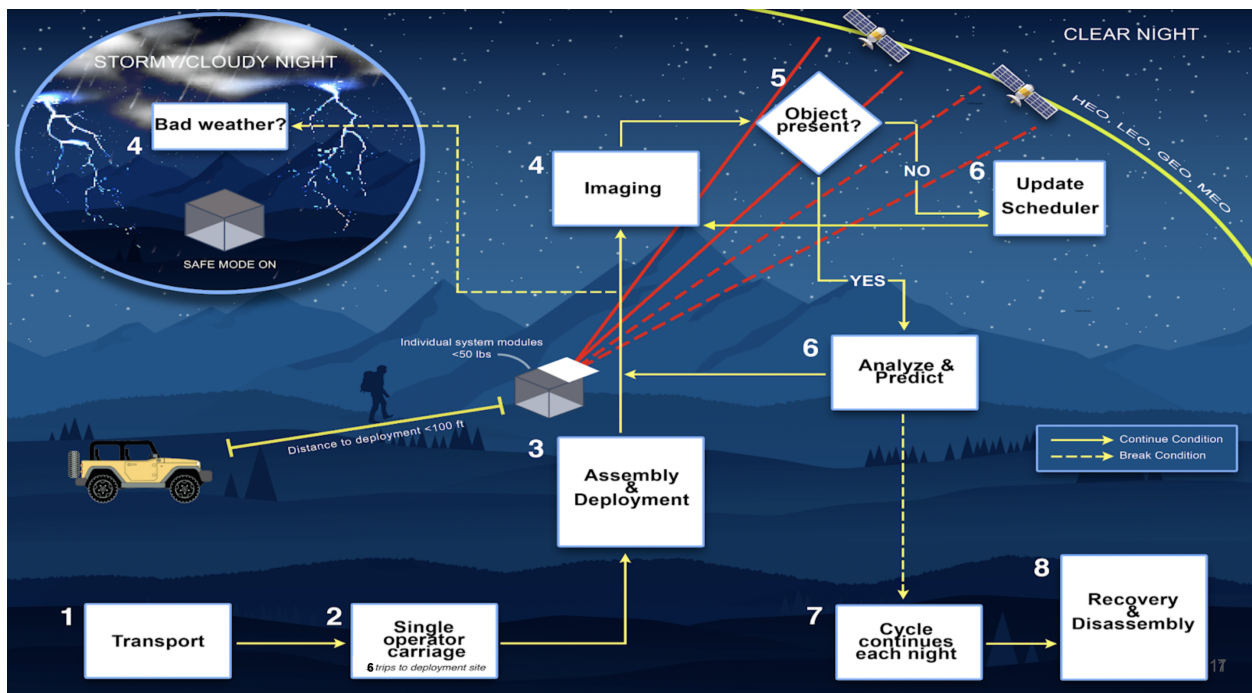


Fig. 4 CONOPS

SHADE's Concept of Operations (CONOPS) can be seen above in Figure 4. The CONOPS depicts what a single deployment of SHADE will look like. The CONOPS will also be used as the foundation for two of the SHADE's three Full System tests; the Single Night Deployment and the Multi-Night Deployment. Below is a comprehensive breakdown of the Concept of Operations:

- 1) A single operator will arrive in a vehicle with the SHADE system modules, parking the vehicle within 100 feet of the deployment site.
- 2) The operator will complete five trips to and from the deployment site, carrying one of the six transport modules on each trip. Each transport module will weigh no more than 50 lbs.
- 3) The operator will assemble the system modules, power-up the system, upload the two line element list, equalize the weather detection sensors and deploy the system. The operator will complete steps two and three all within 30 minutes. The operator will then depart.
- 4) SHADE will then begin its operations, working it's way through the list of TLE elements and determining visibility windows for each. At each visibility window, the camera will take long exposure images of the predict orbit path. Meanwhile, SHADE's weather detection suite will be active, signaling to the active protection enclosure to enter or exit safe mode when necessary.
- 5) The software will determine if the object is present in the images captured of the predicted orbit path.
- 6) If the object is present, SHADE will analyze the images and predict and store a new orbit definition. However, if the object is not present, SHADE will update the scheduler to find the next suitable imaging time.
- 7) Steps four through six will cycle for each night of the deployment. During daylight, the solar panels will charge SHADE's battery.
- 8) At the end of SHADE's deployment, the operator will return to the deployment site, disassemble the system and transport the modules back to the vehicle.

4. System Block Diagrams

Author: Benjamin Vidaurre

1. Functional Flow Block Diagram

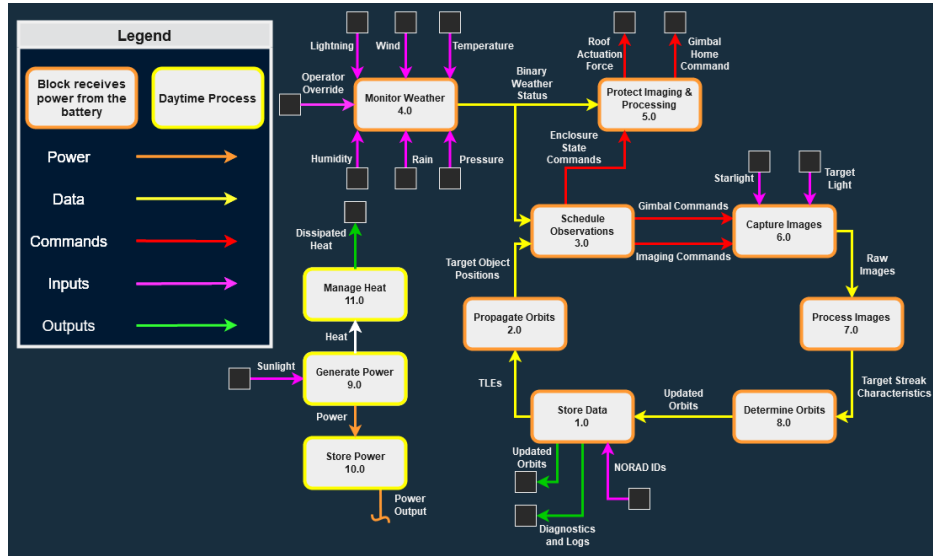


Fig. 5 Overall Functional Flow Block Diagram for SHADE

The functional flow block diagram illustrated in Figure 5 shows the three base processes which take place during the course of a mission and the relevant external inputs to SHADE for each function. The main process is the imaging cycle which runs from functions one through eight. The weather monitoring process sits as a sub-process within the imaging process given its continuous nature and is comprised of functions four and five. The third primary process is the charging process which take place during the day and is composed of functions nine through eleven.

The imaging process forms the basis of the majority of SHADE's primary nighttime operation while also interacting with the weather monitoring process. Having been provided the target objects and determined their last known orbital parameters, SHADE propagates the positions of each target forward in time to search for viable observation opportunities and formulates a schedule for the observations based on the expected quality of a window along with any operator provided information regarding the priority of a target. The observations each have a portion of the sky where they will occur, which is sent from the scheduler to the gimbal to point the camera accordingly. A long exposure image is created which generates a streak as the target traverses the camera field of view. The image is then analysed and the orbit update is derived from the streak characteristics.

The interaction between imaging and weather monitoring takes place whenever the weather is found to be hazardous to SHADE which triggers the gimbal to point to the 'Home' position and then close the roof of the active protection enclosure. Simultaneously, the scheduler is alerted that any observations planned for the time that the roof is closed need to be re-scheduled.

The daytime process performed by the solar panels charges the battery to facilitate further observations. The point of interest in the charging process is the management of the solar panel temperatures to reduce efficiency losses due to heat. The excess heat is drawn from the panels and dissipated from the panels by way of natural convection over the heatsink cooling fins.

2. Full System Physical Block Diagram

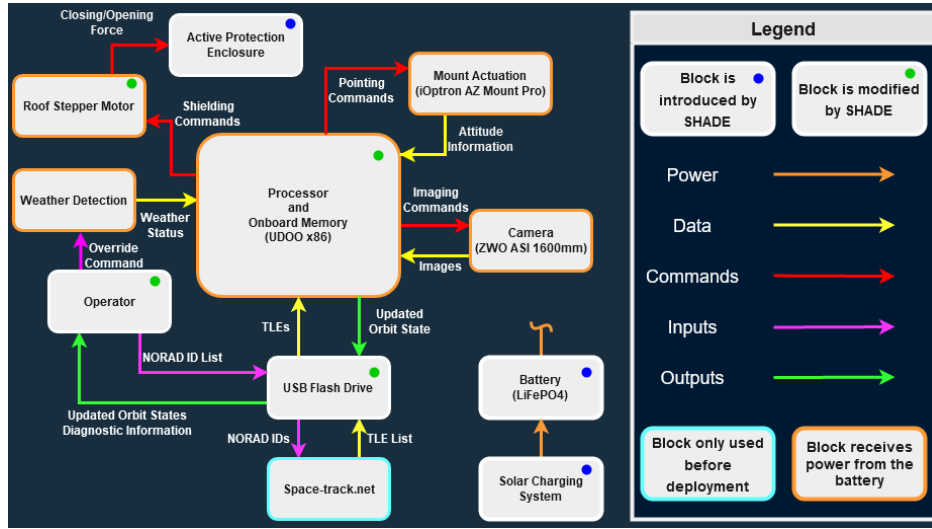


Fig. 6 Full System Physical Block Diagram for SHADE

The physical block diagram of SHADE shown in Figure 6 details the main physical components which make up SHADE. The main component is the processor which drives the operation of each of the other components. The components which drive the three primary processes described in the functional flow block diagram are all represented by the physical block diagram. The imaging process takes place within the processor, the gimbal, and the camera which are grouped in the top right of the diagram. The weather monitoring process is enacted by the weather detection unit comprised of a variety of sensors* and the active protection enclosure whose roof is actuated by the stepper motor. The charging system interacts directly with the battery which then distributes power to the majority of the other components. A more detailed block diagram and description of the charging system can be found in Appendix Section X.6.1.

5. Functional Requirements

Authors: Benjamin Vidaurre, Katherine Nyland, Robert Redfern

Over the course of the conceptual design phase of SHADE development, the functional requirements (FRs) inherited from GHOST and WRAITH were modified as necessary and augmented to account for the additional scope brought by SHADE. The motivation for each of the eight FRs used to develop SHADE will be discussed with respect to the customer needs being addressed and their relevant project elements.

FR 1: SHADE shall schedule predicted locations and visibility windows for objects in LEO, MEO, GEO, and HEO orbits.

In the transition from GHOST to WRAITH, the stipulation relating to the tracking of HEO targets was added to the project scope at the request of the customer. SHADE has not introduced any additional orbital distinctions to the tracking capability of the project, and thus FR 1 has not been substantively

*The sensor suite developed by WRAITH contains an anemometer, lightning detector, IR thermometer, barometer, and a humidity sensor and was not modified by SHADE. As such, it is treated as a single component for the purposes of the physical block diagram.

modified. FR 1 relates specifically to the scheduling capability of SHADE with respect to the different orbit categories, which has been further developed by SHADE, but within the existing constraints set out by the original requirement.

FR 2: SHADE shall function autonomously in standard operating conditions with no human intervention for at least two nights.

The intent of FR 2 as it existed in the WRAITH iteration of the project was to stipulate the autonomous nature of the system as an evolution from GHOST which needed operator interaction throughout the duration of the deployment. While SHADE will retain the autonomous nature of operation, it will also increase the viable duration of the deployment to at least two nights, thus the increase in minimum duration from twelve hours to two nights.

FR 3: SHADE shall autonomously enter and exit a safe mode to protect itself from adverse weather.

FR 3 was introduced by WRAITH as the definition of their weather detection and protection functionality. This was added to reduce the risk associated with leaving the system to run autonomously and the notoriously fickle weather in Colorado. SHADE has not made any modification to FR 3 as it existed upon inheritance.

FR 4: SHADE shall autonomously point to and track objects in LEO, MEO, GEO, and HEO.

Similar to FR 1, FR 4 stipulates system capability with regard to the different orbits being tracked by SHADE but now focuses on the pointing of the imaging system at the target objects. The imaging hardware has not been changed or modified by SHADE, thus the language prescribing the performance of the hardware need not be updated.

FR 5: SHADE shall image objects with apparent magnitude of less than 10.

Although the specificity of this requirement lends itself more to a Type C[†] specification rather than Type A[‡], it was introduced by GHOST to inform their selection of a camera sensor. SHADE will retain the requirement simply to serve as reference for the capability of the system in a *Do no harm* capacity to ensure that other system modifications do not impede the original system capability.

FR 6: SHADE shall create and save an orbit estimate for each object imaged within five minutes of the end of the associated visibility window.

Introduced by WRAITH, FR 6 outlines the necessary processing time to facilitate expedient imaging of a set number of objects over a set amount of time. Generating the updated orbit estimate in less than five minutes allows enough time for SHADE to image at least six objects per hour when accounting for the other system behaviours which must take place in between each observation window. This was not modified operationally by SHADE, though the increase in viable mission duration means that the serialisation of certain functions was modified to take advantage of time spent in safe mode for continued analysis.

[†]Type C specifications are *Product Specifications* which Blanchard describes as "Includes the technical requirements for any item below the top system level that is currently in the inventory and can be procured off the shelf." [22]

[‡]Type A specifications are *System Specifications* which Blanchard describes as "Includes the technical, performance, operational and support characteristic for the system as an entity." [22]

FR 7: SHADE shall be deployed and broken down in 30 minutes by one operator.

This is the first of two novel FRs introduced by SHADE which outlines the intent to make SHADE easier to deploy. WRAITH introduced their own requirement relating to deployment, but required their success on less stringent criteria, namely needing an additional operator to facilitate deployment. The time bound remains consistent between the two iterations of the requirement.

FR 8: SHADE shall be capable of making observations on multiple nights during a single deployment.

FR 8 aims to define the need for SHADE to operate over the course of multiple nights. Certain aspect of this need are represented in FR 1 and FR 2, but FR 8 accounts for all other aspects of the increased mission scope not already accounted for by those modified FRs.

III. Final Design

1. Full System Overview

Author: Jacob Weiner, Robert Redfern

Figure 7 shows the final CAD design of the deployed SHADE system. Centered at the top is the power module, flanked by two, 40-cell solar panels. Directly below is the modified active enclosure with carrying handles and adjustable leveling feet. On the far left is the environmental suit that has remained unchanged since WRAITH. Housed inside the active protection module is the UDOO processor and imaging equipment. The modular design concept of SHADE allows a single operator to fully deploy and recover the entire system in 30 minutes or less. Each module weighs 50 lbs, or less, to increase its portability and reduce risk of injury to the operator. The real version of SHADE and its subsystems is seen in figure 8.

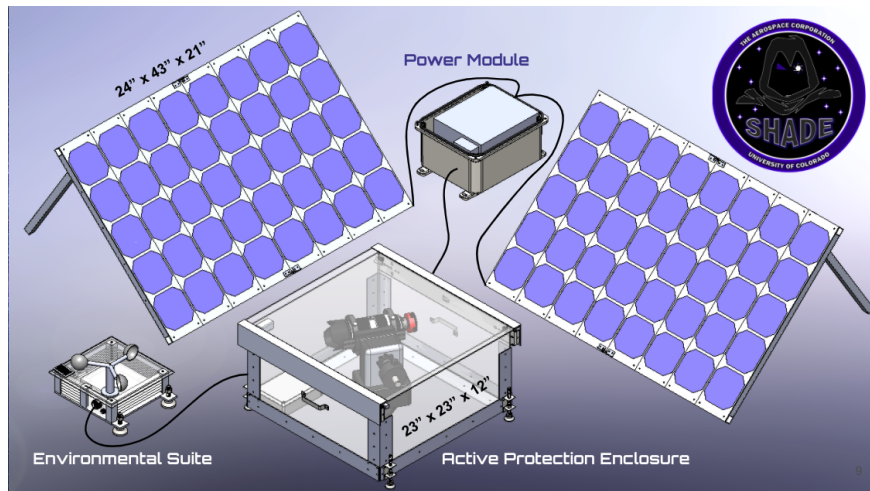


Fig. 7 SHADE Design



Fig. 8 Assembled SHADE System

2. Design Requirements Analysis & Allocation

Author: Benjamin Vidaurre

As listed in section II.5, the FRs for SHADE appear as they currently constrain the in-progress design and development work. Each FR has several associated design requirements (DRs) which detail the technical requirements that facilitate achievement of the performance prescribed by the FRs. The driving motivation for any modifications will be discussed as they relate to each functional requirement along with the justification for each requirement's inclusion.

DR 1.1: SHADE shall accept a series of satellite catalog numbers and TLEs as inputs from the user.

The design of WRAITH with respect to the handling of the input target objects is based on receipt of NORAD IDs for each target in a list which are then converted to Two Line Elements (TLEs) using an internet connection. Although the method for converting the input and the associated operator process has been modified by SHADE, the underlying requirement inherited from WRAITH remained consistent.

DR 1.2: SHADE shall compute predicted observation windows for each input object based on input state information, environmental information, and system location.

This DR, along with DR 1.3, serves as the primary definition of the overall capability of the scheduling system employed by SHADE. Specifically, DR 1.2 highlights the need for the orbit propagator used to identify the observation windows along with other factors which affect the expected quality of an observation such as proximity to the horizon or the phase of the moon.

DR 1.3: SHADE shall create an observation schedule that ensures at least one observation per deployment for each input object, so long as a minimally viable observation window exists.

DR 1.3 stipulates the behaviour of the scheduler and reflects the customer desire to ensure that all targets actually be imaged over the course of the deployment. This may mean that the scheduler must choose observation windows for targets which are not the most ideal window to accommodate

targets with fewer viable or conflicting windows. The trailing clause referring to the existence of a viable window was not included in earlier versions of any requirements lists and has been added to allay any potential to fail compliance tests due to the inclusion of any targets which do not have a viable observation window.

DR 1.3.1: SHADE shall be capable of creating a new schedule if a visibility window is missed.

As an upgrade to the scheduler from its initial design by GHOST, WRAITH introduced DR 1.3.1 to facilitate autonomous function over the course of their targeted twelve hour deployment in the event that an observation could not be made or was unsuccessful. It also serves to make the system more robust to failures which would cause non-compliance with DR 1.3, which was of more importance to WRAITH given that there were fewer opportunities for additional attempts due to their shorter deployment durations. SHADE has bolstered this capability through the generation of a new schedule at the beginning of every night based on results of previous nights observation attempts, but the initial intent driving this requirement remains consistent.

DR 2.1: SHADE shall operate in conditions defined by the Standard Operating Conditions defined in Appendix X.1 with no impact to orbit determination capabilities.

WRAITH's focus on making the system more robust to variable weather conditions motivated their development of the Standard Operating Conditions document defining the environmental bounds for both system function and viable initial deployment decisions. Increasing the mission duration to span more than one night introduced a significant increase in the variability of expected conditions to be experienced during deployment, namely solar heating. While the language of DR 2.1 has not been modified, its connotations regarding module design are plentiful.

DR 2.2: SHADE shall contain a battery capable of supplying operational power levels for 12 hours without recharging.

This is another DR which was introduced by WRAITH when they transitioned from GHOST's assumption that wall power[§] would be available to power the system. SHADE retains this need and driving assumption that no more than twelve hours of continuous observation activity has been sustained. This requirement primarily drives the selection of a battery capable of delivering the required power over the maximum observation period before recharging during the day, when observations are not possible.

DR 3.1: SHADE shall employ active weather shielding to protect the observation platform from adverse weather.

Autonomous initiation and exit of the safe mode by SHADE requires that it be able to monitor weather conditions in real-time and communicate with the active protection system. Additionally, the requirements relating to the accuracy and resolution of the imaging system mean that the camera requires an unencumbered view of the sky which discourages use of a transparent cover as opposed to an active solution for protecting the sensitive electronics and imaging hardware.

DR 3.2: SHADE shall accept a safety override from the operator to activate and deactivate the active weather protection.

While the system will be capable of autonomously activating and deactivating the weather protection,

[§] 120 V, 60 Hz AC power

to mitigate the risk of the weather detection system failing or in the event that the operator identifying potentially detrimental conditions which the weather detection module cannot detect, an operator will have the ability to manually put the system into a safe mode.

DR 4.1: SHADE shall have a pointing accuracy within 4 arcseconds.

The stringent requirement on pointing accuracy is used to assure that the field of view of the camera will capture the entire streak generated by the long exposure. The 4 arcsecond threshold was not present in GHOST's original requirements. WRAITH added the requirement without any quantitative justification, likely to certify that WRAITH would be able to point at HEO targets properly. This addition did not require any additional design work as the iOptron mount used by GHOST has an advertised pointing resolution of 0.1 arcseconds.

DR 4.2: SHADE shall slew at a rate of 2 deg/s.

Similar to DR 4.1, WRAITH added DR 4.2 to ensure that it could properly track HEO objects which represent the targets travelling with the greatest angular rate at perigee. The required slew rate to be able to track these targets was determined using example HEO objects and the 2 deg/s rate represents a factor of safety of two in the maximum slew rate. This slew rate also facilitates the desired observation frequency of six objects per hour, as described in the motivation for FR 6.

DR 4.2.1: SHADE shall contain an on-board control algorithm to actuate the camera gimbal.

DR 4.2.1 arose from GHOST's need to ensure the safety of the hardware during operation and has remained to facilitate autonomous operation in both WRAITH and SHADE.

DR 4.3: The pointing and tracking subsystem shall interface autonomously with the scheduler to receive commands.

Introduced by WRAITH, autonomous interfacing between the scheduler and the imaging system ensured efficient use of observation time and allows the transition from operator driven observations. This communication also facilitates the updates made to the schedule at the beginning of a new night or due to missed observations.

DR 4.4: The computer shall interface with the camera gimbal autonomously.

Control of the gimbal pointing is handled by the gimbal itself, but proper interfacing with the gimbal in issuing commands for pointing as well as calibration remain priorities for SHADE in facilitating the autonomous nature of operation.

DR 4.5: The main processor shall fully interface with the camera sensor autonomously, initiating image capture and receiving the resulting data.

As the camera sensor is not actuated by the gimbal and does not come as a part of the gimbal commercial-off-the-shelf (COTS) unit, control of the camera by the processor must also be regulated to ensure proper imaging of the targets. Proper handling of the images generated is paramount to the success of SHADE, which is also covered by DR 4.5.

DR 5.1: SHADE shall provide at least 6 angular measurements in the inertial frame from a single orbit visibility window.

Introduced by GHOST, DR 5.1 constrains the formulation of the linear algebra problem to be solved by the orbit determination routine and requires that the images produced contain enough information to

produce enough angular measurements to fully define the problem.

DR 5.2: SHADE shall process captured images and screen for quality and missing space objects.

Although the image processor employed by SHADE has been changed from that which was employed by GHOST and WRAITH, it was chosen in accordance with DR 5.2 so as to retain baseline performance with respect to its ability to identify instances where the quality of the observation warrants another imaging attempt.

DR 5.2.1: SHADE shall be capable of identifying and rejecting images that cannot be processed for boresight or space object inertial position.

GHOST used the astrometry.net algorithm for determining the boresight attitude of the camera through analysis of the stars present in an image, a capability which remains with SHADE. DR 5.2.1 mandates that SHADE be able to identify when images are not suitable for processing by the astrometry.net algorithm.

DR 5.2.2: SHADE shall be capable of identifying missing space objects within captured images and reporting that information to the scheduler.

Similar to DR 5.2.1, DR 5.2.2 requires that SHADE be able to identify when the target object is not present in the image to then renew the schedule to allow for another attempted observation later on during the deployment.

DR 6.1: SHADE shall have knowledge of its own location in latitude, longitude, and altitude to within 10 meters.

Precise knowledge of SHADE's position in space is paramount to the accuracy of the orbit updates performed by the orbit determination routine. DR 6.1 was introduced by GHOST to bolster their initial development of the orbit determination capability. As this routine was not modified by SHADE, the language has not been modified but the requirement remained to inform design decisions as they related to modifications made to other system aspects which could have the potential to affect its ability to orient itself.

DR 6.2: SHADE shall save orbit estimates as well as comparisons to previous orbit estimates for each tracked object to the on-board memory.

In transitioning from manned to autonomous operation, WRAITH introduced DR 6.2 to further define the responsibility of the processor in the overall operation of SHADE. While SHADE refined the file system construction, the overall conceit of the requirement remained.

DR 6.3: SHADE shall be capable of converting 6 sets of angular measurements into an orbit estimate within 4 minutes.

As mentioned in DR 5.1, there are to be at least six sets of angular measurements for the orbit determination routine to use in determining the orbit of the target. DR 6.3 stipulates the time in which the OD routine shall provide the updated orbit. This time frame was set by WRAITH to allow for observation of the desired six objects per hour.

DR 6.4: SHADE shall process an image within 10 seconds.

Again, the timing restriction on the operation of the image processor intends to fit the overall processing effort of the system into the time frame which allows for the observation of six objects per hour. The image processor employed by GHOST and WRAITH has been replaced with one better

suiting to the observational environment along with having demonstrated better capability[¶], but still complies with the performance prescribed herein.

DR 6.4.1: SHADE shall maintain a clock drift less than 5 milliseconds when compared with GPS time.

DR 6.4.1 was introduced by WRAITH on the advice of GHOST who struggled to reconcile the inaccuracy of their timing method in the magnitude of the error it produced in the orbit determination results. Although WRAITH stated that they had resolved the issues with clock latency, DR 6.4.1 served as another performance measure for SHADE to ensure proper function.

DR 7.1: The individual system modules shall weigh less than 22.68 kilograms (50 pounds).

As the basis for the modularisation of SHADE, DR 7.1 constrains the extent of any single module to facilitate ease of carriage. SHADE is to be placed in the field by one operator who should be able to lift each module with ease. OSHA standards typically cite 50 lbs (22.68 kg) per person for lifting.

DR 7.1.1: SHADE modules, when located inside their travel casing, shall withstand impulses up to 7 g in any given direction.

This DR serves as a portion of the Type C[¶] specification for the transport casing of each module, with DR 7.1.1 specifying the robustness to shocks imparted to a module either by dropping or through bumps experienced during transport to the deployment site.

DR 7.1.2: SHADE modules, when located inside their travel casing, shall withstand cyclical vibrations ranging between $\pm 2g$ at a frequency of 2 Hz.

Another portion of the Type C spec. for the transport casing, this constrains the expected vibrational environment to be experienced during vehicular transport as described by Grzesica. [6] Although the segregation of the different system components into modules for transport is expected to mitigate some risk of damage incurred by the components during travel, the additional protection will allay further any risk of damage.

DR 7.1.3: SHADE shall utilize passive protection to protect sensitive components not requiring elemental exposure to function from adverse weather.

The modules for SHADE are configured such that the imaging system^{**} is the only environmentally sensitive component that needs to be fully exposed to the environment to function properly. The rest of the components can therefore be enclosed by various degrees of protection to reduce risk of failure due to rain or other hazards.

DR 7.2: SHADE shall be set up and taken down in accordance to the process document titled: SHADE System Operation Manual.

This DR serves to mandate the creation of the Operational Procedure which will detail deployment, recovery, and interfacing with the software systems to aid operators in using SHADE. This aid is meant to further facilitate meeting the time constraint for deployment and recovery of SHADE, in accordance with FR 7.

DR 7.3: SHADE shall be able to startup and perform all tasks with no user input beyond supplying a target list file via external USB drive.

[¶]See section III.5.7 for discussion regarding the Hough Transform image processor

[¶]Type C specifications are *Product Specifications* which Blanchard describes as "Includes the technical requirements for any item below the top system level that is currently in the inventory and can be procured off the shelf." [22]

^{**}Camera sensor, lens, and gimbal

SHADE needs to be set up quickly, and preferably by a person with potentially limited knowledge of SHADE's core design. As such, the onboard operating system will startup and initiate itself as soon as it is powered on and detects the target list on an external USB drive.

DR 7.4: SHADE shall be able to calibrate the boresight attitude of the camera lens autonomously.

As noted in DR 6.1, precise knowledge of the pointing state of the camera is critical to the operation of the orbit determination routine. Because calibration is based on analysis of stars present in an image taken by SHADE, calibration must take place when enough stars are visible. As initial deployment of SHADE is markedly easier, safer, and more convenient during the day, calibration must take place autonomously.

DR 7.4.1: SHADE shall be able to update the boresight attitude calibration autonomously throughout the mission duration.

Following the need for autonomous calibration during system initialisation, increasing the overall duration of the mission introduces greater likelihood of SHADE shifting, settling, or being disturbed. If the disturbance is large enough, the quality of the images taken will suffer and the resulting orbit determination attempts will either fail outright or result in unusable estimates of the target orbits. Updating the pointing state of the camera periodically throughout the mission eliminates the possibility of a disturbance rendering the rest of mission useless.

DR 8.1: SHADE shall be resilient to diurnal temperature fluctuations over the range of temperatures described by the Standard Operating Conditions in Appendix X.1.

GHOST and WRAITH were designed on the assumption that the system would not be left in the field for more than one day-night cycle, allowing for the design to focus on resilience to cold temperature without considering solar heating during the day. Longer missions require that the effects of solar heating now be considered.

DR 8.1.1: During charging, the magnitude of the thermal coefficient for the solar panels shall not exceed -0.5% per °C.

Efficiency of the solar panels varies inversely with the thermal coefficient. Keeping the panels cool during operation is key to extracting maximum efficiency. DR 8.1.1 serves as a Type C spec. criterion used in selecting the solar cells to be used in SHADE's solar panels.

DR 8.1.2: While not in use, the internal temperature of the active protection shall be maintained between 0°C and 40°C.

To avoid damaging the components while not in use, the temperature within the enclosures for each module should be maintained at a safe level. The temperature range is based on the stated limits for the most thermally sensitive component, the camera sensor.

DR 8.2: The solar charging system shall be capable of providing a constant 12.5V input voltage to the SHADE system during adequate solar conditions.

The battery employed by SHADE charges at 12.5V and up to 15A, thus the solar charging system must be able to produce enough electrical power to recharge a depleted battery the following day. This requires that the battery voltage remains above 10.5V such that the power conditioner employed by SHADE can produce an output voltage of 12.5V to avoid any unplanned loss of power.

DR 8.3: SHADE shall predict location of an object at an arbitrary time up to five nights in the future.

Because objects can only be imaged at certain times, the computer must be able to predict the location of a target object in its orbit at an arbitrary point in the future, and determine the portion of sky that must be imaged to track the object. Five nights was chosen as being the longest target mission duration for SHADE. This has connotations about the accuracy of the orbit propagation method employed by SHADE along with the nature of the different orbits as they relate to prediction accuracy and its variation with time.

DR 8.4: When creating the initial schedule, the scheduler shall be able to consider the total mission duration when prioritizing observation windows.

In increasing the mission duration, SHADE will now have more opportunities to make observations of the same object, allowing more flexibility in creating the overall observation schedule. As some orbit categories tend to be less stable than others^{††}, the scheduler should also know how to prioritise the orbits with less stable characteristics so as not to increase the risk of missing observations because the target cannot be found.

3. Solar Charging

Authors: John Hugo, Elliott Tung, Jacob Weiner

1. Overview

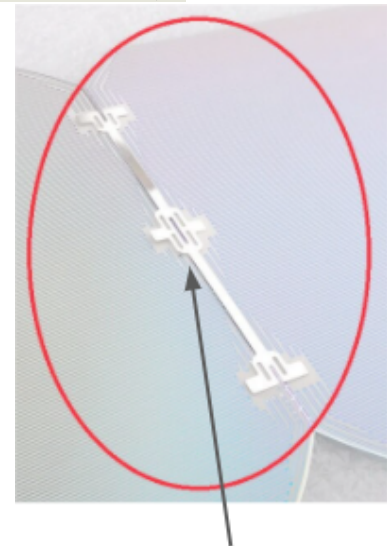
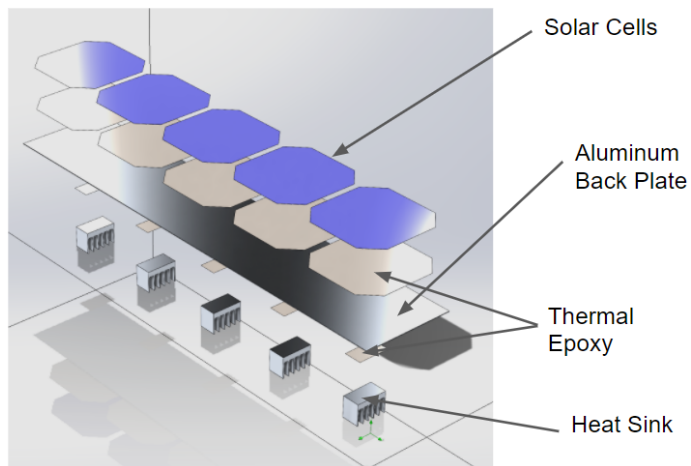
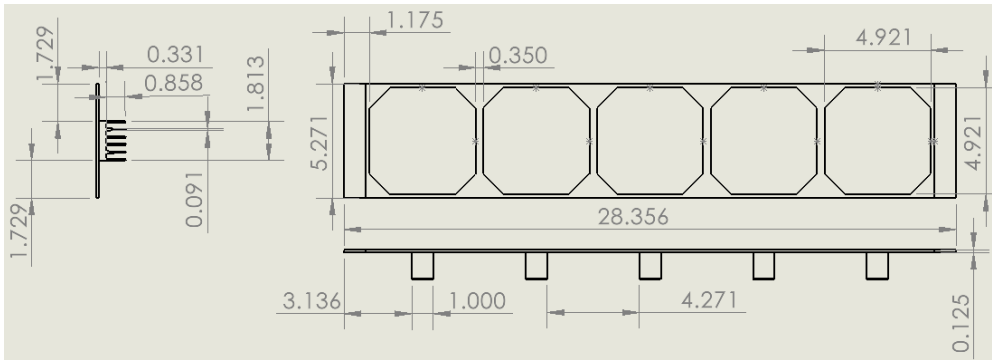
The implementation of a solar charging systems allows SHADE to satisfy FR 2 by replenishing energy spent during a viewing session. Within the solar charging system, the implementation of a new battery technology will reinforce SHADE's ability to meet DR 2.2. The modular nature and light weight components of SHADE's solar charging system is driven by FR 7 and each component is required to meet DR 7.1, 7.1.3, and 7.3. Lastly, FR 8 expands on FR 2 and requires SHADE to view on multiple nights during a single deployment. Design requirements 8.1 - 8.2 were key drivers for the final design of the solar panels and were met using a novel design for solar panels.

2. Panel Construction

Using trade study results and the initial solar charging requirements, a final solar panel design was selected. Figure 7 shows two solar panels each with 40 MAXEONTM Gen III monocrystalline solar cells manufactured by SunPower. The 40 cells are contained on eight, five cell segments. This allows SHADE's operators to quickly manufacture each panel and replace any damaged segment throughout SHADE's lifetime. As noted, adding heatsinks to the back of each solar cell will reduce their surface temperature, increasing their efficiency and electrical output for a given solar incidence. Figure III.3.2 shows how each segment is constructed and key dimensions.^{‡‡}

^{††}Circular, low altitude orbits tend to be the least stable

^{‡‡}Additional dimensions can be found in appendix X.2



**Solderable
"Dogbone"**

Each solar cell is adhered to the aluminum backplate using a thermally conductive epoxy that is also electrically insulating. Each heat sink is adhered to the back side of the aluminum plate using the same thermal epoxy, centered on each cell. The heatsinks are commercially available and extruded from 6063-T5 aluminium. Great consideration was taken in the heatsink sizing and the final design was ultimately driven by the financial and weight budgets for each panel. The current design increases the surface area of each cell by 63.5% and results in a total panel weight of 26.15 lbs. This is well under the 50 lbs requirement and will increase the ease of deployment and recovery. Each of the 40 cells are wired in series using solderable connectors on the back side of each solar cell. Each segment will be connected to the next using insulated wire and the soldered tabs. This highlights the need for the thermal epoxy to be electrically insulating so the panel does not short itself out and damage the cells.

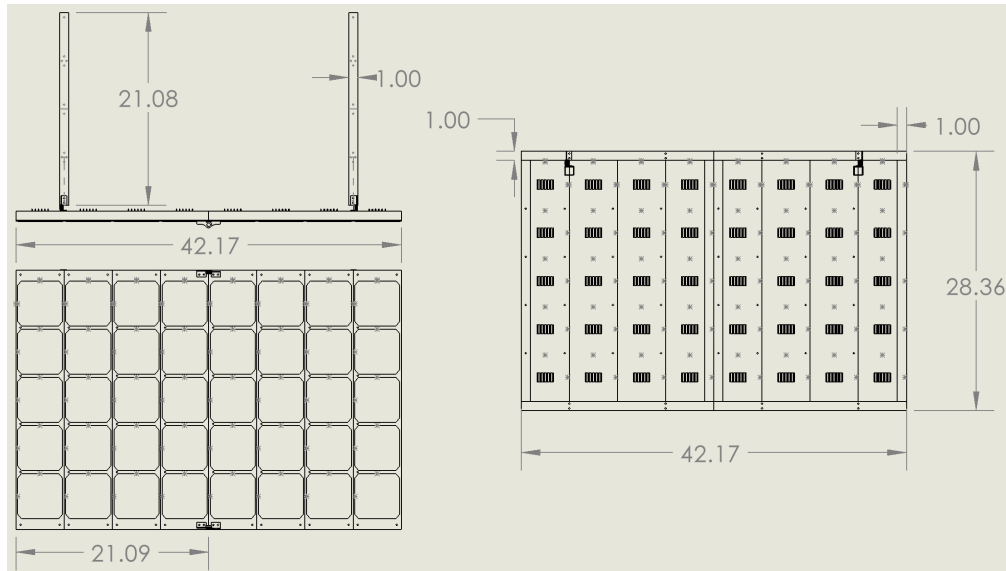


Fig. 9 Dimensioned solar panel

The five cell segments are then screwed into an aluminium square tube frame. The frame itself folds in half for transportation and storage. Friction hinges keep the panel flat when deployed and the legs on the back of the panel employ the same friction hinge. This allows the operator to move the legs so that the panel rests at an angle to allow precipitation to run off the face of the panel. This design also uses the one-inch square tubing as a handle during the transportation phase of each panel to and from the operator's vehicle. Each 40 cell panel will have a nominal P_{mpp} of 148.8 W at a V_{mpp} of 25.28 V.

3. Modeling

Author: Elliott Tung

Initial Steady State Model

Using WRAITH's worst case scenario, their testing data suggest that the system will need 55.14 Ah to operate for a single night. In order to successfully implement a design using solar panels, an initial MATLAB model was devised to ensure that the solar panels are able to collect a minimum of 55.14 Ah during the day. Using solar irradiance data and ambient temperature gathered from the National Solar Radiation Database (NSRDB) from January 2018 to December 2019, a rough estimate of the energy collected on a day to day basis in Boulder, Colorado is shown in Figure 10.

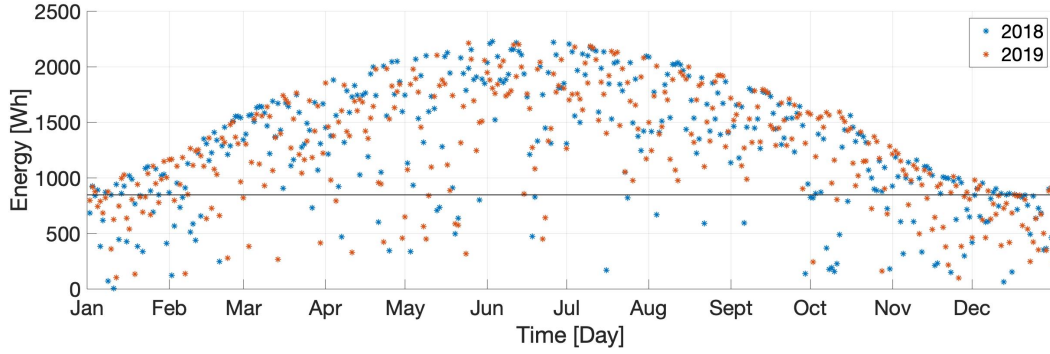


Fig. 10 Estimated Energy Collected By Solar Panels

This model calculates the power produced at five minute intervals based on the solar cell datasheet and is then integrated over the entire day to find the total amount of energy produced. In addition, the solar cell temperature is factored into the efficiency of the cells and is calculated by using the ambient temperature and solar irradiance found in equation 1. The amount of solar irradiance will also be based on the angle the solar panels are set to, which will change based on the time of year. From these results, SHADE will be able to get a full charge 84.25% out of a calendar year.

$$T_c = \frac{T_a + (T_{c,NOCT} - T_{a,NOCT}) \frac{G_T}{G_{T,NOCT}} \left[1 - \frac{\eta_{mp,STC}(1-\alpha_p T_{c,STC})}{\tau \alpha} \right]}{1 + (T_{c,NOCT} - T_{a,NOCT}) \frac{G_T}{G_{T,NOCT}} \frac{\alpha_p \eta_{mp,STC}}{\tau \alpha}} \quad (1)$$

Transient Model

In addition to the steady state model, a more accurate transient model was produced using SOLIDWorks' thermal analysis tool, where the extremes of the current operating conditions were tested. This analysis was able to calculate the solar irradiance and solar cell temperature for a hot day in the summer as well as a cold day in the winter in order to model the battery charge profile which will be discussed more in depth in the section below.

In order to test the efficiency of the heat sinks, the hottest day recorded in Boulder from the last two years (June 28, 2018) was used in the SOLIDWorks' thermal analysis. This was coupled with the longest day of the year (summer solstice), and as shown in Figure 11, a full battery charge was achieved by noon local time.

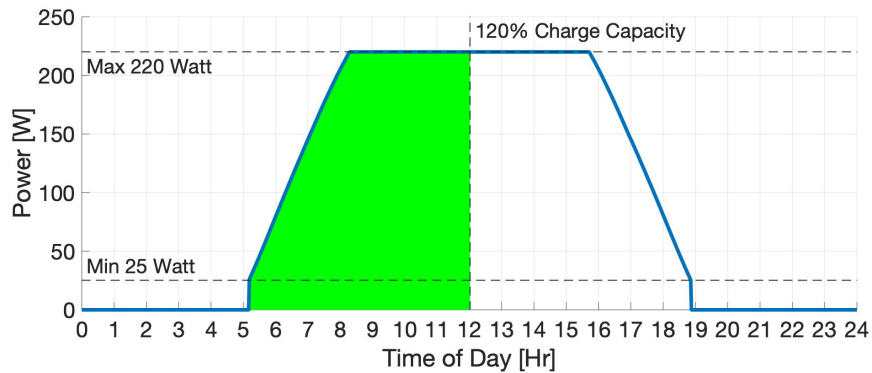


Fig. 11 Estimated Energy Collected By Solar Panels on Hot Day

It is important to note that power generated under 25 W and over 220 W are not included in the graph. As the the voltage of a solar panel does vary and in extremely low light conditions, the panel might not reach a high enough voltage to begin charging. For this reason, the solar panels were given a nominal voltage of more than twice that of the battery. The charger is also unable to charge the battery with any more than 220 W of power. Should the incoming radiation cause the solar array to produce more power than needed, the charger will automatically adjust the resistive load it places on the panel to decrease the panel’s power output.

To find the lower limit of getting enough charge to operate through the entire night, a cold day model was also done through SOLIDWorks’ thermal analysis tool. The tool modeled the coldest day recorded (February 28, 2018) in Boulder, Colorado from the last two years coupled with the shortest day of the year (winter solstice) with 20 percent cloud cover.

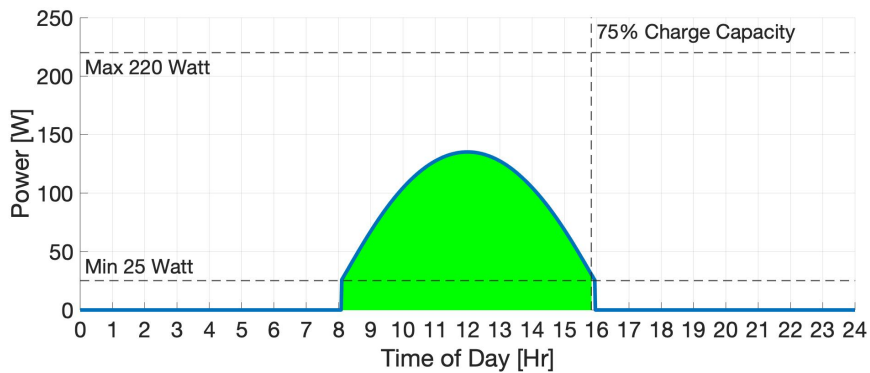


Fig. 12 Estimated Energy Collected By Solar Panels on Cold Day

Figure 12 shows that under these conditions, the battery will be able to charge to approximately 75 percent, or 56.25 Ah. This is fairly close to the minimum threshold of 55.14Ah which was defined as the worst case energy usage in a single night.

Since there are many different variables that can affect the amount of charge the solar panel can collect, only the most feasible edge cases in which SHADE will be deployed, were tested. Operating conditions will be outlined under the Standard Operating Conditions found in Appendix X.1 to prevent SHADE from deploying under unfavorable situations.

4. Charging Simulation

In addition to the transient models, a charging simulation was performed to estimate the battery charge profile for the hot day and cold day case. The battery charging profile is based off of the LiFePo4 battery data sheet.

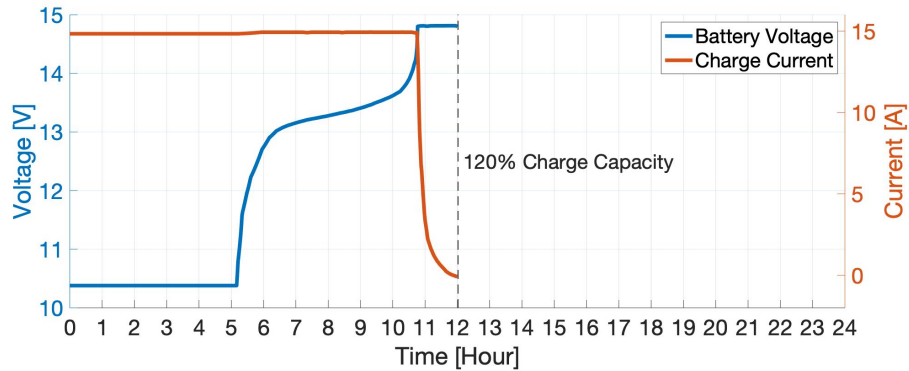


Fig. 13 Estimated Battery Charge Profile on Hot Day

In the hot case shown in Figure 13, the battery does not begin charging until approximately 5:30 AM, which has an initial current of 14.8 A and voltage of 10.2 V. The voltage increases at a logarithmic rate until reaching approximately 80 percent charge. The voltage then increases at an exponential rate until reaching 14.9 V where it flattens out. The current remains constant throughout the charge until reaching a 95 percent charge where it drops off exponentially until it reaches 0 A at 120 percent charge.

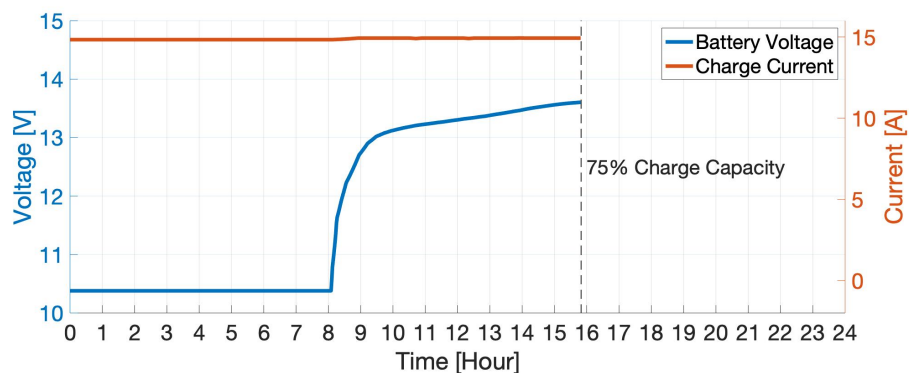


Fig. 14 Estimated Battery Charge Profile on Cold Day

In Figure 14, the battery charge profile follows a similar initial battery current and voltage however, since there is less solar flux received by the solar panels, the battery only gets up to 75 percent charge capacity.

5. Thermal Analysis

Author: John Hugo

As stated before, thermal analysis was conducted on the solar panels, specifically a five cell segment. The reason why to conduct a thermal analysis is that the solar cells degrade in performance at higher temperatures. So, a thermal analysis must be conducted. The main goals of the thermal analysis was to determine the effectiveness of the heat sinks, get an estimate of the expected operating temperatures, and gain data of solar irradiance. This was done through the SolidWorks Flow Simulation feature.

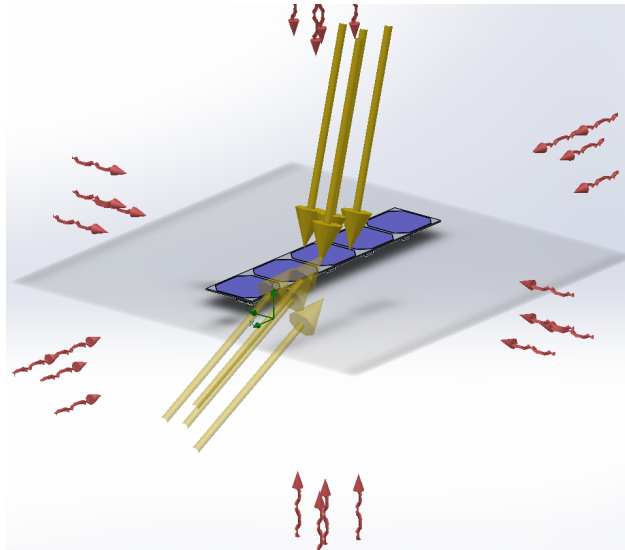


Fig. 15 Thermal Analysis Setup

Through this SolidWorks feature, a simulation can be conducted that accounts for solar radiation throughout a day, ambient temperature, radiation from the objects evaluated, and cloud cover. These conditions can vary depending on location on Earth and local time, which means a full day can be simulated on any location and provide an accurate representation on the the thermal performance of the solar panel. An example of this setup can be seen in Figure 15. Thus, the program was utilized for thermal analysis.

In order to evaluate the thermal performance of the solar panel, two different cases were created: a hot case and a cold case. These were meant to test the expected bounds of performance by selecting a hot summer day near the summer solstice, and a cold winter day near the winter solstice. The chosen location for this analysis was Denver due to proximity and because any field testing would occur nearby. Through analysis of NWS Boulder data, the dates of the hot and cold cases were chosen to be June 28, 2018 and December 28, 2018 respectively. The temperature data from those dates were extracted and then converted to be utilized with SolidWorks.

To test the effectiveness of the heat sinks, two different models were created on SolidWorks: a segment with heat sinks and one without heat sinks. By analyzing the average surface temperature of the solar cells on each model, the overall effectiveness of the heat sinks can be established. This will involve coefficients provided by the manufacturer.

The following sections detail the results of conducting SolidWorks Flow Simulation thermal analysis on both solar panel segment models over a 24 hour period on June 28, 2018 and December 28, 2018. Note that the Cold Case features 20% cloud coverage. Each figure in these sections displays the results around noon (12:00) where the maximum temperatures of the simulation are observed.

Hot Case

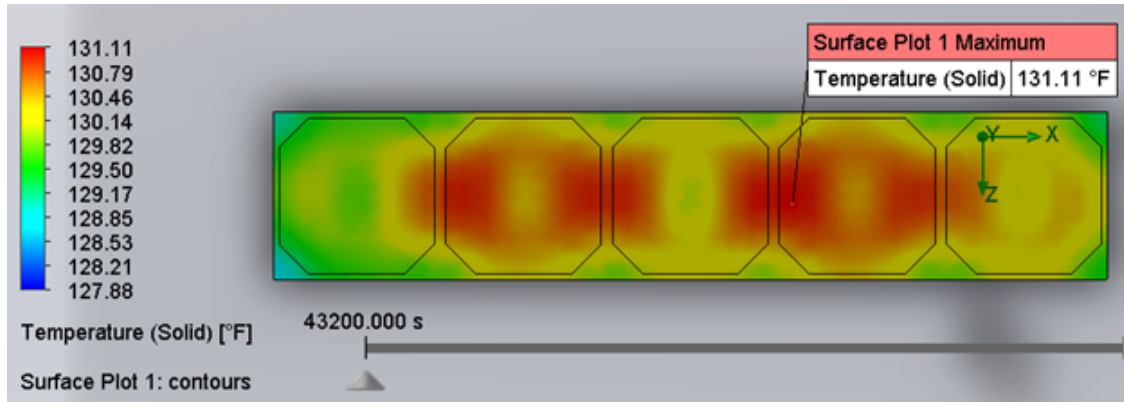


Fig. 16 Hot Case w/ Heat Sinks

Figure 16 shows the surface temperature contours of the hot case with heat sinks. As shown in the figure, the range of temperatures present are between 127.88 °F and 131.11°F with the simulated maximum temperature appearing on the solar cells.

There are some key observations from the figure. Notably, the temperature seems to drop away from the center of the segment in both the vertical and horizontal directions. The reason why this occurs is because the edges are radiating heat, thus the areas with more edges like right and left sides are cooler than other places.

Another key observation is that at the center of the solar cells, the temperature is notably cooler than the rest of the cells. This displays the effect of the heat sinks. While the entire solar cell is not cooled down, this does bring down the average surface temperature of the solar cell down. This means that the solar cells would be more effective.

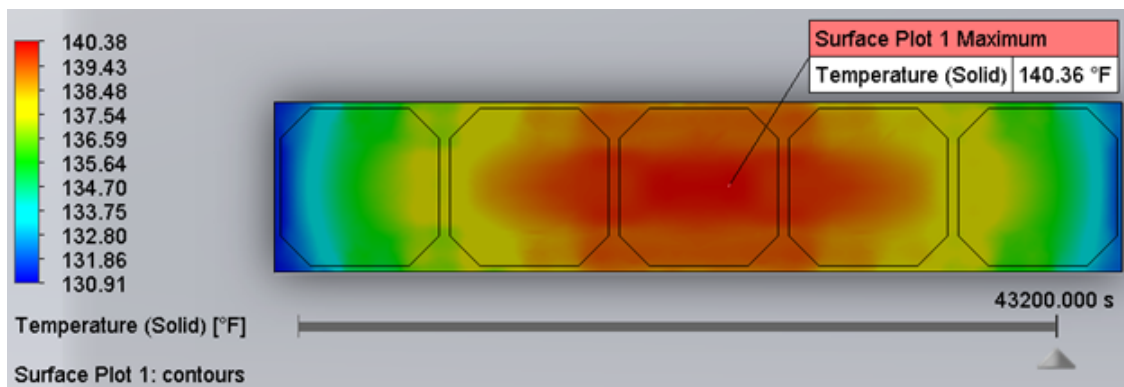


Fig. 17 Hot Case w/o Heat Sinks

Figure 17 displays the surface temperature contours of the hot case without heat sinks. The range of temperatures of the contours are between 130.91 °F and 140.38 °F, with the latter temperature appearing on the surface of the center solar cell.

Comparing figures 16 and 17, there is a stark difference between the two models. Overall, the segment without the heat sink is significantly hotter than the model with the heat sink, making the solar panel more effective with heat sinks during a hot case.

As to the empirical values of effectiveness, the MAXEON Gen III cell data sheet listed the temperature

coefficient of $-0.29\%/^{\circ}\text{C}$ when the temperature is above 25°C . Converting the values displayed in the related figures to Celsius and comparing the difference, the solar panel with the heat sink is 1.4935% more effective than the solar panel without the heat sink.

Cold Case

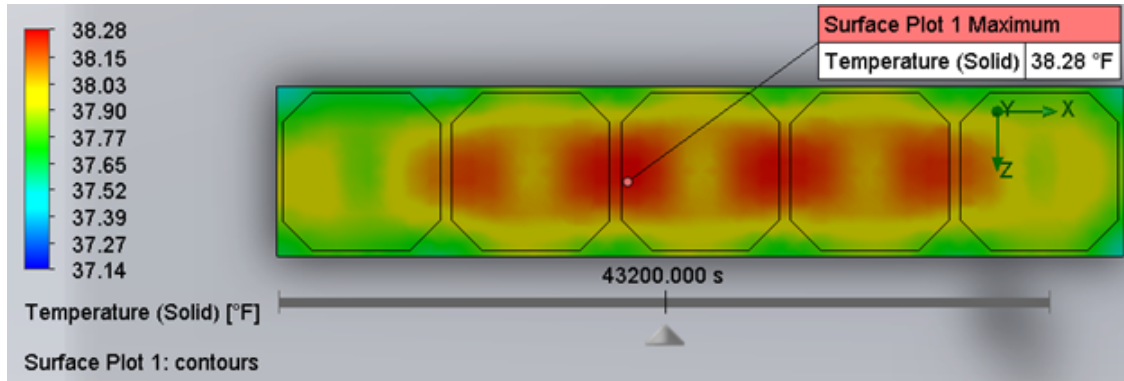


Fig. 18 Cold Case w/ Heat Sinks

Figure 18 displays the surface temperature contours of the cold case with heat sinks. The range of temperatures present are between 37.14°F and 38.28°F .

Again, the same observations as with the hot case is present. At the center of each of the solar cells is the observable effect of the heat sink, which decreases the temperature relative to the other areas of the cell. The pattern is almost identical to that of the hot case, with the obvious difference being the actual temperatures the solar cells are at.

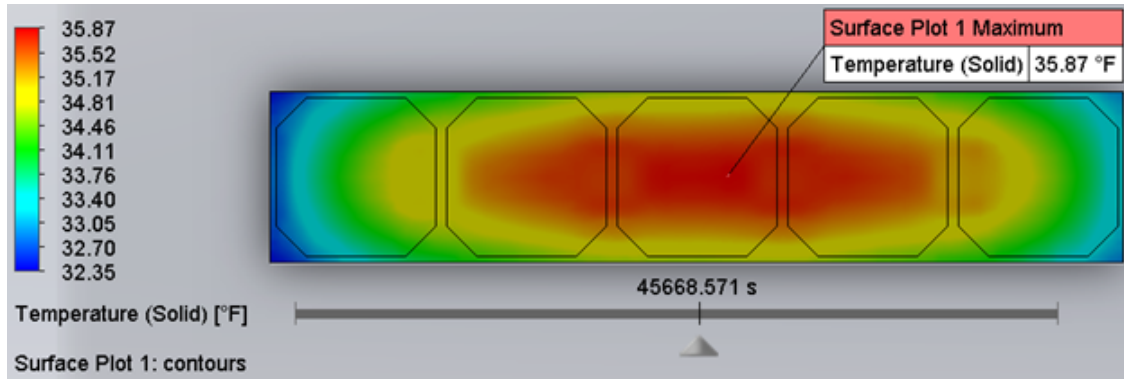


Fig. 19 Cold Case w/o Heat Sinks

Figure 19 displays the surface temperature contours of the cold case without heat sinks. The range of temperatures present are between 32.23°F and 35.87°F .

Like the heat sink model, the contours between the hot case and cold case are nearly identical. The temperature values have changed but the overall behavior of the results in the thermal analysis is as expected.

One obvious observation between the two cases is that the model without the heat sink is actually colder than the model with the heat sink. This could be due to the fact that the heat sinks are retaining more heat

than radiating it away, especially considering the colder ambient temperature. This could also be due to the simulation not having a smaller time resolution, meaning that the simulations would be more inaccurate.

Even with the difference, there is no change in terms of efficiency as the surface temperatures for both models are below 25°C.

Further Discussion on Results

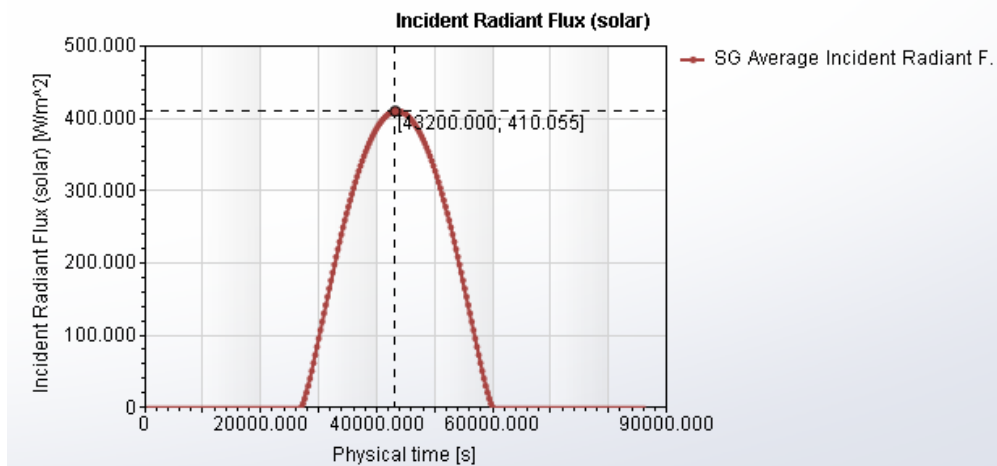


Fig. 20 Solar Irradiance Graph

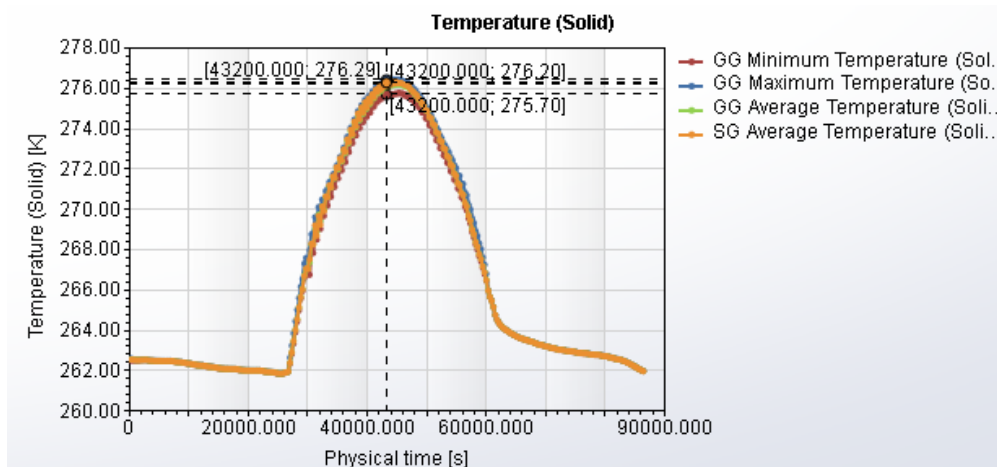


Fig. 21 Surface Temperature Graph

The results shown paint a picture on the expected thermal performance of the solar panels. While the temperature contours are great visual aid, actual temperature data and solar irradiance was needed for further study. SolidWorks could output the data into excel spreadsheets, allowing for analysis into the charging of the power system. Figures 20 and 21 shows the solar irradiance and surface temperature graphs from the cold case that would be produced from the simulation. A charging profile could then be constructed utilizing the data from SolidWorks and coefficients from the MAXEON Gen III data sheet.

The simulations are not perfect however. Notably, calculation time affects the accuracy of the results. With

larger time steps, the accuracy of the simulation is highly suspect. Temperatures would vary and not converge, especially with the transient nature of the simulation. With smaller time steps and more computational time for the simulations, the results would be more accurate.

One other problem with the simulations come from the solar panel models without the heat sinks. Computational times for the associated cases are considerably longer than the models with the heat sinks. For example, the hot case with heat sinks took 30 minutes to run, while the hot case without the heat sinks took about an hour and 30 minutes to run. This is with the same time step. It's why some errors would exist like the model without the heat sinks being colder than the model with the heat sinks. This could be due to how thin the solar panel segment without heat sinks is. Similar thermal analyses on thin objects had extremely long computational times. This should not be a future problem as these thin models were only utilized to determine the effectiveness of the heat sinks, which is self evident in the previous sections.

6. The Power Module

Author: Jacob Weiner

To achieve the required power to fully recharge SHADE's 75Ah battery after a nights long imaging session, two solar panels will be wired in parallel to increase the current into the charger. Both solar panels are wired into an isolation switch which protects the user from the risk of electrical shock while connecting the solar panels to the power module. The output of the isolation switch leads into the Victron BlueSolar MPPT solar charge controller. The Intervolt power conditioner is connected to the charge controller and provides DC power at 12.5 V to the rest of the SHADE system.

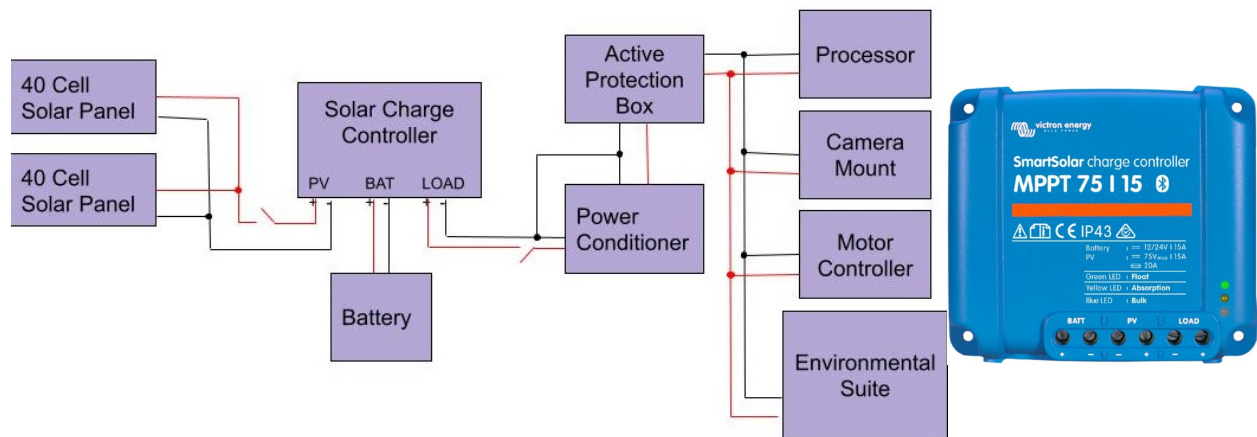


Fig. 22 Solar Charging Circuit Diagram and Charger

The charge controller is the heart and brains of the novel power system and uses maximum power point tracking (MPPT) to adjust the resistive load on the solar panels, forcing them to operate at their maximum power point for a given solar radiation. This allows the charging system to run more efficiently overall. The charger then outputs power at up to 14.4 V and 15 A to charge the battery during the "absorption" portion of the battery charge cycle. Once the battery capacity reaches 98% of its nominal capacity, the charge current decreases and tapers off to prevent damage to the battery. It important to note that temperature will limit the current the a battery can be safely charged at. This risk is mitigated by the SmartSolar charger and its

onboard thermometer. The charger will auto adjust its charge profile as the temperature inside the power module decreases.

The current design uses the charge controller as a mid point between the battery and the rest of SHADE. This provides a redundant level of battery protection since the charge controller can cut power to the power conditioner in the event that SHADE fails to enter low power mode, thus protecting the battery from over-discharging. The box has been painted white and a weather resistant vent has been installed to help keep the internal temperatures below the maximum operating temperatures of the system components.

The final design of the power module is seen below. The blue, Victron charge controller sits on top of the battery in the upper right corner of figure 23. The power conditioner sits on top of the battery at the bottom of figure 23. Both umbilical cables and disconnect switches are through mounted and sealed with either a gasket or silicone to protect the power module from water ingress.



Fig. 23 Power Module Design

7. System and Legacy System Integration

Author: Jacob Weiner

The battery, charge controller, power conditioner, and isolation switches are housed within a COTS box. There are umbilical power cords that are passed through a weather resistant connector for connecting to the solar panels and active protection box. The connectors are an automotive, blade style plug that is weather resistant to reduce risks of shorting out in wet weather conditions. The blue cable to the active protection box includes four wires, two for 12.5 VDC power and two for communicating real time battery voltage to the main processor via a serial port. Communicating between the charge controller and the main processor requires a logic level converter and a common ground to reduce the signal voltage from 5 VDC to 1.8 VDC. The 12.5 VDC power is then distributed to the various SHADE subsystems using a junction box.



Fig. 24 Final Power System

All components of the power system weigh less than 50 lbs. Each solar panel weighs about 26 lbs and the power module weighs in at 29 lbs. The modular nature of the power system allows for easy deployment and minimal effort. The connectors for the solar panels and power umbilical are unique and can only work in one direction. This limits any risk of the operator improperly connecting the solar panels or active protection box. Furthermore, each active component on the power module either has a replaceable fuse or internal protections against over current discharge to prevent component damage.

4. Active Protection System

Author: Marlin Jacobson

SHADE's Active Protection System protects its tracking hardware from inclement weather, heat, harsh environmental conditions, high loads, and vibrations using various passive and active protection elements. SHADE's passive protection elements function to protect the system and its electrical components at all times and to ensure it can survive during nominal to moderate environmental conditions. SHADE's active protection elements protect its internal hardware using an automated sliding roof that opens or closes based on the environmental conditions detected by the environmental suite. Finally, its lightweight and modular design allows the system's operator to easily transport and set up the Active Protection System. The following sections dive into each critical design component and illustrate how the system's final design details were developed to satisfy SHADE's requirements. Figure 25 presents the Active Protection System during non-operational (closed) and operational (open) modes.



Fig. 25 Active Protection System Design

1. Overview

Author: Marlin Jacobson

To precede the detailed design and context for all decisions made for SHADE's Active Protection System, a system overview is presented in Figures 26 and 27. Figure 26 portrays the modeled, labeled system while it is not tracking, and 27 illustrates the system's appearance while in use. The Active Protection System houses the camera, iOptron mount, power distributor, UDOO processor, motor controller, roof actuation motor, COTs boxes to house the electrical components, and wiring.

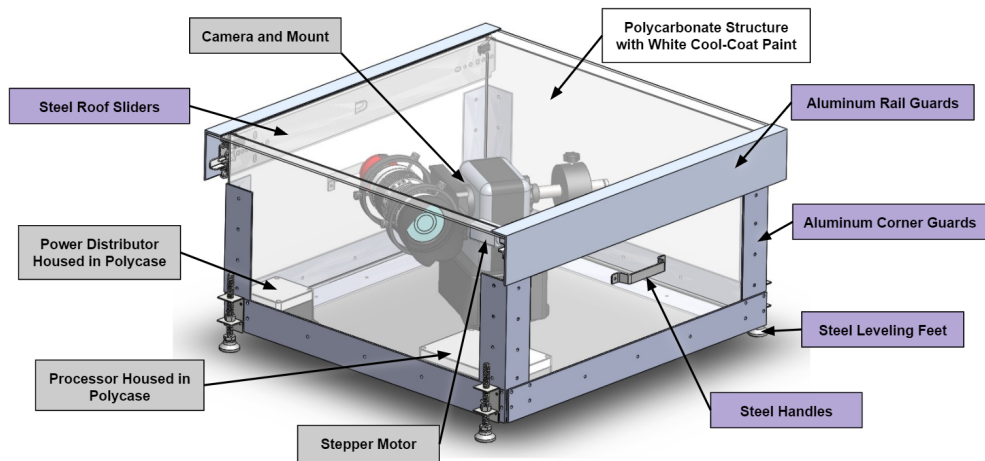


Fig. 26 Active Protection System Overview



Fig. 27 Active Protection System Opened

indicates the direction of liquid flow off of the roof and roof motion direction from a closed state with the blue arrow.

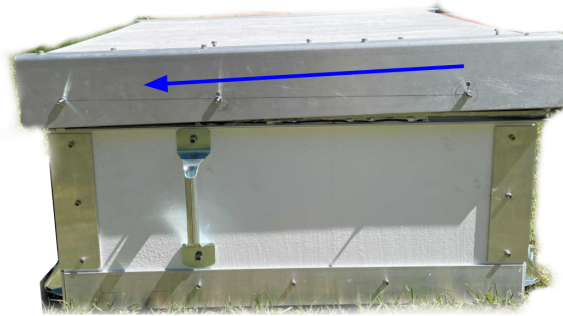


Fig. 29 Active Protection System Liquid Mitigation

3. Active Protection Element

Authors: Marlin Jacobson and Jacob Weiner

The enclosure's active environmental protection element includes a rack and pinion stepper motor. This motor is commanded by the UDOO processor to open or close the roof based upon the data it receives from the environmental suite. SHADE's active protection element satisfies **Design Requirements 2.1 and 3.1** by enabling the system to operate autonomously after setup and to protect all tracking hardware throughout the mission. Figure 30 presents an image of the lid actuation stepper motor.

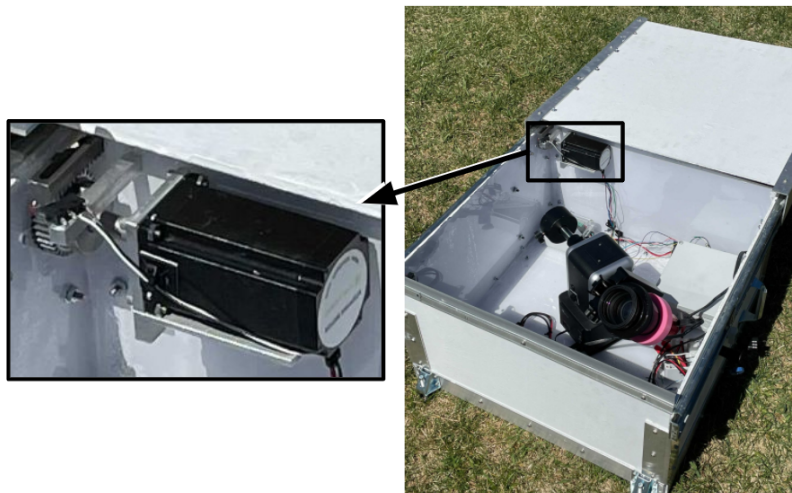


Fig. 30 Lid Actuation Stepper Motor

The stepper motor driver is controlled by a pulse width modulated signal from the UDOO processor. In order to determine whether the system is open or closed, the UDOO processor determines roof states using small limit switches on both ends of the enclosure. There are three states: open, transition, and closed. These states are determined by a combination of which switch or switches are closed. When an open command is given, the roof retracts, the first limit switch breaks contact, and SHADE determines that the roof is in the

transition phase. The roof continues to retract until the second limit switch is released. Now SHADE knows that the roof is nearly open. After the second limit switch is released, the stepper motor driver is commanded to move several additional steps to ensure that the roof is in its fully open position. The same process is mirrored when SHADE commands the roof to be closed. To ensure the successful protection of the tracking hardware when adverse weather is detected, the roof closes within 10 seconds of a command to close the roof.

4. Passive Protection Elements

Author: Marlin Jacobson

SHADE's Active Protection System utilizes four passive protection elements to protect the enclosure itself and its tracking hardware from various environmental conditions. The first passive protection element, which satisfies **Design Requirements 2.1 and 8.1**, is a white, thermally protective paint that covers all external polycarbonate surfaces of the Active Protection System enclosure (Figure 31). The paint's high IR emissivity of 0.95 and low solar absorptivity of 0.3 protects the structure of the enclosure and the internal components from excessive solar heating by absorbing minimal solar radiation and emitting large amounts of contained energy.



Fig. 31 Active Protection System Thermal Protection

The second passive protection element is weatherproofing. These elements include an external gap seal (weatherstrip), internal gap sealant, and a sloped roof design. These elements satisfy **Design Requirement 2.1** by preventing liquid and other contaminants from leaking into the enclosure. One weatherstrip seals the gap created by the angled roof edge and back wall while it is closed. Silicone Caulk was applied internally to each wall-to-wall interface to protect the system's internal components from large temperature gradients, dust, and moisture. Figure 32 indicates where these passive protection elements are used in cartoon-form for clarity. Finally, the sloped roof design described in the previous section prevents liquid from pooling or entering the closed system.

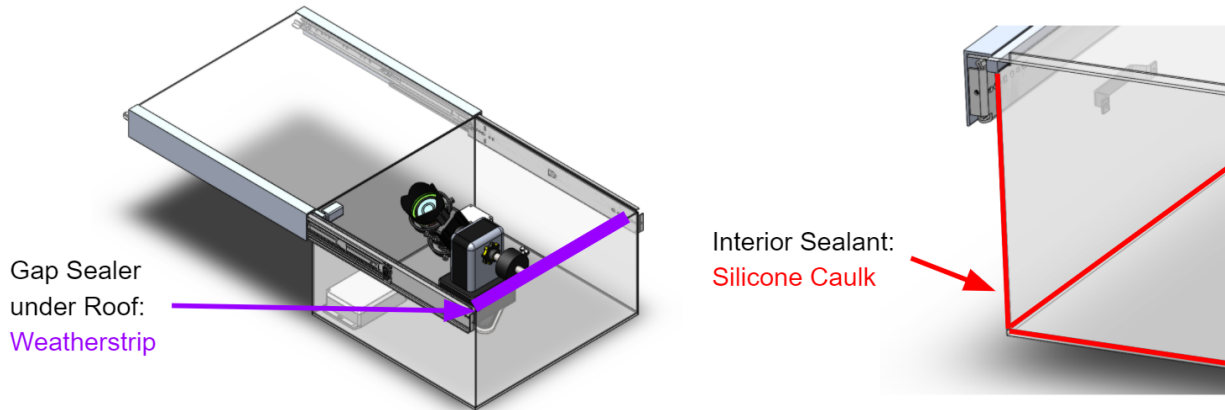


Fig. 32 Active Protection System Edge Protection

The third passive protection element within SHADE’s Active Protection System is the use of three Polycase COTS boxes to protect the processor and power distributor within the enclosure from adverse environmental and temperature conditions or humidity, which help to satisfy **Design Requirements 2.1 and 8.1**. Figure 33 shows the location of each component within the enclosure. The processor will be housed in the Polycase WC-24F, and the power distributor will be in the Polycase WC-31F.

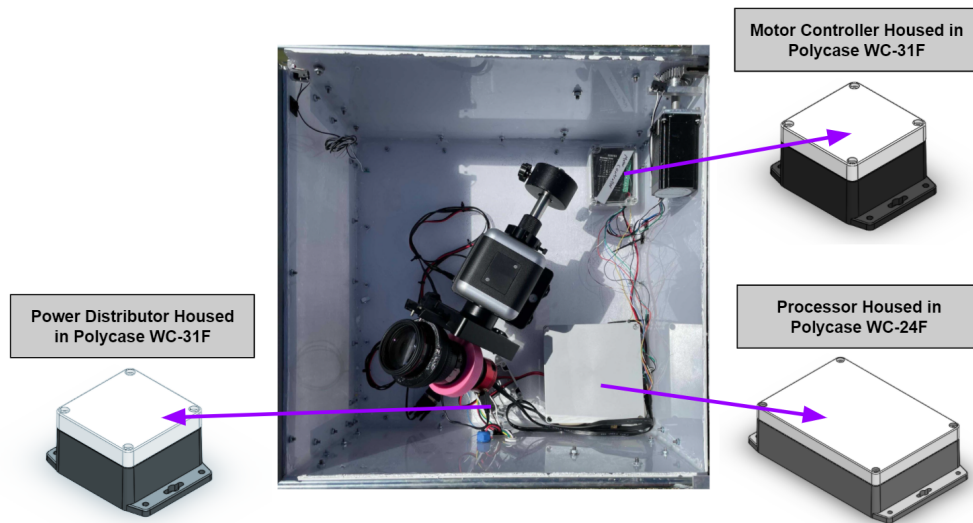


Fig. 33 Active Protection System Internal Component Protection

SHADE’s final passive protection element is the the use of weatherproof umbilical electrical connections. The umbilical ports shown in Figure 34 are weatherproof and enable the power module and environmental suite to be connected to the Active Protection System externally. These external ports are important because they enable the user to easily connect all SHADE modules together quickly and easily, rather than requiring the user to connect each individual electrical component in the Active protection system to each module separately. This passive protection element helps to satisfy **Design Requirements 2.1 and 7.2**.



Fig. 34 Active Protection System Umbilical Connections

5. Software

1. Overall Software FBD

Author: Quinton Dombrowski

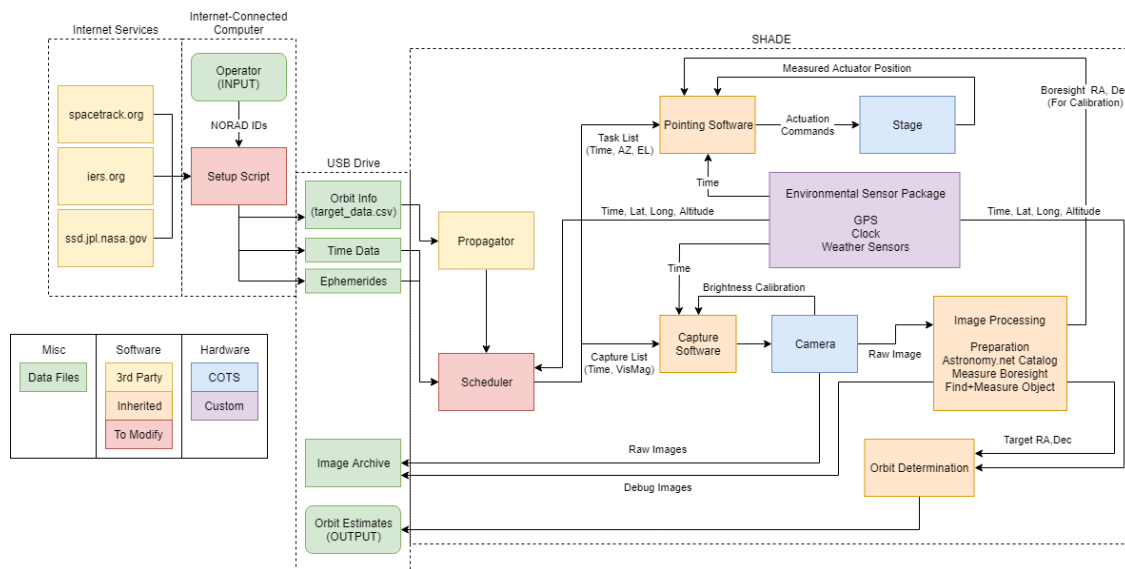


Fig. 35 Overall software functional block diagram, including (from left to right) required internet services, operator's computer, data transfer USB flash drive, and SHADE main computer.

2. Main Computer and Software Dependencies

Author: Quinton Dombrowski

The main computer for the SHADE system is a UDOO x86 II ULTRA single-board computer. The x86 CPU is running Arch Linux, which provides the filesystem and I/O controls used in hardware control and data handling. The on-board Arduino is connected to the main CPU via internal USB and serial, and runs code for actuation of the roof motors.

The operating system, all software (except the Arduino door controller software), and temporary files (such as images and astrometry results) are stored on the 32GB internal flash storage card. Operator inputs (output from the setup script) and system output data (such as logs, observation results and debug information) are stored on a USB flash drive, which is mounted to the Linux filesystem during startup.

The software developed by SHADE (except the Arduino door controller software) is written in Python, though with occasional use of BASH shell scripts. The Linux system will thus require the installation of the most recent Python interpreter, various third-party software dependencies, and third-party Python modules. A complete list of such dependencies is provided in Appendix, Section X.3.

Complete system setup (*SHADE Computer Setup*) and software installation guides (*SHADE Software Setup*) are provided, along with more detailed software documentation, but not included in this document.

3. Software Architecture

Author: Quinton Dombrowski

SHADE and its predecessors rely on a combination of both time-sensitive tasks (i.e. taking images, checking weather) and time-consuming tasks (orbit propagation, image processing, scheduling). As such, it was recognized early on that these tasks must be parallelized. Unfortunately, fundamental limitations of Python, namely the Global Interpreter Lock, prevent true multithreading within a single Python process. While the GHOST system used a pair of independent Python programs, SHADE makes use of Python's multiprocessing module.

At runtime (after the initial startup procedure has been completed) SHADE's software spawns four new processes, dedicated to execution of image sequences, image processing, scheduling/orbit determination, and weather/power system monitoring. Each of these runs independently as separate processes, preventing slow processes (like image processing) or even severe software faults on one process from causing problems in other processes. The data that must be shared between these processes is minimized, and contained within a single class dedicated to state data, which uses multiprocessing-safe data structures (namely Python proxy objects). When the system shuts down (either due to low power, or inactivity) a global flag is set that triggers each process to shutdown safely. Once complete, all state-related data is saved to disk using Python serialization, and the system exits. On the next resume, this state data can be read back from disk, and the system can resume where it left off.

A simplified visualization of the overall structure is provided in Figure 36. Consult the dedicated software documentation included with the source code and the source code itself for more information, such as state transition models, data types, etc.

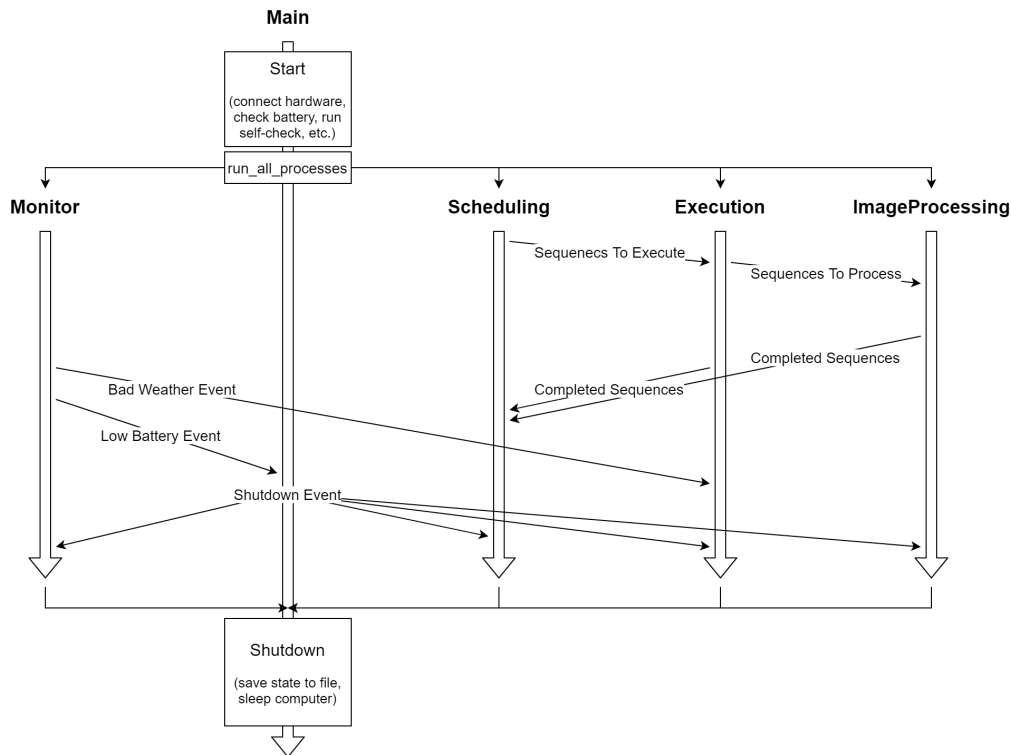


Fig. 36 Flow chart of software runtime architecture. Each large arrow represents a python process. Small arrows show important data passes between these processes as events of queues.

4. Startup Procedure and Data Handling

Author: Quinton Dombrowski

Simplified system startup is a key design consideration of FR 7. The nature of SHADE’s deployment requires that the system operate without an internet connection, and with minimal operator interaction at runtime.

The startup procedure will therefore be split into two portions. The first is a standalone Python script running on the operator’s desktop or laptop computer before deployment. The second involves the main computer, which will include reading the data from the setup script and starting the main software package.

Setup Script

This piece of software takes the form of a single Python script with minimal dependencies, and is intended to make the interfacing process easier for the operator by performing all internet-dependent tasks before deployment. An FBD of this script is outlined in Figure 72, Appendix section X.4.

The setup script’s responsibilities are to 1. parse the list of targets specified by the operator, along with their given priority (if any), 2. retrieve the most recent orbit information from spacetrack.org, using the spacetrack Python module, 3. get the most recent solar system ephemerides and time information using the skyfield Python module, and 4. save all this information in the appropriate format where the script is run (i.e. the operator’s USB flash drive). Running this script allows the system to alert the operator of any data formatting or acquisition problems before deployment, and save the data in a controlled format before being

loaded by the main SHADE software suite, thus minimizing the chance of data input problems at the time of deployment.

Startup Sequence

The second portion of the startup procedure involves the SHADE system itself, and is detailed in Figure 73, Appendix section X.4. During deployment, the operator connects the USB flash drive containing the data from the setup script to one of the SHADE computer's USB ports. When SHADE is powered on, it looks for this flash drive (in the form of an unmounted filesystem) and mount it to the main filesystem. The system then prompts the operator for input. If input is received, the system clears old temporary data and copies the input data from the flash drive, and starts the hardware initialization. This involves opening the door, and letting the operator give a coarse initial calibration. Once done, the stage begins a series of slews around its full range of motion, takes an image with the camera, and acquires a GPS lock. This process allows for the detection of any major hardware malfunctions while the operator is still present. Once this is complete, the operator may detach the monitor and let the system resume autonomously.

5. Scheduler

Author: Quinton Dombrowski, Davis Peirce

A critical piece of software for GHOST, WRAITH, and now SHADE is the scheduler. The scheduler is responsible for determining when to take images of each object, and is the main wrapper for all astronomy and astrodynamics aspects of SHADE (with the exception of orbit determination). This includes finding sunset and sunrise, propagation of target objects, determining the location of solar system bodies (i.e. sun and moon), assessing visibility of objects at a given time, and prioritizing the viewing of each target object.

While much of the scheduler is retained from previous projects, certain issues were addressed for SHADE. The longer deployments as specified by FR 8 mean that the stability of the orbit predictions for each object must be assessed, and greater priority given to those objects that may be difficult to find after a few days. Another change due to FR 8 is the requirement for the scheduler to run for multiple nights. Instead of having the scheduler run once, and plan observations over a timeframe specified by the operator, the scheduler must determine when the next night will occur. Furthermore, the scheduler must prioritize objects that have yet to be observed, by reviewing which objects were viewed on previous nights of the same deployment.

The new scheduler follows the flow chart in Figure 74, Appendix section X.4.

Several aspects of the legacy scheduler were changed to accommodate these new requirements. First, the old scheduler would classify objects into LEO, MEO, and GEO orbits based on their mean motion. Now, a HEO classification has been added with the criterion of an eccentricity greater than or equal to 0.65. The weighting system has been modified, with a boolean tracker in the spaceobject class monitoring whether or not the object has been imaged. If it has, its priority is reduced to $\frac{1}{4}$ of what it would have been. As for how the weight itself is determined, the system now considers whether or not the object is a HEO, offering increased priority if it is. Finally, the time scale has been modified to offer increased priority the older a TLE is, up until one week old. After one week, that TLE will be deprioritized.

6. Orbit Propagation

Author: Davis Peirce

In their critical design review, WRAITH has determined that TLEs are no longer usable in a matter of days due to errors in the TLE itself, the limited precision of the data format, and limitations of the SGP4 propagator. Using Systems Tool Kit (STK), they determined that orbit prediction quality will decay primarily as a function of orbit eccentricity, with lower eccentricities implying more drag on the model and thus decaying faster. For an extended deployment, this may prevent achievement of functional requirements 1, 2, and 8. Thus, it is important to verify WRAITH's results, and if they are valid, to modify or change the orbit propagation method accordingly such that requirements are met.

In order to do this, a third-party SGP4 propagator for MatLab was chosen in conjunction with historical satellite data. The satellite chosen was NOAA-6 from 01/03/1980 to 01/23/1980. This satellite was chosen since it was in a sun-synchronous orbit with a low eccentricity, which would indicate from WRAITH's results that the prediction quality would quickly decay. The time frame used was arbitrarily chosen. The TLE in the time frame was propagated forward to each other TLE in the time frame, and the position vectors were stored. These position vectors were used in conjunction with the dot product to estimate the angle between these predicted values and "true" values obtained by propagating for a time difference of zero.

$$\theta = \cos^{-1} \left(\frac{\vec{a} \cdot \vec{b}}{|\vec{a}| |\vec{b}|} \right) \quad (2)$$

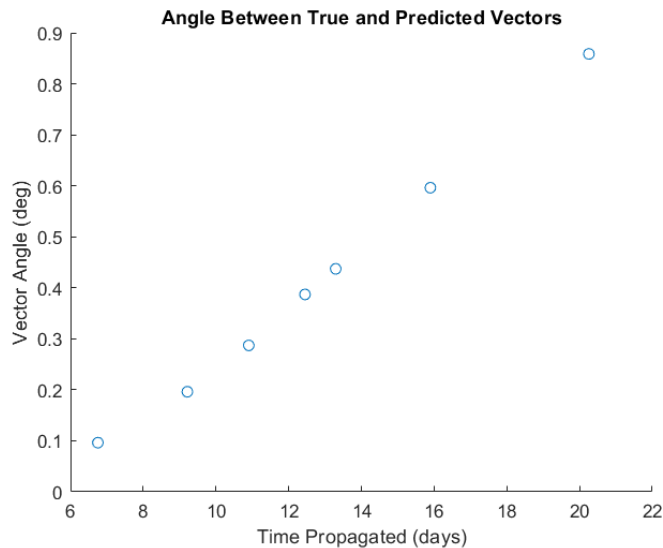


Fig. 37 Angular Error for NOAA-6 Using SGP4

For reference, SHADE's camera has a field of view of $5.22^{\circ} \times 3.95^{\circ}$. This graph shows that the error increases roughly linearly with respect to time, increasing to nearly a degree over three weeks. However, for this test case, the predicted error falls safely within SHADE's field of view.

However, this test case is not perfect. It's a single case for an object in LEO, and there may be cases where the error is large enough. Thus, a model for the error with respect to several key orbital parameters was developed. For this model, each TLE is propagated until the next TLE so that the true and predicted values can be compared over a shorter time span. This approach was chosen to reduce the effect of any errors in an

individual TLE. Next, the error is found between the true and predicted values and a linear fit is created by holding all but one orbital parameter constant and allowing that one to vary before taking the average of the linear fits for each parameter.

Inputs to the model included NOAA-6, NOAA-17, DMSP-F16, GOES-4, AO-10, and AO-13, which range from sun-synchronous orbits to GEO orbits to HEO orbits. Using this model, SHADE shall be able to predict the error for a chosen viewing and schedule objects with higher errors earlier in the deployment. When using this model to predict errors, inputs must be scaled according to the following equation:

$$\hat{x} = \frac{x - \bar{x}}{\sigma_x} \quad (3)$$

Where \bar{x} is the mean and σ_x is the standard deviation. This scaling factor is required due to a lack of variation within several of the chosen orbital parameters. This model, when fully implemented, did not provide meaningful predictions for the error. This is likely due to the averaging approach not being a good approximation when comparing different types of orbits. However, this model was still useful in that it confirmed that time and eccentricity are the most important parameters for estimating the error of an orbit. Future work may involve the implementation of models for different types of orbits to avoid this error. Thus, the weighting system involving time was modified so that orbits with increased eccentricity will have increased priority.

7. Image Processing

Author: Quinton Dombrowski

The image processing software in SHADE is used to identify a streak created by a target object. Testing of the legacy image processing revealed significant shortcomings, mainly a propensity to identify a streak either in the wrong location, or when no valid streak exists. This is a particular issue in terms of risk mitigation, as accurate image processing is necessary for FR 5 and 6. As such, this streak detection system was revisited by SHADE.

The new image processor uses a series of pre-processing steps followed by a Hough transform, which detects all linear features in the image. These lines correspond to streaks or part of streaks. Parallel, adjacent streaks are combined to produce a set of all complete streaks in the image. Using an astrometric calibration of this image, the previous orbit estimate can be used to produce a predicted streak shape. This expected shape can then be matched to the streaks extracted from the image to determine which, if any is most likely to correspond to the target object. The endpoints (or single endpoint, if only a partial streak was extracted) can then be used (along with the astrometric calibration and time information of the image) to determine precise time and location information of the object for orbit propagation.

8. Automatic Calibration

Author: Quinton Dombrowski

The operator startup procedure outline above includes a coarse calibration of the pointing hardware at deployment. However, such a calibration is not sufficiently accurate, and must be refined.

Initial calibration will be performed at the beginning of the first night, and can be re-run at any subsequent

time (after dark) if the system invalidates the calibration. This procedure involves pointing the camera at arbitrary right-ascension and declination coordinates (with sufficiently high elevation) and taking a single image. Astrometric calibration can then be run on this image to determine the real camera bore sight. This real data is then fed back into the pointing hardware, which updates its internal pointing model. This procedure is repeated five times to give the pointing hardware an accurate model of its orientation.

One unimplemented feature that was considered in the initial design was a pre-image calibration correction. This would occur when there is sufficient time before an imaging sequence, and would involve taking an image at the location of the expected streak. This image could then undergo astrometric calibration, and the results fed back to the stage. This would ensure highly accurate pointing for the upcoming image sequence, even if the calibration in the pointing hardware contained some error.

Both the initial calibration procedure and pre-image correction are detailed in Figure 76 in Appendix section X.4.

IV. Manufacturing

1. Power System

Author: Jacob Weiner

The manufacturing of the solar panels proved both challenging and sometimes frustrating. The panels were each built from scratch using aluminum tubes, aluminum sheet metal and screws. The individual solar cells themselves were purchased from a retailer and they were soldered by the team into strings of five cells. The solar panels were all manufactured at the Ann & H.J. Smead Department of Aerospace Engineering Sciences Building with the help of the Aerospace Machine Shop staff

1. The Solar Panels

To build the individual solar panels, the team took the CAD measurements and used hand tools to measure lengths of tube and locate holes. The team decided to use this method rather than more accurate CNC machine work since it was decided that the increased accuracy was not worth the additional time it would have taken to produce each piece. This decision resulted in its own set of challenges however.

The biggest problem that SHADE encountered during the manufacturing process of the solar panels was the accumulation of compound errors resulting from the imprecise measurements. In some cases, the drill bit had wandered out of the center punch divot or the center punch divot may have been miss placed. After the holes were drilled, the team tapped the holes so that the back plates could be screwed into them for assembly. This was another challenge.

The back plates were slightly out of spec from what the team had ordered and as a result to not fit together perfectly. This highlighted the greatest oversight the power team had in their solar panel design - tolerance. There was zero acceptable tolerance built into the design of the parts and this was a massive oversight. As a result, the manufacturing of the solar



Fig. 38 Solar Panel Fitment Fix

panels became an arduous process. Holes had to be wallowed out and washers had to be put in place increasing the budget and weight of the panels. Other holes had to be meticulously measured individually to help limit the same kind of fitment errors.

2. The Heatsinks and Thermal Epoxy

The addition of heat sinks to the solar panel design was not difficult from a manufacturing perspective. The team prepared the surfaces for attachment and mixed the epoxy before applying a coat to the backside of the heatsink. With the heatsinks placed on the backplates, the solar panel sections were placed in the oven to cure.

After the cure was finished the team took the panels out of the oven to cool. Once cool, the team then gently tapped the heatsinks to ensure that they were adhered to the aluminum backplate. Several heatsinks fell off and the team had to re-sand and re-cure the backplates with a new coat of epoxy. This resulted in an increased usage of the first thermal epoxy.

However, upon arrival the team also noticed that the first epoxy was electrically conductive. This would have resulted in complete failure of the solar panels if it was used to adhere the PV cells to the aluminium back plates since the PV cells have electrical traces that run along the backside of each cell. A new thermal epoxy was ordered that was electrically insulating and could be cured at room temperature.

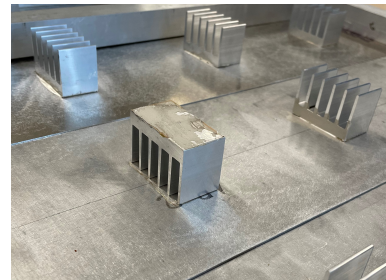


Fig. 39 Broken Heatsink

3. PV Cell Soldering and Adhesion

The soldering of the individual cells proved to be straight forward. The team first dabbed the contact pad with some flux, pre-tinned the dog-bone connectors and then applied heat to the backside of the dog-bone connector. This process made strong connections both physically and electrically. The first PV cell challenge came from aligning the cells with the backplates. The error from drilling and placing holes meant that the cells no longer fit onto a single backplate resulting in the heat sinks not lining up with the middle of the PV cells. During this process, there were also several "high spots" from the first layer of thermal epoxy. While the team members were gently pressing down on each cell to ensure good adhesion, a cell cracked. The electrical connections remained so the string had not been completely broken but it had become too difficult to correct given the budget and time constraints. Additionally, the team had to purchase extra epoxy after cross contamination between the resin and hardener rendered the first batch useless.

4. Power Module and Integration

The power module was the last item to be assembled. This was more of an integration problem than manufacturing. The final design of the power module required a jumper from the input and output terminals of the power conditioner. Since the power conditioner electrically isolates the upstream connection from the downstream connection, a floating ground was introduced. The main processor is required to interface with the charge controller which has a different ground reference and voltage than the main processor. To remedy this, a logic level converter was implemented to bring the 5 VDC signal down to 1.8 VDC (See Fig. 77). The 12.5 VDC power is carried along the same cable bundle into the active protection box. Inside is a COTS box

with all the terminations for the various electrical components of the system. They are all wired together with a wire nut and secured with a zip-tie.

While testing the power system, the COTS box that houses all of the components overheated. This was due to the box being made of black ABS plastic and the fact that the charge controller also produces heat. To maintain temperatures that would be within the operational envelope, the team added a vent and painted the box with the same thermal paint that was used in the active box. It is expected that the surface temperature would be reduced by as much as four degrees Celsius.

2. Active Protection Enclosure

Author: Marlin Jacobson

The Active Protection System manufacturing was a long but rewarding process. Its manufacturing process lends itself to four main parts: gathering materials, machining, assembly, and modification. This section will describe each step in detail to portray the overall manufacturing process of the system.

1. Gathering Materials

The Active Protection System is comprised of the enclosure components, including the polycarbonate walls, aluminum rail guards, stainless steel roof sliders, leveling feet, handles, weatherstrip, nuts, bolts, screws, and gear rack, as well as the internal components, including the COTs polycase boxes and stepper motor. Components that were bought off-the-shelf are the COTs boxes, leveling feet, roof rail guards, and handles. Polycarbonate sheets of the required wall, floor, and roof dimensions were bought and pre-cut; however, these sheets were modified slightly and painted. Additionally, various legacy components were reused, including the stepper motor, Accuride roof sliders, gear rack, and the weatherstrip. Once all materials were bought and gathered, the manufacturing machining process began.

2. Machining

The machining process took place at the Aerospace Building in the Project Space and Machine Shop. The aluminum rail guards required the most machining out of any other Active Protection System part. Other items that required machining were the polycarbonate walls, pre-cut roof corner guards, and the gear rack.

The side aluminum corner guards were all machined and cut from the same two right-angled bars in the Machine Shop. The corner guard CAD drawings with dimensions were used to guide this process. The horizontal band saw was used to cut each guard from the full bar, and the vertical band saw was implemented to cut parts of the floor corner guards at 45° angles. After all guards were cut to their correct lengths and angles, a metal file was used for deburring. Lastly, a power drill was used to pre-drill all of the holes required for assembly. The team decided to pre-drill the holes because it helped ease the guard-to-polycarbonate assembly process.

Next, in the project space, holes were drilled into the polycarbonate walls using the dimensions in the CAD part drawings. This step was done to ensure proper assembly of the enclosure. Holes were drilled along the edges of each wall and on the roof. The wall holes were drilled for the corner guards and Accuride roof sliders, and the roof holes were made for the roof corner guards and gear rack. Although the system should ideally be symmetric, walls were labeled with designated locations and corner guard groupings to ensure the

enclosure fit together correctly during assembly.

The final part of the enclosure that was machined was the roof gear rack. This part is a legacy item from WRAITH, so it needed to be modified to fit SHADE's new system. Holes were drilled and threaded into the rack to be assembled to the roof using the power drill and threading materials from the Machine Shop. All holes were drilled to speed up the assembly process. Once all materials were machined, the assembly process began.

3. Assembly

The Active Protection System assembly process occurred at one of the team members' houses near the Aerospace Building. Before the final assembly of the enclosure, each drilled and precut polycarbonate wall was painted using the white Cool Coat thermal paint, paint rollers, and brushes. Only the external sides of the polycarbonate walls were painted, and two layers were applied to each wall. Once the paint dried, basic tools including nuts, bolts, screws, screw drivers, power drills, and Allen keys were used to assemble the enclosure.

4. Modification

The Active Protection System modification process also took place at the house, and it covers the steps required to integrate the enclosure with all other system modules. First, using a hole saw and power drill, a hole at the center of the box was drilled for venting and drainage purposes to ensure moisture would not build up inside of the system. The two umbilical chord holes were also drilled, shown in Figure 34, to allow the power and environmental suite modules to be connected. The silicone caulk was then applied to the internal edges and corners of the enclosure using a caulk gun to protect the system from external contaminants or moisture.

Small aluminum square stands were added to the system near the gear rack in order to attach the limit switches correctly. Finally, using adhesive foam strips, a mold was created on the bottom of the enclosure to fit the footprint of the iOptron mount to ease user setup. Small holes for wiring and connections between electronic components were drilled into the COTs Polycase boxes, and wires were organized within the system using clips and fasteners on the polycarbonate walls.

5. Summary

Many challenges were faced by the team throughout the Active Protection Enclosure manufacturing process. While these challenges were sometimes frustrating and time consuming, the team worked together to find a solutions to each problem. The first challenge faced was caused by the machining process of the corner guards and polycarbonate walls. As described previously, holes were drilled separately into the guards and walls to aid in the assembly process. Although this step was taken to facilitate assembly, every hole was drilled by hand. Each hole was inherently inexact and differed slightly from the CAD drawings. During assembly, the group realized that many of the guard and wall holes did not line up correctly, which made it impossible to fasten the enclosure together correctly. This challenge caused the group to have to re-drill or enlarge many of the holes already drilled in the polycarbonate. Although this challenge caused delays in assembly, the group was able to efficiently fix the issue. All exposed unused holes were filled in to ensure the system remained protected. A lesson learned from this challenge is that it is important to focus on dimension tolerances and account for them during manufacturing. Due to the manual use of hand tools during machining,

it was difficult to impossible to account for tolerances with such small holes. In the future, the team should consider using automated machines for drilling and cutting parts.

The second challenge was gear rack, motor, and roof connection process. This issue was also a result of the imperfections in the design caused during machining because everything was machined and built by hand. The design of the slanted roof required the gear rack to be angled off of the roof ceiling and parallel to the tops of the walls. The rack must be flat to maintain a connection with the stepper motor as the slanted roof moves. While drawings were made to account for this design, implementing it was difficult. Varying screw sizes and methods used to hold each screw in place were required to properly hang the rack at an angle from the roof. Fine tuning of the angle that the rack made with the roof was required to keep it in contact with the motor gear at all times. This challenge was frustrating and, at times, concerning because a failure of the roof design meant mission failure. The team was able to get the roof working through teamwork. A major lesson learned is that it is vital to consider even the smallest of measurements when designing a system for production.

V. Verification and Validation

In order to validate the SHADE system, the design was verified against various predictive models through a series of tests. SHADE's testing was broken down into two preliminary categories; Component testing and Full System testing. The purpose of the Component testing was to verify that the individual project elements are functioning properly before the system is tested as a whole. The Component testing was further broken down into SHADE's critical project elements; Power, Active Protection, Weather Detection and Software. Individual tests, specific to each element, were developed to validate each component and verify its related requirements.

1. Component Testing

Power Tests

Authors: Katherine Nyland, Robert Redfern, Jacob Weiner

1. Battery Duration

Test Design:

In order to verify that a fully charged LiFeP04 battery can power the SHADE system for a full night, the team performed a battery duration assessment. This test monitored the battery voltage and capacity over a duration of 12 hours, through the use of a battery cycle tester (purchased by WRAITH). To test the worst case scenario, a discharge of 55.12 Ah was used to derive the test current from the following equation:

$$I = \frac{\text{discharge}}{\text{duration}} = \frac{55.12Ah}{12hrs} \quad (4)$$

Resulting in a current of 4.61 A. With this current, the fully charged LiFeP04 was attached to the load and the voltage was recorded over the course of the 12 hour testing window. The rate of change of capacity was determined to verify that the battery will be capable of powering SHADE for a full night of deployment.

This test was conducted with the battery initially at a full charge. Then the battery load tester drew

a current of five amps over an eight hour period at room temperature and a four hour period at a colder temperature. The battery voltage was monitored using the PowerSonic iPhone application that gave real time battery temperature, voltage and current draw. Measurements of temperature and battery voltage were taken during the course of the test to allow analysis of the discharge curve.

The expected results of this test were that the variation of the voltage would match the discharge curve provided by the supplier. This test was designed to permit more accurate mission planning and scheduling through empirical knowledge of the discharge curve. As well as to increase the confidence that the battery will last a full 12 hour observation period (DR 2.2).

Test Results: Complete

This test was designed to validate Functional Requirement 8. Due to time constraints, the test was only conducted for eight hours at room temperature and 4.5 hours at 10°F. However, it still validates the battery performance since the region in which SHADE can safely operate has a linear relationship between the battery voltage and percent capacity.

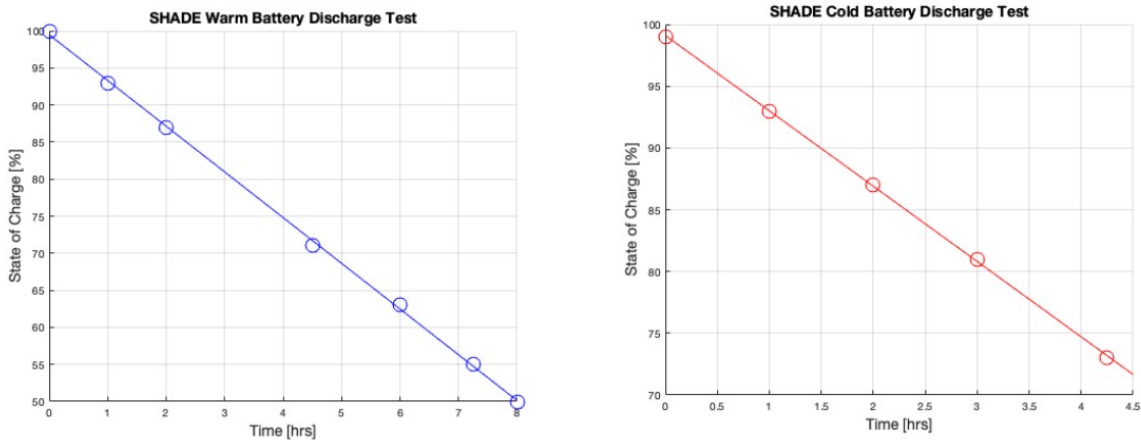


Fig. 40 Battery Discharge Percentage vs Time

2. Low-Power Shutdown

Test Design:

To ensure that insufficient power would not result in sensitive components being exposed to the elements, SHADE needed to be able to safely stow itself until the battery regains enough charge to continue deployment. Utilizing the Victron Connect iPhone application, the test involved using a battery load tester to place a dummy load on the power system to temporarily cause a measurable decrease in the battery voltage. The power module was connected to the active protection box and the battery load tester was powered by the same electrical connection that the camera mount uses. After a voltage drop of about 0.5 V was recorded for a five amp dummy load, the UDOO was reprogrammed with the new cutoff voltage to simulate the process should the battery actually have a low state of charge.

Test Results: Complete The charge controller read the battery voltage as 13.27 V and the low power shutdown threshold was set to 13.2 V. Using the battery load tester, an artificial five amp load was placed on the system decreasing the battery voltage to 13.17 V. SHADE was successfully able to read the change in voltage from the serial connection to the charge controller, identify that it was less than the low power threshold value,

close the lid of the active box and enter a lower power mode. While 13.2 V is by no means a critically low battery, it validated the systems logic and ensure that low power shut down process was functional. After the test, the low voltage condition was reset to 11.5 V for future use.

3. Solar Panel Connection Test

Test Design:

In order to assess that the individual solar cells were adequately connected before use in the final product, a multimeter was be used to measure the voltage output of each five-cell segment. If there was an appreciable voltage potential, the segment was deemed satisfactory and production continued with the next segment.

Test Results: Complete

This test was performed several times during the construction of the solar panels. After each five cell segment was soldered and at the end of each solar panel construction. During this process, the team was able to ensure that each string had a proper electrical connection. At the same time, the team also measured the voltage output of each cell in indoor conditions. The nominal string voltage was 2.5 VDC. Some strings had a slightly lower reading at 1.9 VDC and may have contributed to a worse than expected overall performance. For the string that did have a lower voltage reading, the team inspected each segment and could not find any noticeable flaws in the soldering or solar cell.

4. Solar Charging Test

Test Design:

In order to assess that the solar panels are properly functioning and have been manufactured correctly, the team performed a solar charging test. This test was executed using both real and artificial sunlight. To ensure the accuracy of the panels' charging capabilities, the experimental charge values for both cases were compared to their corresponding theoretical models provided by the manufacturer. Additionally, this assessment was used to verify that the off-the-shelf charger was performing properly.

This test was conducted outside on a clear sunny day, using the solar panels, a multimeter and the VictronConnect iPhone app. The test was started with the battery at 70% capacity. The multimeter and VictronConnect were used to record power generation and battery voltage throughout deployment.

The expected results of this test were that the theoretical and experimental power generation and open-circuit voltage would closely match and that the solar cells would not short. This test was designed to ensure that the system has a continual power source and was able to perform on days without clouds. Additionally, it was designed to ensure that the solar cells do not make contact with the back plate, resulting in a short.

Test Results: Complete

The solar charging test was conducted on April 2nd, 2021 from 12:30pm MDT to 3:00pm MDT, a mostly sunny day with an average solar irradiance value of 941 W/m^2 and an average ambient temperature of $21 \text{ }^\circ\text{C}$. The battery was charged from 70% to 100% capacity by the end of the testing period and the results showed that the max solar power provided was 199 W. This was well off the expected result of 250 W which was determined to be caused by damaged PV cells during manufacturing. From these results, the initial steady state model was modified with an efficiency factor of 73% and shown in Figure 41 is the energy that can be collected in its current configuration based on 2019 data.

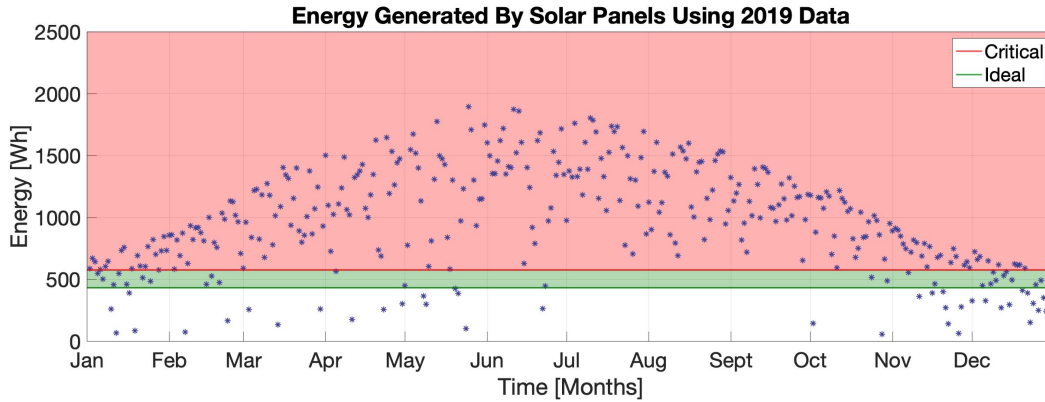


Fig. 41 Energy Collected By Solar Panels Based off 2019 Solar Irradiance Data

The green region and above, also known as ideal situations, represents a best case scenario where SHADE can recharge the day after a single night deployment and have enough remaining charge for a full second night of imaging. The red region, called critical situations, represents day that SHADE can recharge from a critically depleted battery and still have enough reserve energy to power another full night of imaging. Based off of 2019 weather data, 88.36% of the days in the year are ideal situations while 80.96% of the days are critical situations. This test satisfies Functional Requirements 2, 4, 7 and 8.

5. Thermal Solar Cell Test

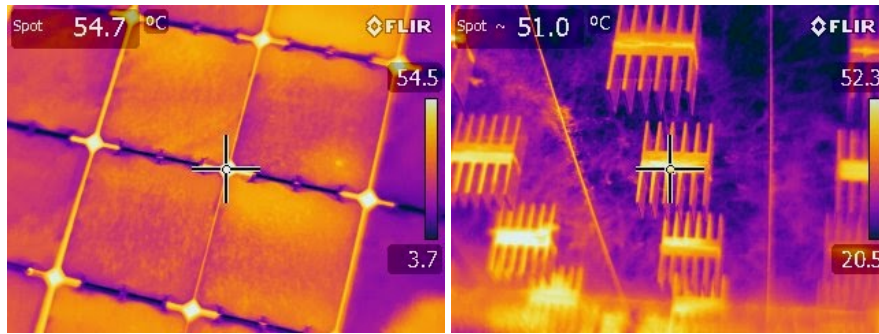
Test Design:

Simultaneous to the Solar Charging test, an assessment was run to conduct a thermal analysis on the individual solar cells and the effectiveness of the coupled heat sinks. This assessment used a thermal imaging system to measure the temperature gradient on a sample of solar sells with and without heat sinks.

This test was conducted in an open outdoor space, using the solar cells, and IR Camera and an ambient temperature sensor. The open circuit voltage of the test pieces was recorded prior to the test. Then the ambient and solar cell temperatures were recorded at 30 minute intervals. The IR camera was used to capture heat sink and solar cell face temperatures. At the end of the test, the open circuit voltage was again recorded. Finally a SolidWorks model was built using the test day's data to ultimately compare to the empirical data.

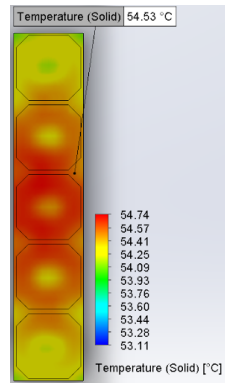
The expected results of this test were that the solar segments with heat sinks would be observed to be at a lower temperature compared to those without heat sinks. Additionally, it was expected that the IR camera temperature contours would match similarly with the model developed in SolidWorks. This test was designed to mitigate the risk of failure to fully recharge the battery after a full night deployment.

Test Results: Complete

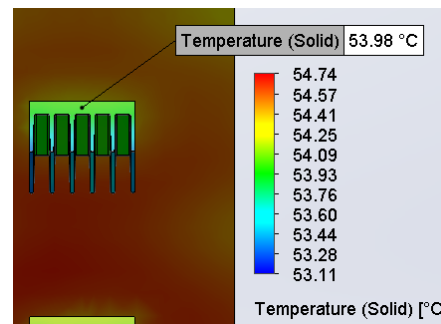


(a) IR of Backplate

(b) IR of Heat Sinks



(c) Simulation of Backplate



(d) Simulation of Heat Sinks

Fig. 42 Thermal Test and Simulation Images

The model that this test was designed to validate was the SolidWorks Flow Simulation Model, which simulated the steady-state thermal solution of a solar panel segment at prescribed conditions. Once this simulation is complete, temperature contours over the entire segment are generated. Other initial conditions and output can be drawn from the simulation, but for this case, temperature was the main analytical focus.

Figure 42 displays the results of an April 2nd test conducted in Boulder from 12:30 - 3:00 PM. The IR images represent the experimental data and the SolidWorks images represent the simulated data. These figures also display the temperature spots as well as the range of temperatures on the back plate and heat sinks.

As seen in figures 42a and 42c, the backplate has an experimental temperature of 54.7°C and a simulated temperature of 54.53°C. This difference in temperature is less than one degree. Thus, this indicates that since the temperatures are relatively close to being equal, the simulation could be considered accurate.

Yet, as seen in figures 42b and 42d, the experimental and simulated heat sink temperatures differ more than the backplate. The experimental temperature of 51°C is approximately three degrees less than the simulated value of 53.98°C. The reasons for this discrepancy vary, but the most reasonable answer would be the ideal nature of the simulation. Gusts of wind, which would cause forced convection, is not accounted for. Since the heat sinks have a high surface area, gusts of wind would cool the heat sinks faster.

While the heat sink discrepancy is notable, the main concern for the thermal test would be the backplate temperature, as solar cell temperature matches closely with the backplate. This means that losses due to temperature would match with the backplate. Thus, the test validates the thermal model. This means

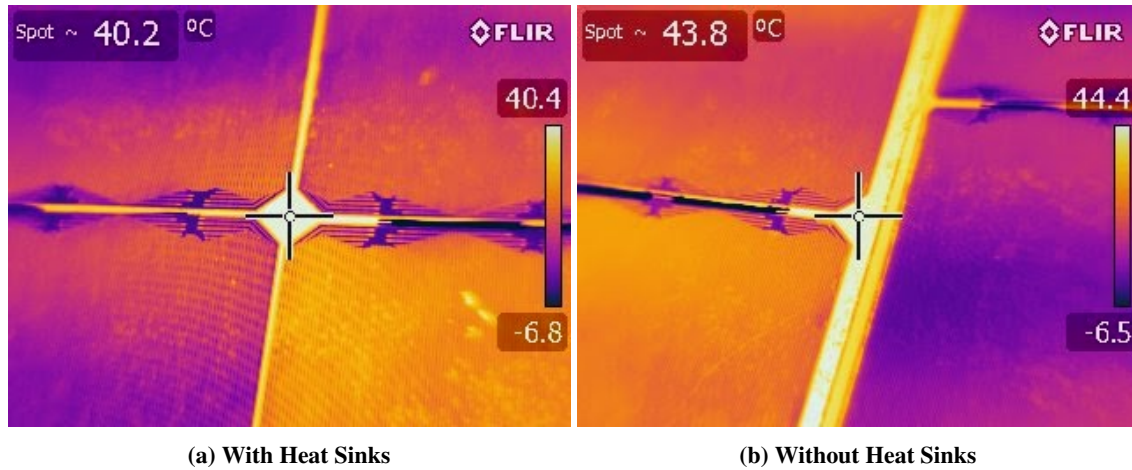


Fig. 43 IR images of Heat Sink Effectiveness

that the thermal model could be used to analyze performance with different conditions, allowing for the characterization of solar panel working conditions.

Figure 43 shows results of a deployment two different solar panel segments, one with heat sinks and one without. Notably, the temperature of the segment with the heat sink is lower than the segment without, whose temperatures are 40.2°C and 43.8°C respectively. While both panels will see efficiency losses, this difference of 3.6°C would make the solar panel with the heat sink produce more power than the panel with no heat sink by approximately 1.82%. The values were calculated utilizing coefficients from the solar cell manufacturer. Thus, this validates the design choice of having heat sinks on the panel.

This test was designed to satisfy Functional Requirements 2 and 8.

Active Protection Tests

Authors: Marlin Jacobson

6. Thermal

Test Design:

The first test conducted for the Active Protection System was its thermal test. This test was performed to validate the accuracy of its thermal model in order to further predict worst case scenario temperatures and to ensure that all components remained within their thermal limits for the duration of the mission. This test satisfies **Functional Requirement 2**, which states that the system shall operate in standard operating conditions for a least two nights by itself.

The materials used for this assessment were the empty active protection enclosure, an forward-looking infrared (FLIR) camera temperature sensor, a barometric sensor and a pyrheliometer. The steps followed to conduct the thermal test began with the enclosure's setup. First, the active protection enclosure was placed in an outdoor location with the roof open. After one hour, the roof was closed and the temperature of the hot and cold side walls, apparent solar flux, and ambient pressure were recorded. At the beginning of each hour for three total hours, these measurements were recorded again. After the physical test was finished, the initial

temperature parameters recorded were input to the Solidworks thermal model and rerun. The thermal model results were then compared to the physical test results to determine the accuracy of the model.

Before the test, it was expected that the thermal model would provide similar wall temperature results to the experimental thermal test after three hours. Additionally, it was expected that the physical results would validate the thermal model and, therefore, enable the team to predict other temperature scenarios using the model. Overall, this test was designed to mitigate the risk of extreme temperatures prohibiting component functionality.

Test Results: Complete

Figure 44 presents the results recorded during the physical thermal test. The blue and red lines plot the wall temperatures over time, the green line plot the ambient temperature, and the yellow line plots the solar flux recorded. From the graph, it is apparent that the Active Protection System wall temperatures are largely driven by the solar flux into them; therefore, as flux decreases, the temperatures at the walls also decrease. It is also important to note that, while they follow the same trends, the shaded (cold) wall is warmer than the sunny (hot) side wall. This trend may have been caused by the placement of the enclosure during test setup. The enclosure was set up near a house. The sunny side was open to the environment, and the shaded side faced the house. This setup may have actually cause more heating on the shaded side due to the radiant heat from the house onto the enclosure and less forced convection in the more enclosed area. On the sunny side, temperature may have been lower because this side was more open to the environment, allowing for greater forced convection and, therefore, cooler temperatures on the face.

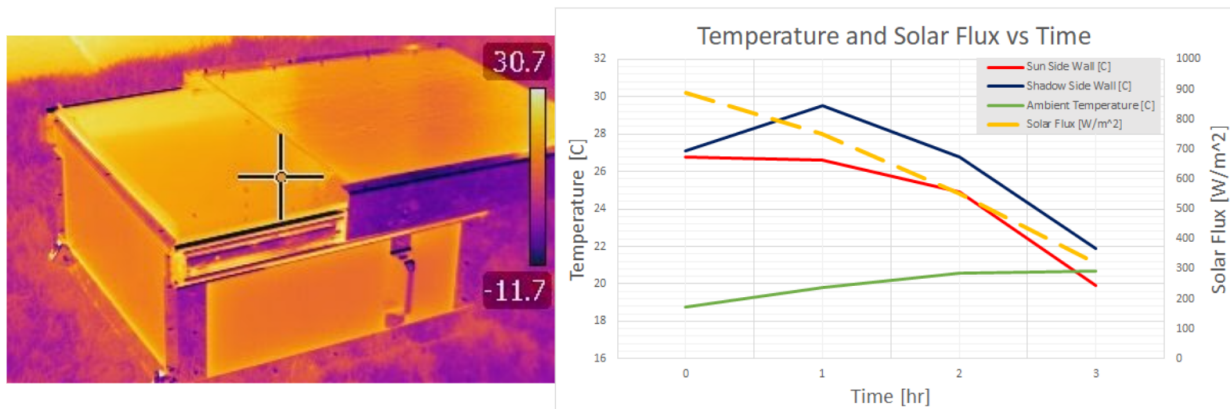


Fig. 44 Thermal Test Results

The recorded initial temperatures from the test were then input to the thermal model for comparison. Figure 45 illustrates the thermal model test setup implemented in Solidworks. It is important to note that the solar flux applied in the model does not vary with time. The final test hour's solar flux value was used in the model due to constraints using the Solidworks program. When testing this model with the greater flux values, temperatures were much greater than those recorded in the physical test.

Test Setup:

- Solar flux on roof and wall:
 $G_{\text{absorb}} = G_{\text{solar}} \cdot \alpha = 96 \text{ W/m}^2$
- 18.8°C ambient air.
- 26.9°C initial structure temperature.
- Natural convection (BTU/hr/ft²/F):
 $h_{\text{Horizontal}} = 0.5459$
 $h_{\text{Vertical}} = 0.4403$
- Internal and external radiation.
- $\Delta\text{Time} = 3 \text{ hrs}$

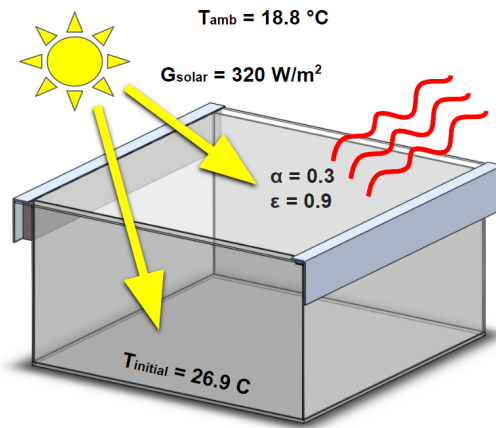


Fig. 45 Thermal Model Setup with Test Inputs

Figure 46 compares the results of the thermal model using the test inputs to the actual thermal test performed. As shown in the images, the model predicted a maximum temperature of 41.7 degrees Celsius, while the thermal test provided a max of 26.6 degrees Celsius. Moreover, the model maximum wall temperature is about 15 degrees greater than the physical result. After an investigation into the causes of this discrepancy, the team concluded that the largest source of error is most likely the fact that forced convection was not modeled in the thermal analysis. Only natural convection was modeled on structure surfaces. During the real test, there was a small breeze, which can remove heat and greatly affect temperatures felt on the structure. While there are not ideal and large discrepancies between the test and model, the comparison indicates that the model over predicts temperatures and shows that it is conservative.

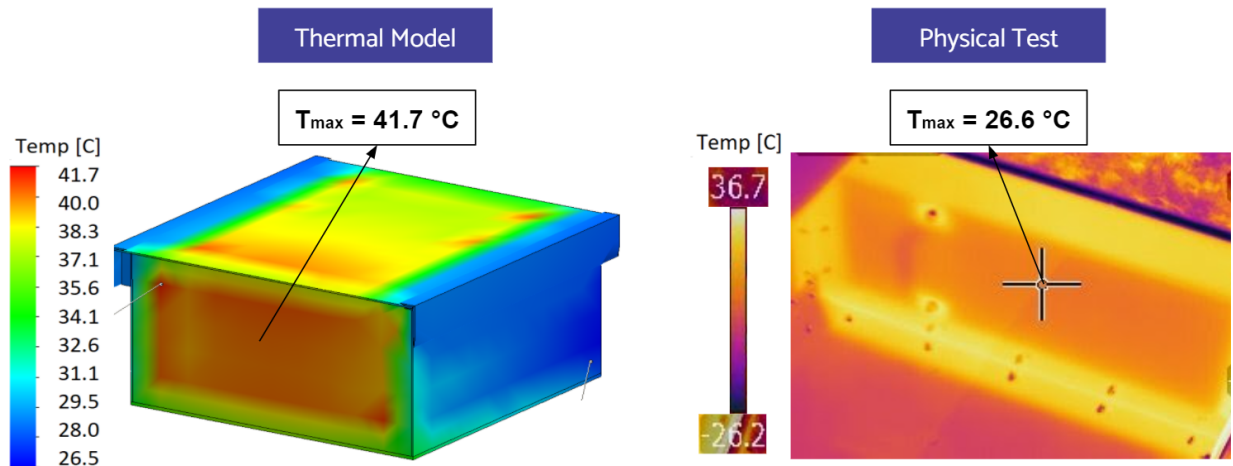


Fig. 46 Thermal Model-Test Comparison

Using the results of the thermal model and test, the team confident that the system will remain within its thermal limits, even in a worst-case hot scenario. Figure 47 presents the thermal model setup and results of a worst case hot scenario. The greatest solar flux measured in Denver, CO during the year was applied to all sides of the enclosure except for the bottom, and a hot summer environment was modeled externally. Even using this overly conservative, worst-case hot setup, the enclosure components remain within their thermal

limits. The group, therefore, is confident that the Active Protection System and internal components will remain within all material limits for the duration of its mission.

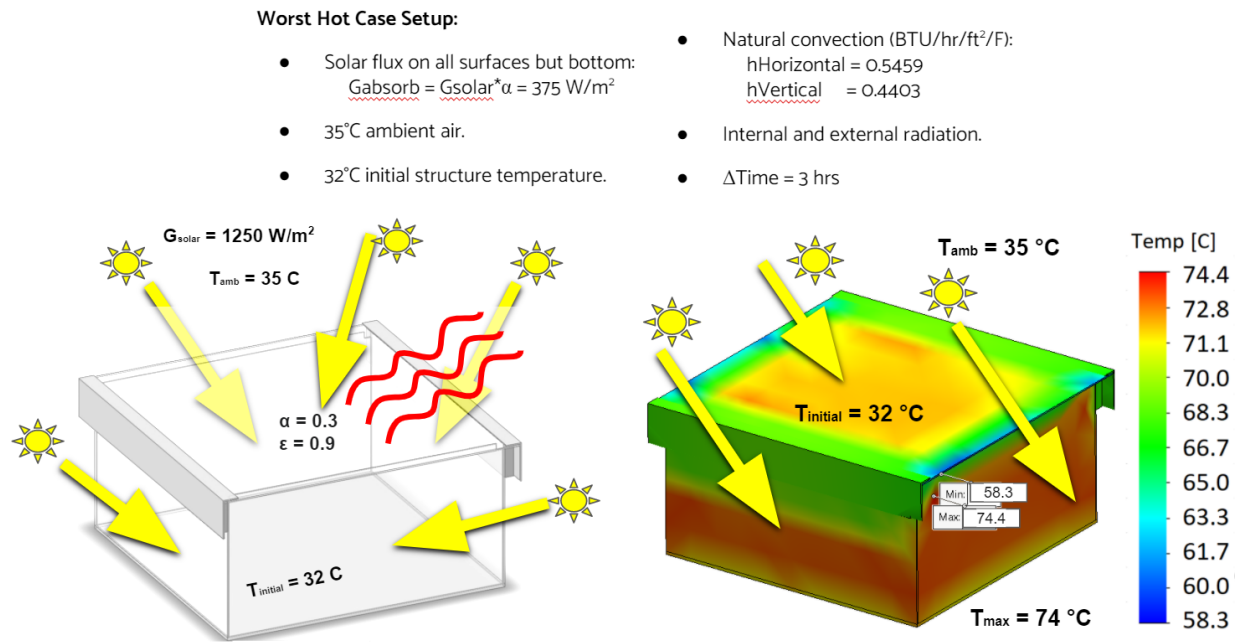


Fig. 47 Thermal Model Hot Case

7. Structural

Test Design: In order to ensure that the Active Protection System Enclosure can handle possible high loading scenarios without breaking, two different tests were conducted. The first test verified that the polycarbonate floor would not sag due to the applied load of the camera and camera mount. The second test was a tip-over test to validate SHADE’s ability to withstand a high load on its open lid and to verify that the system would tip over before breaking. This test also satisfies **Functional Requirement 2** and mitigates risks of mission failure caused by a broken roof. The most likely cause of such a failure would be a small animal interfering with the lid.

The materials required for this test included the active protection system with weights inside to model the hardware and increments of known weights to apply to the roof. Based on the tipping model shown in Figure 48, it was expected that the system would withstand 26 lbs on the end of its open roof before tipping over and that the system would tip rather than breaking the roof. To perform this test, small 2.5 lb weights were incrementally to the edge of the open roof until the system began to tip.

Determine max allowable moment at fulcrum before box tips over

$$CG_{total} = \frac{W_{lid}d_{lid} + W_{box}d_{box} + W_{hardware}d_{hardware}}{W_{lid} + W_{box} + W_{hardware}} = 9.095 \text{ in}$$

$$\Sigma M_{fulcrum} = L_{max,tip}d_{max,tip} - W_{total}CG_{total} = 0$$

$$L_{max,tip} = \frac{W_{total}CG_{total}}{d_{max,tip}} = 25.7 \text{ lbf}$$

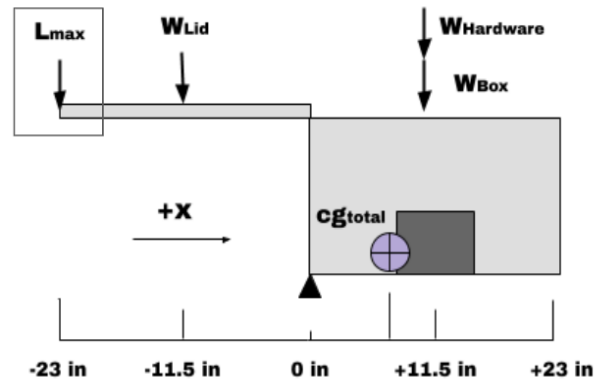


Fig. 48 Tipping Model

Test Results: Complete

The results of both tests were definitive. For the first test, it was apparent that the bottom of the enclosure did not sag in any appreciable way. The tip-test resulted in 26 lbs causing the system to tip and not break. Considering the predicted tipping load was 25.7 lbs, the group is confident to say that the model accurately predicts this maximum tipping load. Figure 49 presents this tip test. Overall, the fully-set up active protection system can withstand about 26 lbs on the edge of its open roof before tipping over, and the system will tip over before breaking.



Fig. 49 Tip-Over Test Results

8. Lid Actuation

Test Design:

The final Active Protection System test performed was the lid actuation and motor test. It was completed to verify the successful operation of the motor, gear system, and limit switches on the roof. Additionally, it served to verify that the lid was able to open and close in 10 seconds, a success criteria imposed by WRAITH. Figure 50 presents the roof velocity model and indicates that it should open or close within 10 seconds.

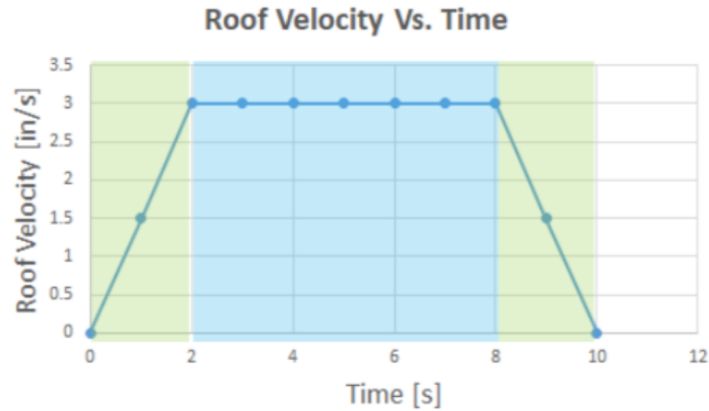


Fig. 50 Roof Velocity vs Time Model

The proper functionality of the lid actuation is crucial, as it is the main aspect of the active weather shielding, protecting the sensitive components from adverse weather conditions (DR 3.1). The test, therefore, helps to satisfy **Functional Requirement 3**, which states that the system shall autonomously enter and exit a safe mode to protect itself from adverse weather conditions. This test was designed to mitigate the risk of quickly developing precipitation causing system damage as the result of untimely roof actuation. The materials needed for this test were the Active Protection Enclosure, UDOO processor, motor controller, roof motor, limit switches, and the battery.

Test Results: Complete

Through the lid actuation and motor test, the group validated the reliability and success of the roof stepper motor. The test showed that motor is able to fully open or close the Active Protection System roof in 10 seconds. Additionally, the results of this test meet WRAITH’s legacy design point. Figure 51 plots the motor manufacturer’s data of the applied motor torque versus gear speed. The green dot is WRAITH’s design point, which indicates that a speed of 30 RPM is required at 141 oz of torque to close the roof in 10 seconds. Overall, the results of the lid actuation test indicate that SHADE is able to meet this design point, verifying the functionality and reliability of the motor.

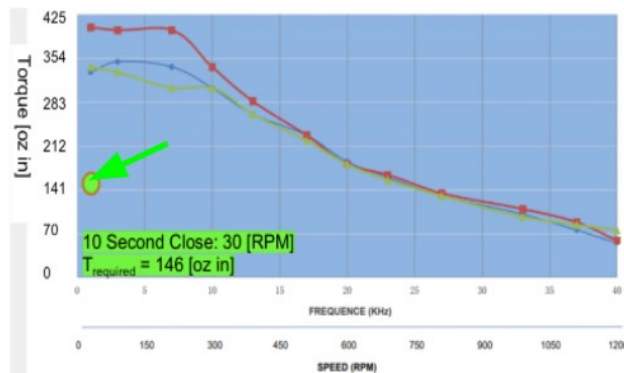


Fig. 51 Lid Actuation Design Point

Weather Detection Tests

Authors: Katherine Nyland

Test Design:

Functional Requirement 3 defines SHADEs autonomous weather protection, which has been addressed through the Weather Detection module. An assessment of the functionality of the individual sensors was conducted by WRAITH. However, in order to assess the functionality of the Weather Detection module as a whole, a full system weather detection test was conducted. The purpose of this test is to ensure each weather shutdown case triggers the appropriate signals, in turn telling the system to enter or exit safe mode.

The test was conducted in an open air environment with a clear view of the sky. For this test, only the Weather Detection module, the battery and a computer were used. The Weather Detection module is powered by the battery, negating the need of a wall outlet. A laptop monitored the serial output from the Electron micro-controller via USB. The execution of this test took place on multiple nights with varying weather conditions. The success of the test is assessed by observation and inspection. Concurrent to the analysis of the sensor data streams, a team member periodically made qualitative observations of the weather conditions. Based on their observations, the team member concluded whether or not they believe SHADE should have been in safe mode. These qualitative observations were directly compared to the data logged by the weather detection sensors and the decision made by the Electron as to the safety of the weather. This decision made by the Electron used the safe mode trigger conditions, seen below:

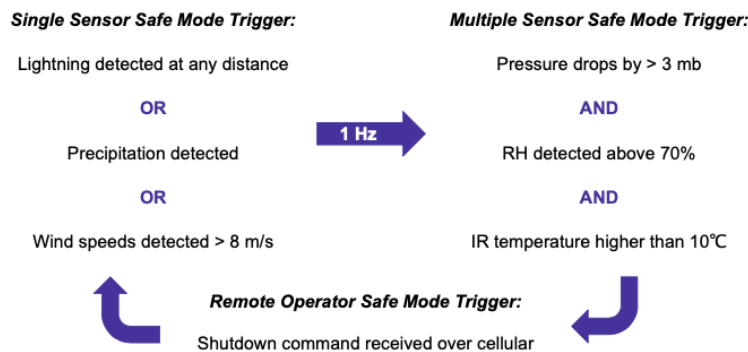


Fig. 52 Safe Mode Trigger Conditions

If both the operator and the safe mode trigger conditions reach the same conclusion, the results will be deemed satisfactory.

Test Results: Complete

This test was designed to satisfy Functional Requirement 3. This test was completed in tandem with other attempts at completing imaging sequences. With the serial monitor open, the raw data outputs from the Electron were monitored along with the Electron's decision as to the safety of the weather. As was noted by WRAITH in their assessment of the various sensors, the IR thermometer, barometer, and relative humidity sensor displayed a delayed transient response at the beginning of the tests. It appears that the sensors took approximately ten minutes to acclimate to the outdoor environment after being brought outside from a warmer indoor environment. Because the expected deployment time for SHADE is during the day, this will allow ample time for sensor equalisation to occur prior to observations, thus the nominal operation is not affected and FR 3 was validated and compliance was verified.

Software

Authors: Katherine Nyland, Quinton Dombrowski, Davis Peirce

9. Week-Long Dynamic Scheduling

Test Design:

The scheduler was designed to only run for a single night. However it must consider previously collected data and orbit stability in subsequent nights. In order to verify this, the scheduler was run on the same target set, with varying amounts of existing data. This existing data would cause the scheduler to simulate its behavior as if it was the second night, third night or even a later deployment. This assessment was to be deemed successful if the scheduler proves to de-prioritize objects that have been already observed, while prioritizing those that have not.

Test Results: Complete

This test was conducted initially using three satellites: the ISS, Galileo 22, and Meridian 8. These satellites were chosen as they are in LEO, MEO, and HEO orbits respectively. Running a test script for the scheduler and plotting the imaging sequences resulted in the following azimuth-elevation plot:

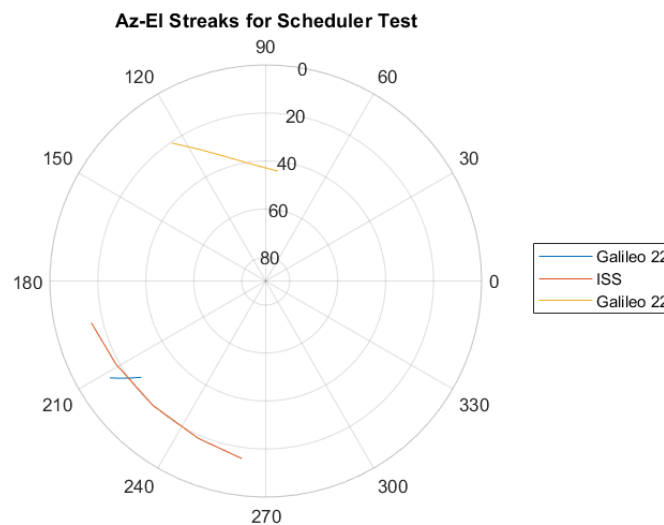


Fig. 53 Scheduler Test: Azimuth-Elevation Plot with Meridian 8

Figure 53 shows the scheduler output for the initial test. Two sequences were scheduler for Galileo 22 and one was scheduler for the ISS. However, no sequences were scheduler for Meridian 8, and subsequent attempts to run this test were also unable to provide sequences for Meridian 8. This is likely due to the fact that Meridian 8 is in a Molniya orbit and spends the majority of its time over Russia. Thus, a new HEO satellite was chosen to verify SHADE's capability to scheduler objects in HEO orbits. The chosen satellite was SDS-F6, and the scheduler was tested again with this input.

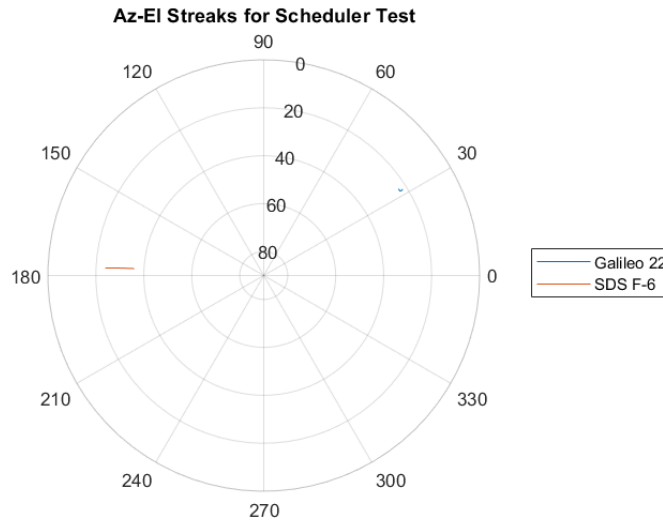


Fig. 54 Scheduler Test: Azimuth-Elevation Plot with SDS-F6

Figure 54 shows the scheduler output with the modified input. Although the ISS was unable to be scheduled, that capability had been verified in the previous test. Furthermore, this test showed that the scheduler is able to predict imaging sequences for HEO orbits.

Finally, the boolean tracker for whether an object has been imaged or not was manually modified to the "imaged" condition, and the scheduler was run. This resulted in reduced weight for those objects with the modified boolean indicator, verifying the ability to deprioritize objects that have already been imaged.

10. Image Processing

Test Design:

In order to assess the functionality of SHADE's Image Processing, an assessment was conducted to compare SHADE's imaging sequence coordinates to the coordinates predicted by orbit propagation. A set of images captured by the camera, containing streaks of various sizes and shapes, was input into the image processing system. The image processing system was to then be able to identify the correct streak in each image and turn the streak's endpoints into RA-Dec coordinates. This assessment was to be deemed satisfactory if the RA-Dec coordinates found by the imaging sequence match those predicted from orbit propagation. This test was designed to mitigate the risk of the image processor improperly identifying streaks, as well as the risk of the image processor identifying the wrong streak if multiple streaks are present.

Test Results: Partially Complete

The lack of long-duration full system tests meant that the image system could not be tested on real data. As a substitute, a set of synthetic streaks, with varying quality (brightness, noise, dark or bright objects on screen) and geometries (multiple streaks, intersections, locations, angles) were created to test the image processing system. The results of these tests are shown in Figure 55. These demonstrate that the streak detection algorithm is capable of detecting partial and complete streaks, selecting the best streak based on a predicted shape, and still operates if the steak is being intersected by another. However, these tests should

be considered no more than a basic proof of concept until more tests can be run on a full suite of real data, collected by a full system deployment. Once complete, this will fully validate FR 5.

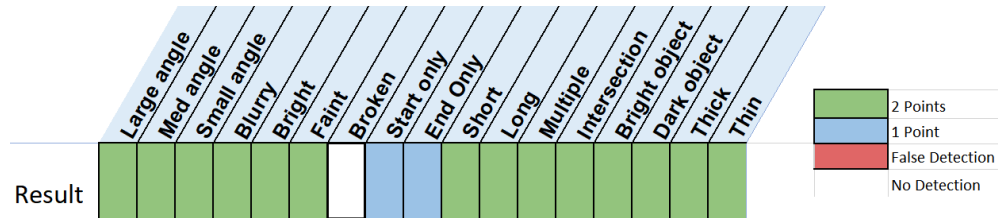


Fig. 55 Image Processing Test: Result of streak detection and selection on a suite of synthetic test images

11. Timed Software Setup

Test Design:

In order to validate Functional Requirement 7, which defines SHADE’s 30 minute transport and assembly constraint, an assessment was conducted to verify that the software can be setup in a timely manner. For this test, an operator timed how long it takes to attach the USB drive, power up the system, and receive either the all systems go message or a detailed error report if something is wrong. This assessment was to be deemed satisfactory if the software setup could be conducted in a reasonable time, less than 10 minutes. The software setup was to be assessed again, in coordination with the full Time Budget test.

Test Results: Complete

Repeated deployment tests yielded a typical software setup time of four to five minutes. This included about one minute of hardware attachment (USB drive, monitor HDMI cable, monitor power), and less than a minute of detaching the monitor when complete. The remaining two to six minutes was spent manually calibrating the mount and waiting for a GPS lock. The wide range of times is mostly due to the GPS lock, which might have achieved a lock while other tasks were completed, or may require a few minutes, if performing a cold-start. The time budget outlined here will hold if the GPS requires seven minutes or less to get a first-fix. Along with the deployment tests, this validates FR 7.

2. Full System Testing - Test Plan (TP)

Author: Katherine Nyland

The following three Full System tests are the pinnacle of the SHADE system validation. They were designed to verify the end-to-end functionality of SHADE, as well as to demonstrate the fulfillment of SHADE’s novel Functional Requirements.

1. 30-Minute Transport & Assembly

Test Design:

The first of the three Full Systems tests was designed to validate Functional Requirement 7. In addition to SHADE being transported and deployed by a single person in 30 minutes, this requirement also insinuates the following parameters; the transport vehicle will be within 100 feet of the deployment site and the system modules will weigh no more than 50 lbs.

The initial Time Budget (Fig.56), seen below, was developed to provide an estimate for how the 30 minutes will be spent.

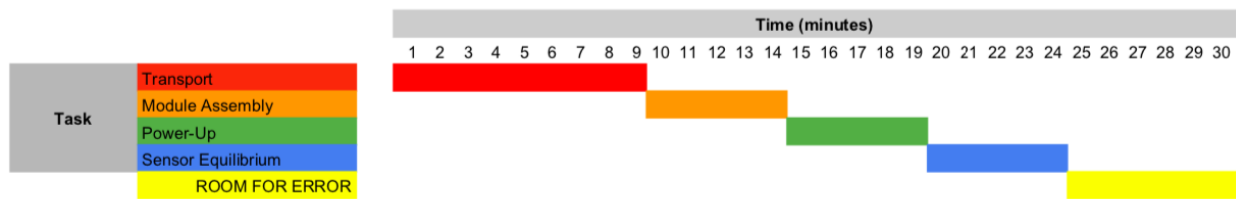


Fig. 56 Time Budget

Nine minutes were budgeted for the transport of the modules, one minute each way. Five minutes were budgeted for both the system assembly and power-up. Sensor equilibrium was also budgeted five minutes, however this value came from Sensor Equilibrium testing conducted by WRAITH. The WRAITH team tested how long it took for each of the sensors to reach equilibrium and found that the relative humidity sensor took the longest to equalize, equalizing in 250 seconds. This left six minutes of room for error. This initial Time Budget was used as a guide throughout the duration of the test and was adjusted at the conclusion of testing.

The test was conducted in the field behind the Aerospace building and shall be conducted using the following procedure:

- 1) Two SHADE team members arrived at the Aerospace building, parking their vehicle in SEEC lot 556.
- 2) One team member measured a distance of 100 feet from the vehicle to a location in the field. This team member remained at this location and act as the timer.
- 3) The second team member acted as the operator. The timer started the stopwatch and signaled to the operator to begin the module transport.
- 4) The operator completed each of the six trips from the vehicle to the deployment site and back. The timer recorded the time at the completion of the module transport.
- 5) The operator then assemble the modules. The timer recorded the time at the completion of module assembly.
- 6) The operator conducted the power-up of the SHADE system. The timer recorded the time at the completion of the power-up.
- 7) Next, the operator equalized the weather detection sensors. The timer recorded the time at the completion of the sensor equilibrium.
- 8) The timer stopped the stopwatch.
- 9) Both the timer and the operator powered-off and disassembled the system modules and transported the modules back to the vehicle, concluding the test.

Test Results: Complete

A single operator was timed transporting and assembling the SHADE system. This resulted in a hardware setup time of 10 minutes and 17 seconds and a software setup time of slightly less than 8 minutes. The resultant total deployment time was approximately 18 minutes, below the 30 minute limit. Figure 57 shows the resulting deployment time budget, with 12 minutes of room for error. The success of this test satisfies Functional Requirement 7.

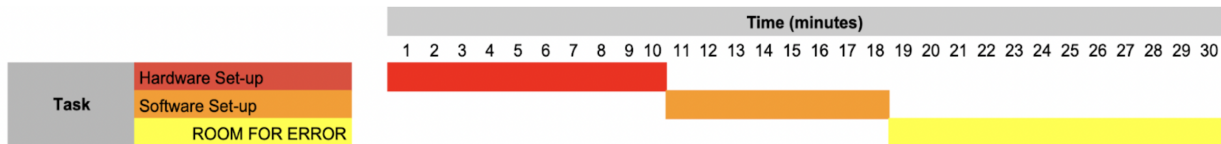


Fig. 57 Experimental Time Budget

2. Single Night Deployment

Test Design:

The second of the Full System tests was designed to validate Functional Requirements 1, 3, 4, 5, and 6. The test was to be conducted on the roof of the Aerospace Building, as the team felt this was the most controllable outdoor location. Special access to the roof was necessary and was to be obtained through the building manager with the help of Professor Rhode. The test set up was to look similar to that of the CONOPs with two exceptions; the transport and assembly of the system were not be restricted to the 30 minute, single operator limitations due to the roof being an unrealistic deployment location. The second exception being that for the purpose of this test, SHADE was to be only be deployed for one night (12 hrs) and not multiple nights. The logic behind this was to verify that the system was functioning properly for a single night, before a multi-night deployment was to be attempted.

The test was to be conducted using the following procedure:

- 1) At dusk, the SHADE was to be transported to the roof of the Aerospace Building.
- 2) The SHADE modules was to be assembled in a location with clear view of the sky.
- 3) An operator was to conduct the power-up of the SHADE system.
- 4) An operator was to equalize the weather detection sensors.
- 5) An operator was to upload the TLE list for automated scheduling.
- 6) An operator was to deploy the system and depart.
- 7) 12 hours later, the operator was to return to the roof of the Aerospace building, power off, disassemble and transport the system back to their vehicle.

During the test's 12 hour duration, the scheduler was to determine the viewing window for each object. At each objects viewing window, the actuation stage was to be commanded to point the camera in the correct location. SHADE was to then capture a background and three streak images of the object, then the image processing system would determine the streak endpoints. This data was to then be passed to the orbit propagation software and provide a final updated TLE. Concurrently, SHADE's weather detection suite was to be active, communicating with the active protection module on whether or not to enter safe mode.

Test Results: **Incomplete**

The two final full system tests, the Single-Night Deployment and the Multi-Night Deployment, were not completed. This can be attributed to various unprecedented challenges the team encountered. The first of these challenges was a GPS lock that required a manual override to resolve. Secondly, an issue with the camera focus arose. This is strictly a hardware issue. The camera has a very short window of time to focus on each object and any slip of the camera inhibits accurate calibration. It was also found that the camera is not focused at infinity, resulting blurry streak images. Additional software issues arose as well, however these have since been debugged.

The largest issue the team faced in completing these final two full system tests, was the weather conditions

in Boulder, CO during the planned testing week as well as the weeks following. The precipitation and heavy cloud cover made it infeasible to launch the system with the desire of testing any functionality other than the weather detection suite. In industry, the team would have more schedule contingency, permitting the tests to be pushed back until weather conditions cleared.

3. Multi-Night Deployment

Test Design:

The third and final Full System test was the culmination of the SHADE system validation, designed to validate all Functional Requirements, yet notably validating Functional Requirements 2 and 8. For the same reasons listed previously, the test was to be conducted on the roof of the Aerospace building. The test set up was to again look analogous to that of the CONOPs, with the omission of the 30 minute transport & assembly restriction.

The test was to be conducted using the same procedure listed for the Single Night Deployment, the only discrepancy being that for this test SHADE was to be deployed for two nights. (36 hours), instead of one. Thus, this test would verify the functionality of the solar panels, in that they are capable of providing adequate power to the system.

Test Results: **Incomplete**

See Single-Night Deployment Test Results

3. Satisfaction of Functional Requirements

Author: Katherine Nyland

Functional Requirement 1- Satisfied

FR 1: SHADE shall schedule predicted locations and visibility windows for objects in LEO, MEO, GEO, and HEO orbits.

Relevant Tests: *Single Night Deployment, Multi-Night Deployment, Orbit Propagation, Week-Long Scheduling*

Satisfaction: If SHADE is successful in the Orbit Propagation assessment, the Week-Long Dynamic Scheduling assessment, and accurately predicts locations and visibility windows for 90 % of the requested objects in the Single and Multi-Night Deployment assessments, FR 1 will be satisfied.

Functional Requirement 2- Satisfied

FR 2: SHADE shall function autonomously in standard operating conditions with no human intervention for at least two nights.

Relevant Tests: *Multi-Night Deployment, Week-Long Dynamic Scheduling*

Satisfaction: If SHADE is successful in the Week-Long Dynamic Scheduling assessment, adequately powered for the duration of the Multi-Night Deployment assessment, completes 80 % of its requested tracking, enters/exits safe mode when signaled, and accurately predicts and stores orbit information for both nights, FR 2 will be satisfied.

Functional Requirement 3- Satisfied

FR 3: SHADE shall autonomously enter and exit a safe mode to protect itself from adverse weather.

Relevant Tests: *Single Night Deployment, Multi-Night Deployment, Lid Actuation, Weather Detection Tests*

Satisfaction: If SHADE is successful in the Lid Actuation Assessment, the Weather Detection Tests, as well as enters/exits safe mode when signaled in both the Single and Multi-Night Deployment assessments, FR 3 will be satisfied.

Functional Requirement 4- Satisfied

FR 4: SHADE shall autonomously point to and track objects in LEO, MEO, GEO, and HEO

Relevant Tests: *Single Night Deployment, Multi-Night Deployment, Week-Long Dynamic Scheduling, Image Processing, Orbit Propagation*

Satisfaction: If SHADE is successful in the Week-Long Dynamic Scheduling assessment, the Image Processing assessment, the Orbit Propagation assessment and accurately points to and tracks 80 % of the requested objects in both the Single and Multi-Night Deployment assessments, FR 4 will be satisfied.

Functional Requirement 5- Partially Satisfied

FR 5: SHADE shall image objects with apparent magnitude of less than 10.

Relevant Tests: *Image Processing*

Satisfaction: This requirement has been partially satisfied through WRAITH team testing. WRAITH verified that the camera was capable of imaging objects with apparent magnitude of less than 10. If SHADE is successful in the Image Processing assessment, verifying that the captured images are sufficient for accurate imaging sequence results, FR 5 will be fully satisfied.

Functional Requirement 6- Satisfied

FR 6: SHADE shall create and save an orbit estimate for each object imaged within five minutes of the end of the associated visibility window.

Relevant Tests: *Single Night Deployment, Multi-Night Deployment, Image Processing*

Satisfaction: If SHADE is successful in the Image Processing assessment and accurately creates and saves the orbit estimate for 90 % of the objects within five minutes of the end of the associated visibility window in the Single and Multi-Night Deployment assessments, FR 6 will be satisfied.

Functional Requirement 7- Satisfied

FR 7: SHADE shall be deployed and broken down in 30 minutes by one operator.

Relevant Tests: *30-Minute Transport & Assembly*

Satisfaction: If a single operator is capable of transporting, assembling and deploying the SHADE system within 30 minutes, FR 7 will be satisfied.

Functional Requirement 8- Satisfied

FR 8: SHADE shall be capable of making observations on multiple nights during a single deployment.

Relevant Tests: *Multi-Night Deployment*

Satisfaction: If SHADE is adequately powered for the duration of the Multi-Night Deployment assessment, completes 80 % of its requested tracking, enters/exits safe mode when signaled, and accurately predicts and stores orbit information for both nights, FR 8 will be satisfied.

VI. Risk Assessment and Mitigation

Author: Benjamin Vidaurre

In undertaking a project with two years worth of associated work with that work having been completed to various degrees of success, the risks to SHADE both inherent and discovered are plentiful. Figure 58 shows the categorisation of all the identified risks for SHADE. Each risk was rated in terms of its likelihood of failure and recoverability on a scale from one to five. The product of these scores gives the measure of the risks overall severity.

		Recoverability				
		Trivial	Easy	Difficult	Very Difficult	Unrecoverable
Likelihood of Failure	Near Certainty			SOC	SLS, DIH	
	Highly Likely		CLC		TOI, SPF	
	Likely		LDN, ITC, RMA, PRH	PBA, SLP		
	Unlikely		WFT	CMM	SDA, WDC, BOP, SDP	
	Not Likely		WLD			RCR, GPS, THF, SPO, ACA

Fig. 58 The full risk matrix for SHADE prior to mitigation

Both for demonstration and internal organization, the risks have been categorised by their nature into Technical, Management, and External risks. All of the risks identified for SHADE can be found in appendix X.5, while the highest severity risks which were realised are discussed in detail here.

Risk: Diurnal Heating

ID: DIH

Category: Technical

Risk Statement: If solar heating experienced by SHADE increases the temperature of the components past their heat tolerance, operational failure or permanent component damage can occur.

Likelihood: 5 **Recoverability:** 4 **Severity:** 20

In increasing the minimum mission duration of SHADE, we departure from the assumption used by GHOST and WRAITH that solar heating would not play a significant role in the operating conditions

experienced by the system. Although the majority of the operational activity takes place during the night, SHADE will be sitting in safe mode over the course of the day being heated by the sun.

Mitigation: Insulation of sensitive components, addition of heat sinks and radiative fins to the solar panels, and application of thermally protective paint to the active protection enclosure and power module will reduce the severity of temperature fluctuations and help to maintain a lower individual component temperature. Additionally, a waterproof vent was installed on the power module to aid temperature control during the day.

Likelihood: 5 **Recoverability:** 1 **Severity:** 5

Risk: Single Point of Failure

ID: SPF

Category: Management

Risk Statement: Due to the serial nature of SHADE's observational operation, if any one component fails the entire mission could be compromised.

Likelihood: 4 **Recoverability:** 4 **Severity:** 16

While the classic solution to the risk of single point failure is to introduce component redundancy to the system to allow a failure not to cripple the system, program limitations mean that the individual components should be made more robust against failures which would otherwise render it inoperable. Increasing the mission duration increases the difficulty of recovery from SPF along with increasing its likelihood, resulting in an overall more risky mission than was undertaken by WRAITH.

Mitigation: Providing an operator procedure reduces the risk of hardware initialisation error, self-diagnostics can help identify operator error, the new image processor is more robust to confounding confounding factors, the orbit propagation study reduces the risk of generating an invalid observation schedule, and the automated calibration functionality accounts for shifting and settling over time.

Likelihood: 2 **Recoverability:** 4 **Severity:** 8

Risk: Schedule Slip

ID: SLP

Category: Management

Risk Statement: If work for any scheduled development, integration, or testing processes which fall on the project critical path takes longer than planned, the dependent work must be pushed back to accommodate for the time spent which extends the entire duration of the project.

Likelihood: 3 **Recoverability:** 3 **Severity:** 9

Given the breadth of the work being done for SHADE, much of this work can take place concurrently. This does not mean that a critical path does not exist for the overall schedule, rather than the critical path is more important to track than it may be for a project with more serial development. The effects of slipping on the critical path tasks can have effects both on critical path tasks downstream of the slip as well as tasks which now end up on the critical path which were not there previously. Due to the tightly constrained nature of our schedule due to the class enforced deadlines, schedule slip can also

exacerbate the risk of schedule driven progress (**SDP**), which would mean that the team must move on from graduation-type events without SHADE necessarily meeting the targeted graduation criteria.

Mitigation: Designing the schedule with some margin allows for slip to be accommodated without affecting the entire schedule. Enhanced monitoring of task progress for those on the critical path also helps to identify possible issues which might induce slip to allocate additional resources to the task prior to the target completion date.

Likelihood: 3 Recoverability: 2 Severity: 6

Figure 59 shows the expected categorisation of all the identified risks for SHADE after mitigation methods have been enacted.

		Recoverability				
		Trivial	Easy	Difficult	Very Difficult	Unrecoverable
Likelihood of Failure	Near Certainty	SLS, SOC, DIH				
	Highly Likely	TOI				
	Likely	LDN, ITC	SLP			
	Unlikely		PRH, SDP, RMA		SPF	
	Not Likely		WLD, SDA, ACA, WFT	PBA, CMM	WDC, BOP	RCR, GPS, THF, SPO

Fig. 59 The full risk matrix for SHADE following mitigation

The two risks which still indicated a severity score of greater than five are Schedule Slip (**SLP**) and Single Point of Failure (**SPF**). Rather than indicate that the risks required more effort to mitigate them further, their scores indicated that they warranted especially close attention from the team. It should also be noted that both fall under the Management category which placed further onus on those in positions of higher leadership to monitor these risks, lest they manifest negatively within the project.

Over the course of the spring semester, eight of the 24 identified risks, and two of the five most severe risks were realised during integration and testing. Three were technical risks (**DIH**, **RCR**, & **GPS**), four were management risks (**SPF**, **SLP**, **SDP**, **RMA**), and one was an external risk (**BOP**). Because the majority of the risks were initially formulated via FMEA, expectations for situations most likely to induce realisation of a risk were known ahead of time. Depending on the nature of the risk, those associated with the actual operation of SHADE could only manifest during testing and were much easier to track. This is true for all of the technical risks along with **SPF** and **BOP**.

For a risk with many different associated failure modes like **SPF**, the failures produced by other risks will end up inducing **SPF** as was the case with Roof Closing Routine (**RCR**), GPS Signal Acquisition (**GPS**), and Operator Error (**BOP**). If **RCR** manifests when the Weather Detection module detects hazardous weather, the

imaging hardware will be exposed to that weather and then is especially likely to become damaged. Failure to acquire a GPS signal lock during setup renders the orbit determination routine incapable of producing accurate updates which represent terminal failure of SHADE. Depending on the nature of any operator error left unfixed during setup, there is the potential for terminal failure of SHADE. Due to the initial severity along with the various associated failure modes for **SPF**, SHADE implemented a number of technical solutions looking to preempt some of these failure modes and deployment testing allowed refinement of the operator manual to prevent possible operator errors during setup.

Tracking and mitigation of the management risks was the main focus for the management team as these risks could not be directly addressed with technical solutions. A major aspect of mitigating the potential for **SLP** was accomplishing the majority of legacy system testing in the fall semester. This allowed for more effective use of the limited time afforded to us by the restrictions for on-campus operations. These restrictions were the main driver of **RMA** manifesting. Not being able to draw on all of the team members on a regular basis meant that the majority of the physical manufacturing and development was undertaken by four of the ten team members.

The schedule for spring semester manufacturing was built on the assumption that we would be able to rely on more of the team than ultimately was possible. This meant that a reallocation of workload was needed to effectively accomplish tasks in a relatively timely manner. Ultimately, this was a contributing factor to much of the schedule slip we encountered. Although we built the initial schedule with a considerable amount of slack, most was consumed fairly early in the semester. Despite having achieved requirement compliance and the targeted success levels for the various project elements, there was a fair amount of schedule driven progress (**SDP**) where components represent a minimum viable product rather than a more complete solution which could have been implemented with more time.

VII. Project Planning

1. Organization Chart

Author: Robert Redfern

The organizational chart for SHADE is shown below in Figure 60. This chart lists all ten members of the SHADE project along with their primary focus area. It is important to note that the job title under each name is meant to reflect the area of the project that person *led*. Team members also help in other areas of the project as well and were not confined to their titled position. The chart is broken down to show duties relating to SHADE's hardware, software, and finance. These are highlighted in red, blue, and green respectively. Additionally the purple "float" outline indicated that these primary roles are focused on the combination of the other three. The three float roles are Project Manager, Systems Manager, and Testing/Safety Lead. The finance manager position worked in tandem with project management in order to accurately assess the needs of the hardware and software teams as well. Team leads played an important role in testing as well in order to effectively troubleshoot issues as they arose. Communication with the Aerospace Corporation and other stakeholders was primarily the responsibility of the Project Manager, though system specific inquiries could be made by all team members.

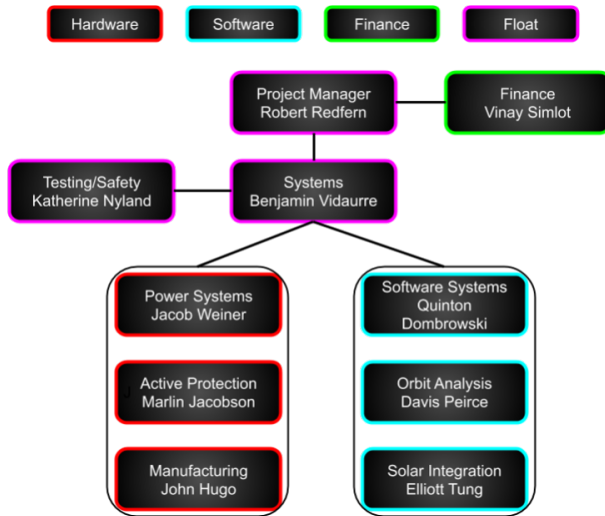


Fig. 60 Team Organizational Chart

2. Work Breakdown Structure

Author: Benjamin Vidaurre

The work breakdown structure (WBS) for SHADE is organized by the major categories of activity with the associated subordinate tasks and functions for each to show the flow of associated work to the relevant project areas. The SHADE Summary Work Breakdown Structure (SWBS) is shown in Figure 61 and describes the two uppermost levels of detail which are the the major activity categories and their primary work areas. The logic in selecting these major activity categories stems from the intent to limit duplication of work across different categories while still maintaining high-fidelity tracking of the different work packages at the lower levels of detail.

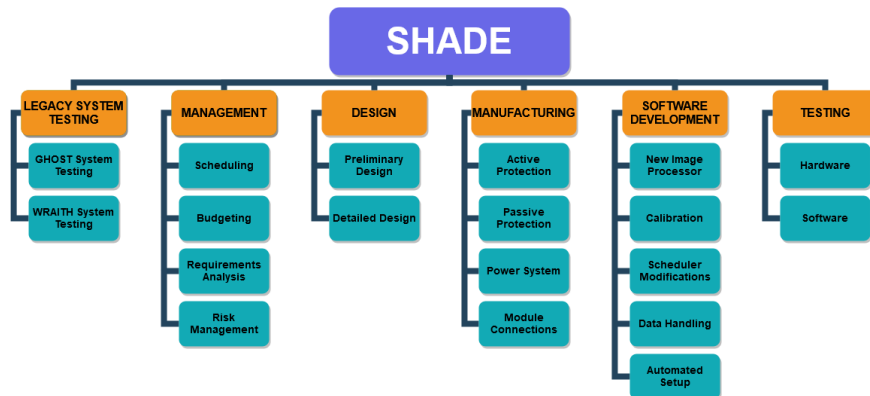


Fig. 61 SHADE Summary WBS

The full WBS developed for SHADE can be found in appendix X.7 and details individual work packages to five levels of detail. Figure 62 focuses on the Manufacturing and Software Development branches of the WBS and indicates an additional level of detail which summarises the major areas of work associated with the critical project elements as they relate to each development category.

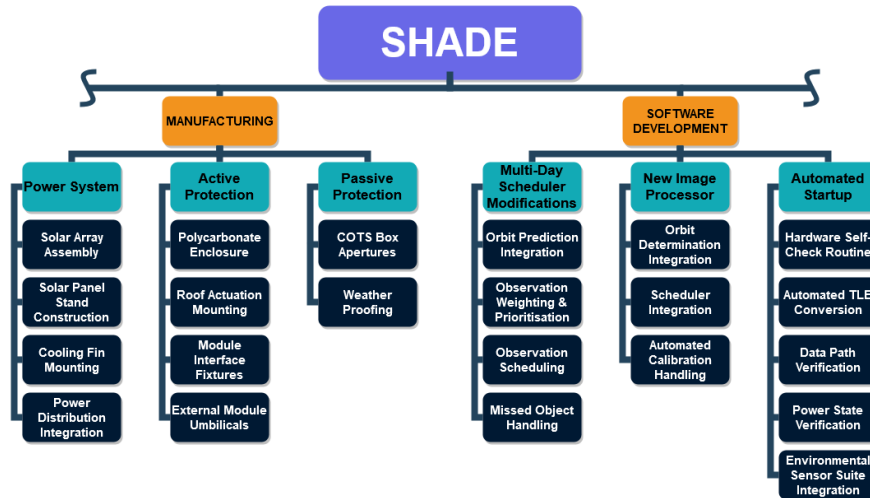


Fig. 62 SHADE WBS - Third Level of Detail, Development Product Work Packages

The other benefit of organizing the WBS based on the activity areas is the ability to cross-reference the related work being done in one area to other areas where a work package may be dependent on the results from others, either in a developmental or organizational capacity for easier tracking of overall progress through the evolution of the program schedule where each of the work packages can be found.

3. Work Plan

1. Overview

Authors: Robert Redfern

This work plan section shows the full project timeline and works to demonstrate the structured completion of all development, testing, and integration plans for the SHADE project. This begins with our legacy systems, which were tested throughout the fall semester to assess their current state. Legacy weather detection testing was pushed into the spring semester due to previously damaged hardware that could not be replaced until spring. The spring semester focuses on SHADE’s development and testing schedule and is broken down by each SHADE subsystem. The work plan is completed with successful integration and functional system tests.

2. Fall Legacy Testing

Authors: Robert Redfern, Benjamin Vidaurre, Jacob Weiner

Throughout the fall semester, legacy component and system level tests were required to assess the state of the inherited system. Upon inspection it was clear the timing of the spring stoppage had a significant impact on the project as a whole, resulting in limited documentation and functional components. This fall testing process was partially inhibited by university COVID policies while also being completed in parallel with the design of new SHADE systems. Legacy power distribution worked as intended and the team was able to conduct further tests on the UDOO processor and lid actuation motor.

At a component level, the iOptron Base, Zwo ASI camera, and Cannon lens were also found to be functioning as intended. This was verified through running specific UDOO commands to the iOptron to

point in a certain direction to ensure that the iOptron and UDOO could still interface with one another. Other legacy hardware did not work as intended, specifically the actuation of the active protection roof and environmental suite. While the lid actuation hardware functioned as intended, the actuation software lacked proper integration, resulting in non-functional hardware control. This meant that the roof could only be opened and closed once before the UDOO would crash. In contrast mainly hardware issues were uncovered in the environmental suite.

A power issue with the Particle E series board was uncovered during initial component testing. This was the result of an incorrectly wired WRAITH umbilical cord. The new board was ordered once P-cards were distributed to teams in January. Software for the environmental suite was never completed by WRAITH, adding to the scope of SHADE’s development. Similarly, the GHOST scheduler and imaging software was found to be in a state of disrepair and were unable to perform as intended based on previous group’s documentation. SHADE’s design incorporates a new dynamic multi-day scheduler, as well as a new image processing system, the decision was made to shift focus to the novel design of these software components.

Overall the fall legacy testing was very beneficial to assess how much technical debt had been inherited by the SHADE team. Even though this process required the team to be temporarily split between new design and component testing, it was vital to accurately assess the true scope of the project. Sufficient legacy testing also aided in the creation of the spring work plan. While not all legacy issues were uncovered prior to the winter break, those that were mission critical were accounted for and received higher priority during the spring semester.

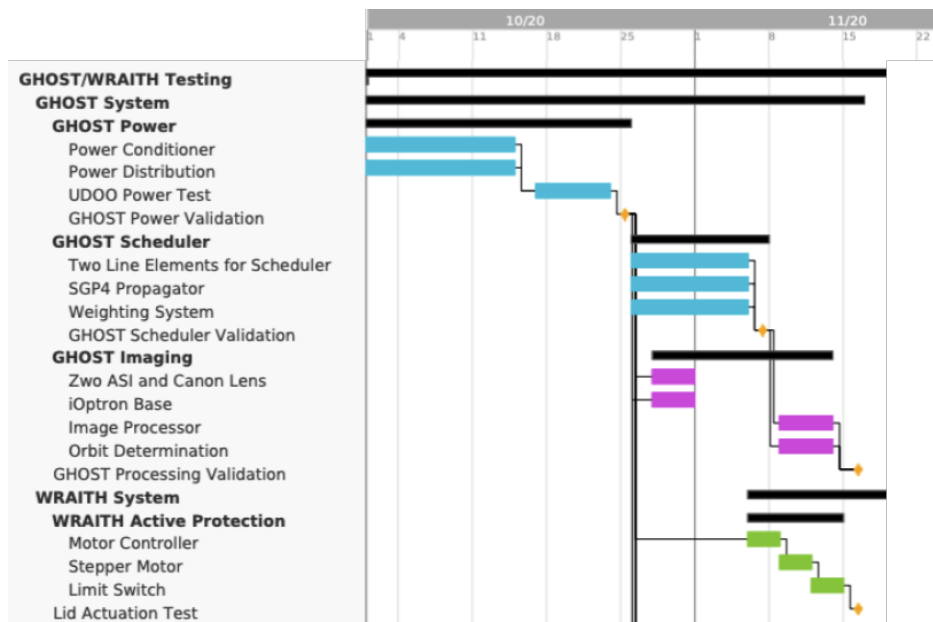


Fig. 63 Gantt Chart of Fall 2020 Legacy Testing

3. Spring Legacy Testing

Authors: Robert Redfern, Benjamin Vidaurre

These two legacy subsystems were not able to be tested before the end of the fall semester, and instead

underwent testing in the spring. Upon initial assessment, the architecture of the Weather Detection module appeared sound and the extent of testing in the spring was to verify correct function of the sensors before integration with the Active Protection module and communication with the main processor took place. During this testing phase, the anemometer was found to be non-functioning along with the Particle Electron micro-controller which drives data collection for the Weather Detection module. Additionally, the firmware for the Electron was only partially complete. Following replacement of these two components and completion of the firmware, the Weather Detection module was integrated with the rest of SHADE. The WRAITH scheduler has been replaced by a new multi-day scheduler, and therefore was a low priority for testing in the fall.

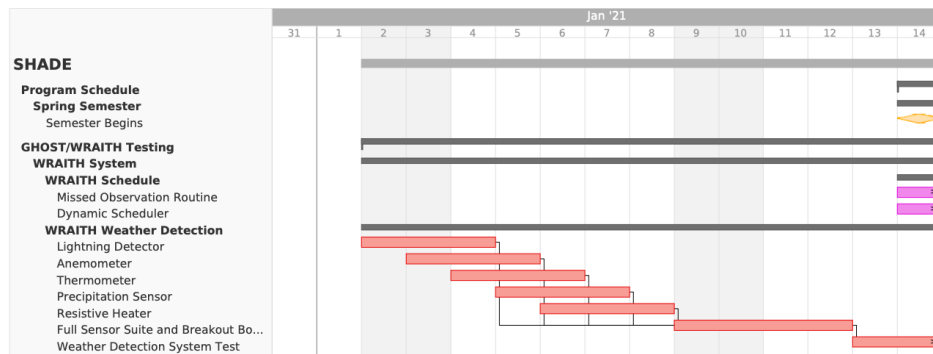


Fig. 64 Gantt Chart of Remaining Legacy Testing

4. Spring Work Plan

Authors: Robert Redfern, Benjamin Vidaurre

This next section examines SHADE’s completed work plan for the spring semester. This plan focuses on the development of each critical project element, as well as demonstrates the integration time required with legacy systems. The overarching timeline with this plan was to complete manufacturing and component development by the end of March. This then leaves April for system level tests and resolving other integration issues. The reasoning for this choice, and its subsequent execution will now be discussed in detail. At the beginning of the spring semester, a two-week delay to university Return to Research (R2R) access pushed back initial manufacturing timelines. This gap reduced development slack and compacted the integration schedule even further, as can be seen in each of the system schedules.

Power System

SHADE’s multi-day power system is the first critical area of SHADE’s development. This system required manufacturing of two unique solar panels and the SHADE power module. The panels themselves are designed to be easily manufacturable, however CAD tolerance issues and the R2R delay added on development time. Once manufacturing began in early February, the aluminum stands were completed followed by heat sink adhesion to the back-plates through a thermal epoxy curing process. Once the cells were connected and tested, the first solar charging tests were able to be completed in mid-March. Thermal testing was also completed in March to assess how the cooler cells were preventing additional power loss. In parallel with hardware development, power related software, including low power shutdown tests, was finalized. Some schedule slip

occurred in the integration phase due to a serial voltage discrepancy between the power module and UDOO processor, though this error was rectified quickly with the addition of bi-directional level shifters. Overall the power system was able to remain close to its predicted timeline, with no significant delays stemming from the systems ability to power SHADE.

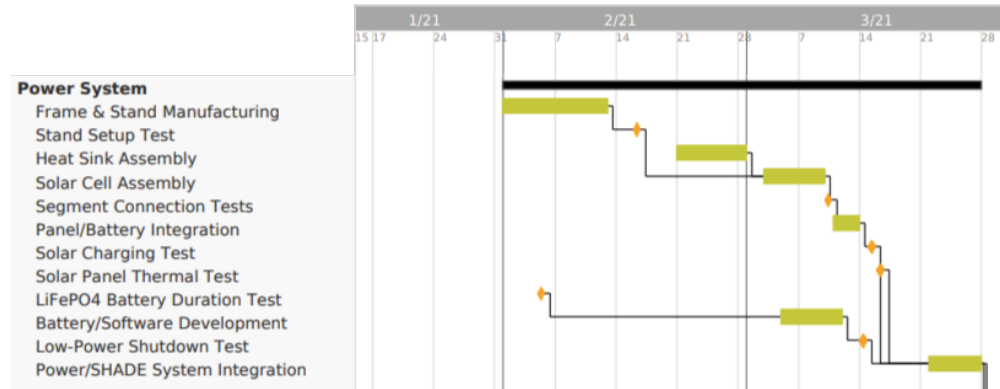


Fig. 65 Gantt Chart of Power Work Plan

Active Protection

SHADE’s active protection is the remaining hardware dominant system, which works to protect imaging hardware during deployment. The new polycarbonate enclosure began its manufacturing and assembly once R2R was received in early February. This process took a week longer than expected due to restriction to lab hours. Once the shell was completed the sliding rails and roof was mounted. A water-draining roof angle of one degree was designed to be accomplished by the leveling feet, however a redesign was required once calibration issues with the a non-level camera mount were discovered. With the lid and rails finished, both thermal and structural tests were performed to validate fall design models. With thermal paint applied and structure verified, SHADE components such as the polycases and motor hardware could be installed. The second half of March focused on the the validation of lid actuation models, as well as final integration steps including umbilical and handle placement. Overall the active protection schedule was impacted the most by the R2R delay, but was able to complete its manufacturing in time for integration in early April.

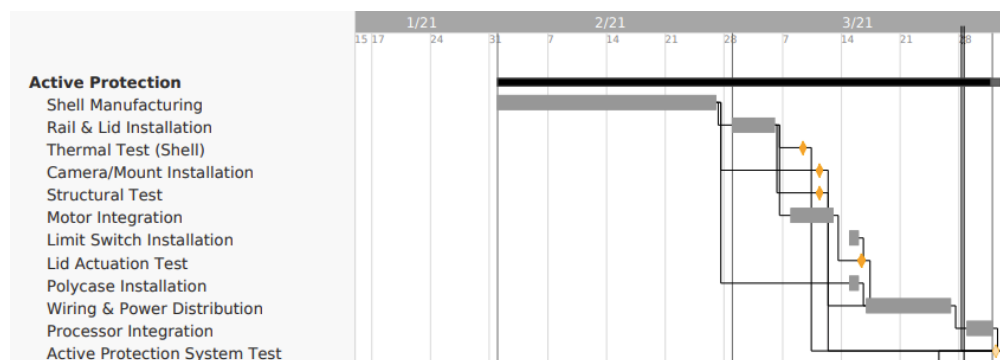


Fig. 66 Gantt Chart of Active Protection Work Plan

Software

SHADE's software systems are comprised of multiple novel and legacy components. The core imaging processes are dependent on software, therefore this subsystem is defined as the critical path for development. Software development began over the winter break and therefore avoided most of the schedule slip associated with the R2R delay. Development was also broken down into a parallelized structure to allow for easier task delegation. A gradual integration approach was also implemented allowing for hardware control to be tested as manufacturing was completed. A full suite of software component tests was added to the schedule at the end of March and early April, but was inhibited by poor weather conditions and hardware integration issues.

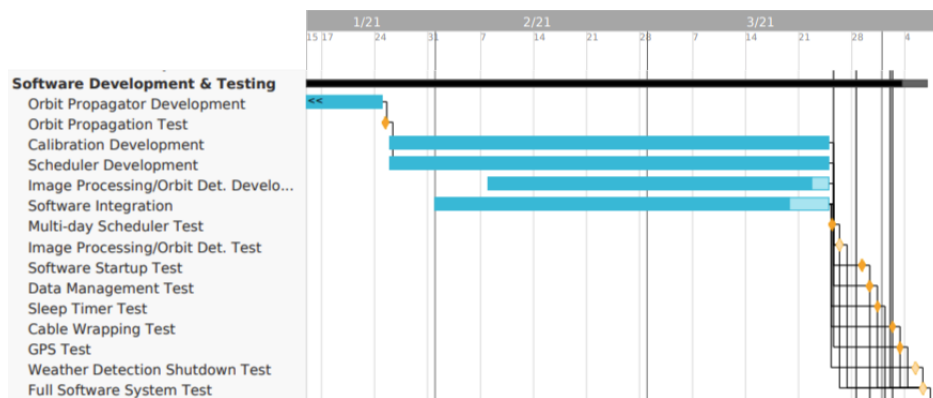


Fig. 67 Gantt Chart of Software Work Plan

System Tests

The original work plan targeted a shift to full system tests on April 3rd. However the combination of the R2R delay, along with compounding integration errors pushed this target back approximately a week. An unfortunate turn in April weather conditions resulted in a ten day period of no imaging opportunities. Though this weather concern was accounted for initially in the schedule, the systems testing margin had already been consumed due to the aforementioned delays early in the semester. With system testing delayed, the team shifted focus to the two class deliverables both due between April 16-19. During this period, the 30min deployment test was able to be completed as the system setup does not necessarily require subsequent imaging to take place. This verified FR 7 and was the first system test completed on April 12th. Temporary clearing in weather conditions toward the end of April allowed for some single night deployment attempts. These were completed with an operator present to assist in rapid trouble-shooting.

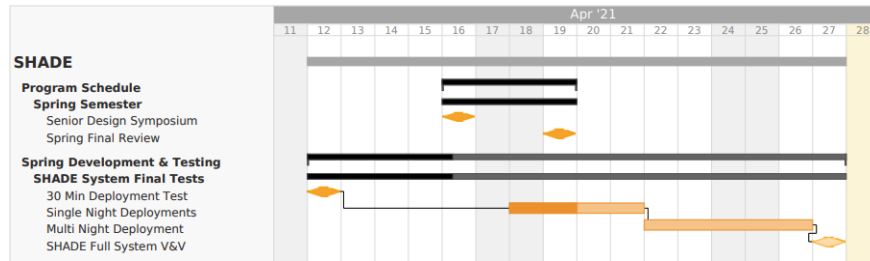


Fig. 68 Gantt Chart of Full System Work Plan

4. Test Plan & Testing Hardware

Scheduling of all component and system tests can be seen in SHADE’s work plan, and is broken down by subsystem. Additional hardware for the power system included a battery load tester that was provided by the WRAITH team. Personal multi meters were also used to assess connection stability. All thermal tests with the power and active protection systems were conducted with a forward looking infrared (FLIR) camera. This allowed the verification of the respective thermal models. The camera along with an oscilloscope was checked out from the electronics shop in the CU Aerospace Building. Active protection structural tests were completed with weights corresponding to the limits defined in the models. SHADE’s system tests require a clear area no more than 100ft from a transport vehicle. The 30min deployment tests and imaging were completed in a clearing between SEEC and AES building.

5. Cost Plan

Author: Vinay Simlot

SHADE’s budget, actual cost and margins are shown in figure 69. SHADE ended up over-budget in nearly every category. Because of testing errors, the SHADE team was forced to reorder the UDOO x86 processor, twice, costing the team an extra \$600. Additionally, the original amount of thermal epoxy ordered was not enough to cover both solar panels. The extra cost incurred after purchasing the thermal epoxy was \$270. Lastly, the team opted to purchase screws, building materials, and hardware from McGuckin’s and Home Depot in Boulder, rather than cheaper online outlets. The team was confident that there were enough funds to pay a premium for convenience, and avoid shipping delays. The full list of items purchased and their costs are in the appendix.

	Cost	Budget	Margin
Active Protection System	\$ 902.61	\$ 650.00	-39%
Power	\$ 2,429.55	\$ 2,320.00	-5%
Software	\$ 867.68	\$ 280.00	-210%
WRAITH Recovery	\$ 159.00	\$ 300.00	47%
Deposit	\$ 200.00	\$ 200.00	0%
Total	\$ 4,558.84	\$ 3,750.00	-22%

Fig. 69 SHADE's Cost Plan

VIII. Lessons Learned

Authors: Robert Redfern, Benjamin Vidaurre

1. Appropriate Scoping

One of the first hurdles encountered by the SHADE team in the fall was the complex scope of the project. SHADE worked to expand the design of previous projects inherently depends on the functionality of previous work. Due to the unexpected shutdown in spring 2020, much of this needed functionality was not present. Through a tedious re-evaluation of the project as a whole, the team was able to find new design areas to satisfy course requirements, while also leaving room to build up conceptual legacy systems. This re-scoping was a stressful time where many project deliverables were required by the course in rapid succession. This process illustrated the importance of appropriate scoping and showed how an ill-advised scope would have resulted in project failure.

2. Proactivity

Much like the benefits inherent in effectively determining the scope for the project, being proactive in discussions with course leadership along with the customer is immensely valuable. Understanding expectations as to the nature of work to be done and how that work will be valuable to overall project success was paramount to being able to rely on work already done when it became useful later on in the development process. Rarely were deliverables requested that were not useful in another contexts either as a reference or even as the basis for further deliverables. This meant that better work done earlier on allowed equally good work to be done later at the expense of less effort, which was especially important given the degree to which work can accumulate.

3. Subsystem Team Tag-Ups

With much of the design process taking place remotely throughout this year, the importance of communication became more apparent than ever. Team meetings multiple times a week did well to update the project status and tackle larger system issues. However, sometimes smaller subsystem issues would not be addressed. This if left unchecked resulted in insufficient knowledge transfer and small design flaws. Overall the SHADE team learned the importance of smaller team breakouts, which worked to help facilitate more proactive communication and efficient problem solving. This also helps to avoid large knowledge gaps, where team leads feel as though they are isolated in helping push the project forward. The final benefit of subsystem tag-ups is to improve task delegation. Not every task can be properly allocated in full team meetings, and the smaller discussions allow for each team member to understand what areas of the project need to be focused on next.

4. Component Design Reviews

A third lesson learned was the importance of formal design reviews. These reviews are baked into the foundation of the projects course and serve as the best way to identify potential risks. Not everything can be covered in these large reviews however, and smaller reviews are vital to save time in the future. For example, a more rigorous review of the solar panel stand design would have most likely uncovered the need for more tolerance, which in turn would have cut down a significant amount of manufacturing time. Additionally a discrepancy in cell solder tab sizes could have prevented a string of cells from cracking along a back plate seam line during testing. For the active protection hardware a calibration issue was discovered a non-level floor, and the lid had to be adjusted to prevent pooling water. No project will be able to foresee all hardware integration issues, however the risk can be mitigated by small, thorough design reviews taking place in between course deliverables.

IX. Individual Report Contributions

1. Robert Redfern

- **Project Purpose:** Required need, industry impact, legacy work.
- **Project Objectives:** Levels of success, functional requirements.
- **Final Design:** System Overview
- **Verification and Validation:** Power & Active Protection test design.
- **Project Planning:** Organizational chart, work plan, test plan, special equipment.
- **Lessons Learned:** Scoping, tag-ups, component design.

2. Benjamin Vidaurre

- **Project Objectives and Functional Requirements:** System block diagrams, functional requirements
- **Final Design:** Design requirements analysis & allocation
- **Verification and Validation:** Weather detection tests
- **Risk Assessment and Mitigation**
- **Project Planning:** Work breakdown structure, work plan
- **Lessons Learned:** Proactivity

3. Quinton Dombrowski

- **Final Design:** Software
- **Verification and Validation:** Software Tests

4. John Hugo

- **Final Design:** Solar Charging, Thermal Analysis
- **Verification and Validation:** Thermal Solar Test

5. Marlin Jacobson

- **Active Protection System Final Design:** Overview, design materials and geometry, and active and passive protection elements
- **Manufacturing:** Active protection system sections
- **Verification and Validation:** Active protection thermal, structural, and lid actuation tests
- **Appendix:** Active Protection trade studies, conceptual design, models, and development

6. Jacob Weiner

- **Final Design:** Full System Overview; Solar Charging: Overview, Panel Construction, The Power Module System and Legacy System Integration; Active Protection System: Active Protection Element
- **Manufacturing:** Power System
- **Verification and Validation:** Power Tests: Battery Duration, Low-Power Shutdown
- **Project Planning:** Work breakdown structure, work plan
- **Lessons Learned**

7. Vinay Simlot

- **Project Objectives**
- **Functional Requirements and Levels of Success=**
- **Project Planning:** Budget, cost plan

8. Davis Peirce

- **Final Design:** Software: Scheduler, Orbit Propagation
- **Verification and Validation:** Software: Week-Long Dynamic Scheduling Test

9. Katherine Nyland

- **Project Objectives and Functional Requirements:** Concept of Operations, Functional Requirements
- **Verification and Validation**
- **Lessons Learned**

10. Elliott Tung

- **Final Design:** Modeling: Initial Steady State Model, Transient Model, Charging Simulation
- **Verification and Validation:** Solar Charging Test

References

- [1] Kennewell, John A, and Ba-Ngu Vo (2013). An Overview of Space Situational Awareness. Institution of Electrical and Electronics Engineers. http://Ba-Ngu.vo-Au.com/ba-ngu.vo-au.com/vo/KV_SSA_FUSION13.pdf.
- [2] UCS Satellite Database. (n.d.). Retrieved September 07, 2020, from <https://www.ucsusa.org/resources/satellite-database>
- [3] United States Government Accountability Office. (n.d.). Retrieved September 08, 2020, <https://www.gao.gov/products/gao-16-6r>
- [4] Libre Space Foundation. (n.d.). Retrieved September 08, 2020, <https://libre.space/2020/03/02/space-situational-awareness/>
- [5] OSHA procedures for safe weight limits when manually lifting. (2013-06-04). Retrieved September 08, 2020, <https://www.osha.gov/laws-regs/standardinterpretations/2013-06-04-0>
- [6] Grzesica, Dariusz (2018). Measurement and analysis of truck vibrations during off-road transport. MATEC Web of Conferences https://www.researchgate.net/publication/328194182_Measurement_and_analysis_of_truck_vibrations_during_off-road_transportation
- [7] Types of solar panels. (n.d.). Retrieved September 29, 2020, from <https://www.energysage.com/solar/101/types-solar-panels/>
- [8] Posted in Batteries amp; Charging. (n.d.). What is Maximum Power Point Tracking (MPPT). Retrieved September 29, 2020, from <https://www.solar-electric.com/learning-center/mppt-solar-charge-controllers.html/>
- [9] Anemometer Wind Speed Sensor w/ Analog Voltage Output DataSheet (2014). Retrieved September 29, 2020, from https://media.digikay.com/pdf/Data%20Sheets/Adafruit%20PDFs/1733_Web.pdf
- [10] Bosch Sensotec (2018). BME280 Data sheet. Retrieved September 29, 2020, from https://cdn.sparkfun.com/assets/e/7/3/b/1/BME280_Datasheet.pdf
- [11] Microelectronic Integrated Systems (2009). MLX90614 family Data sheet. Retrieved September 29, 2020, from <https://www.sparkfun.com/datasheets/Sensors/Temperature/SEN-09570-datasheet-3901090614M005.pdf>
- [12] SparkFun (2016). AS3935 Franklin Lightning Sensor IC Data sheet. Retrieved September 29, 2020, from https://cdn.sparkfun.com/assets/learn_tutorials/9/2/1/AS3935_Datasheet_EN_v2.pdf
- [13] Components101 (2009). Rain Sensor Datasheet. Retrieved September 29, 2020, from <https://components101.com/sensors/rain-drop-sensor-module>
- [14] Particle docs (2020). E Series Module Datasheet. Retrieved September 29, 2020, from <https://docs.particle.io/datasheets/electron/e-series-datasheet/>
- [15] UDOO (2017). UDOO x86 Manual. Retrieved September 29, 2020, from https://udoo.org/download/files/UDOO_X86/Doc/UDOO_X86_MANUAL.pdf
- [16] iOptron (2017). iOptron AZ Mount Pro Altazimuth Mount Instruction Manual. Retrieved September 29, 2020, from http://www.ioptron.com/v/manuals/8900_AZMP_Manual.pdf
- [17] ZWO (2020). ZWO ASI1600 Manual. Retrieved September 29, 2020, from https://astronomy-imaging-camera.com/manuals/ASI1600_Manual_EN.pdf

- [18] MatWeb (2020). Retrieved September 29, 2020, from <http://www.matweb.com/>
- [19] Honeywell. Digital Compass Solution. Retrieved September 29, 2020, from [https://media.digikey.com/pdf/Data %20Sheets/Honeywell % 20PDFs/HMR3000_Rev2015.pdf](https://media.digikey.com/pdf/Data%20Sheets/Honeywell%20PDFs/HMR3000_Rev2015.pdf)
- [20] Analog Devices. ADXL 103/203 Data Sheet. Retrieved September 29, 2020 from https://www.analog.com/media/en/technical-documentation/data-sheets/adxl103_203.pdf
- [21] Firgelli Automations. Premium Linear Actuators. Retrieved September 29, 2020 from <https://www.firgelliauto.com/products/premium-linear-actuators>
- [22] Blanchard, B. S., & Blyler, J. E. (2016). System Engineering Management (5th ed.). Hoboken, NJ: Wiley.
- [23] SunPower Corporation. SunPower Module Degradation Rate. Retrieved November 1, 2020 from <https://energyhub.org/wp-content/uploads/2018/05/SunPower-Module-Degradation-PDF.pdf>
- [24] SunPower Corporation. MAXEON GEN III SOLAR CELLS. Retrieved November 1, 2020 from [https://cdn.enfsolar.com/Product/pdf/Cell/5b91fcf3916df.pdf?ga = 2.202701717.521940106.1607470678 – 130959401.1601147093](https://cdn.enfsolar.com/Product/pdf/Cell/5b91fcf3916df.pdf?ga=2.202701717.521940106.1607470678-130959401.1601147093)
- [25] Power Sonic Corporation. PSL-SC-12750-G24 Technical Documentation. Retrieved November 1, 2020 from <https://www.power-sonic.com/wp-content/uploads/2020/04/PSL-SC-12750-G24-Technical-Documen.pdf>

X. Appendices

1. Standard Operating Conditions

The operating conditions for the SHADE system are focused on defining suitable environmental and topographical conditions for deployment. The *Deployment* characteristics focus on the conditions present at the observation site prior to deployment while the *In-situ* characteristics focus on the dynamic atmospheric conditions during the observation period.

Deployment

- 1) The temperature range shall be between 0°C and 40°C.
- 2) The average relative humidity shall not exceed 50%.
- 3) The maximum ground grade shall not exceed 10°.
- 4) The minimum Sky Quality Meter (SQM) shall exceed $20 \frac{mag}{arcsec^2}$
- 5) The forecasted weather shall have less than 10% chance of precipitation.

In-situ

- 1) The temperature range shall be between 0°C and 40°C.
- 2) The wind speed shall not exceed $8 \frac{m}{s}$.
- 3) Lightning shall be further than 15km from SHADE.
- 4) The relative humidity shall not exceed 80%.

2. Supplemental Solar Panel Dimensions

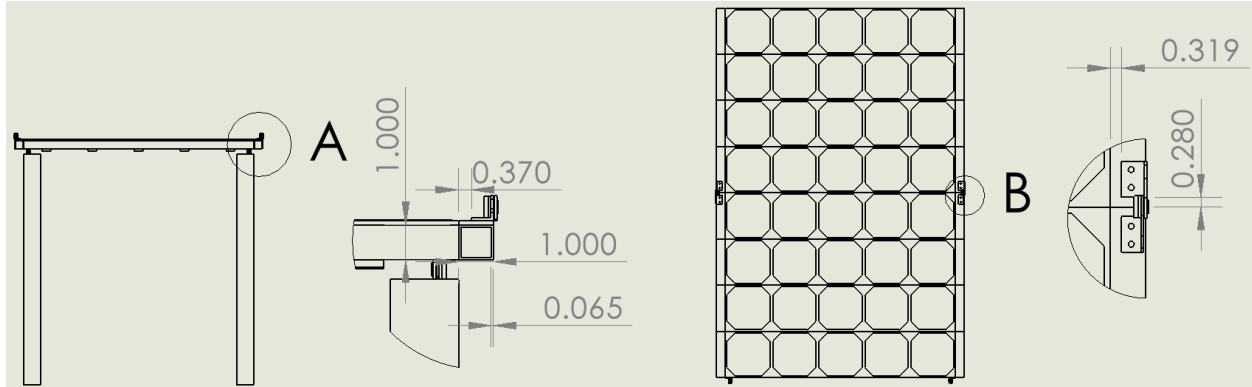


Fig. 70 Solar Panel Hinge Location

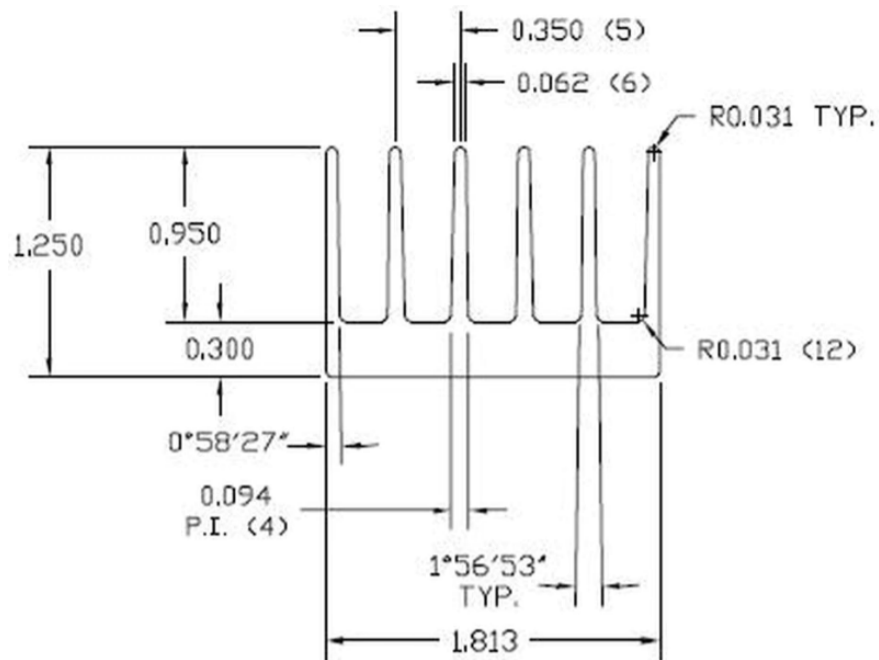


Fig. 71 Dimensioned Heatsink

3. Software Dependencies

SHADE is dependent upon the following pieces of third-party software:

- 1) **Arch Linux:** Main operating system for the SHADE computer
- 2) **Core Linux Utilities:** Basic components required to run SHADE (but are not part of the core Arch distribution) include NetworkManager, vim, vi, GRUB, efibootmgr, sudo, libusb
- 3) **git:** Version control software used during development, and best way to install SHADE software on a new machine
- 4) **Arduino CLI IDE:** Required to program the on-board arduino

- 5) **astrometry.net:** Software for generation and use of astrometric calibration data. This code is built from source.
- 6) **astrometry index files:** These are used by the astrometric
- 7) **Python and pip:** All core SHADE software is written in Python and requires a python interpreter. Pip is used to install third-party python modules.
- 8) **ZWO ASI SDS:** Development kit for the SHADE camera. This handles all USB communication with the camera, and is used with a python wrapper
- 9) **wcslib, cairo, netpbm, libpng, libjpeg, bzip2, swig:** Required for building astrometry.net software

SHADE is dependent upon the following third-party Python modules:

- 1) **Skyfield (1.36):** Skyfield is a powerful open-source astronomy package, and SHADE uses it extensively for handling timescales, planetary motion, coordinate transformation, propagation, and much more.
- 2) **scipy (1.6.3):** Used by legacy math components, including orbit determination
- 3) **dill (0.3.3):** A more powerful serialization library, used for saving state data to disk
- 4) **pyproj (3.0.1):** Used by legacy math components
- 5) **pyserial (3.5):** Used for communication with all serial devices, including power module, weather module, door control arduino and stage
- 6) **opencv-python-headless (4.5.1.48):** Version of the opencv module (used in image processing) that does not require an active X UI running
- 7) **zwoasi (0.0.22):** A python wrapper for the ZwoASI SDK. This is required for interfacing with the camera through Python
- 8) **python-pillow (8.2.0):** Fork of python image library (PIL), required for image processing and manipulation
- 9) **numpy and astropy:** Required for building astrometry.net software

The setup script is dependent upon the following Python modules:

- 1) **Spacetrack:** Spacetrack's Python module allows for the simplification of API calls to the spacetrack.org database, such as user account control, request throttling, and controlling data format.
- 2) **Skyfield:** Skyfield must be available to the startup script so that ephemerides and time information can be fetched from various remote databases.
- 3)

4. Software Diagrams

1. Setup Script FBD

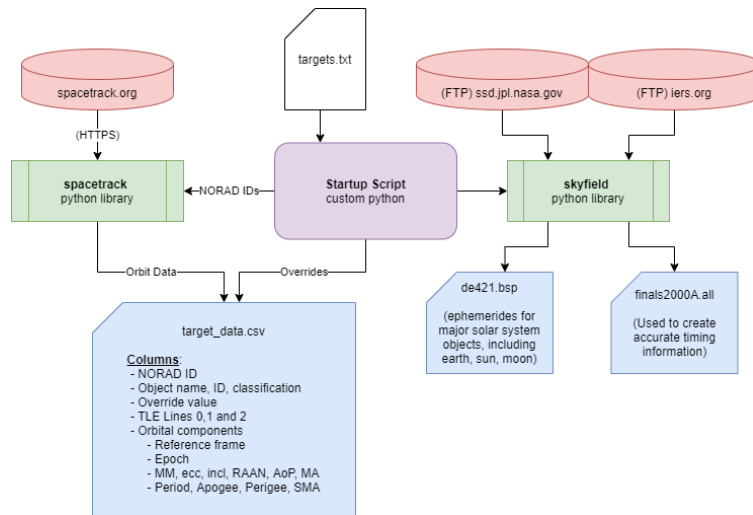


Fig. 72 FBD of the setup script

2. Startup Process

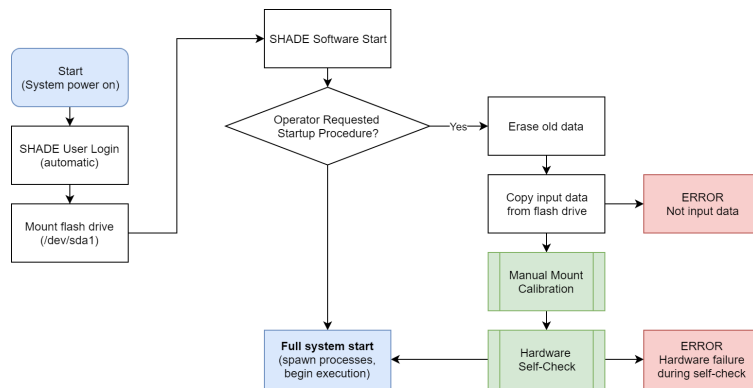


Fig. 73 Flow chart of the on-board computer's startup sequence

3. Scheduler Flow Chart

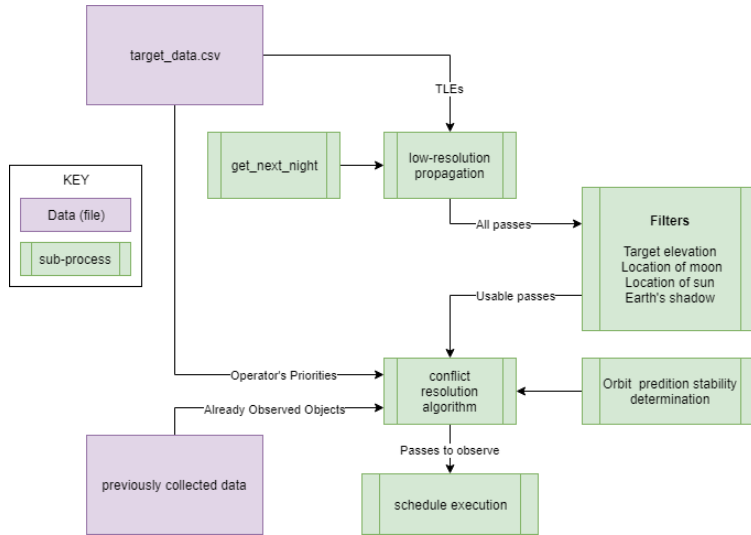


Fig. 74 Flow chart of SHADE scheduler

4. Image Processor Flow Chart

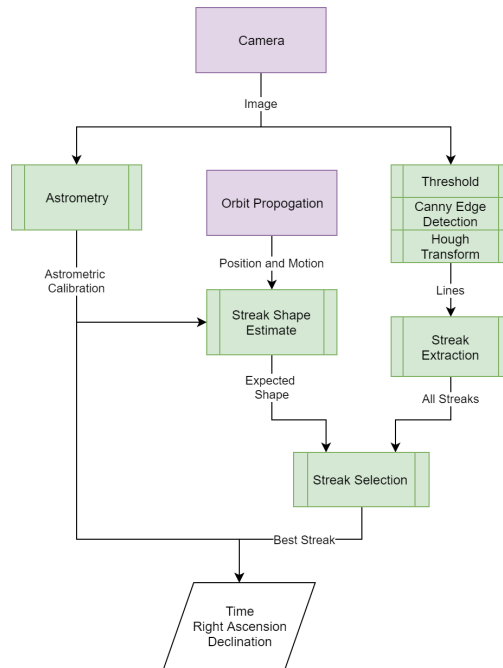


Fig. 75 Flow chart of SHADE image processor

5. Calibration Flow Chart

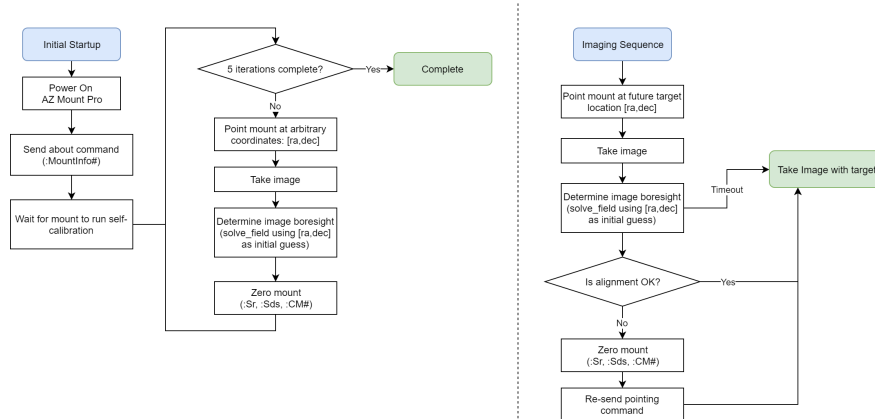


Fig. 76 Flow chart for both the initial (left) and pre-image (right) portions of the calibration process.

6. Wiring Diagram for UDOO Arduino and Braswell Pinouts

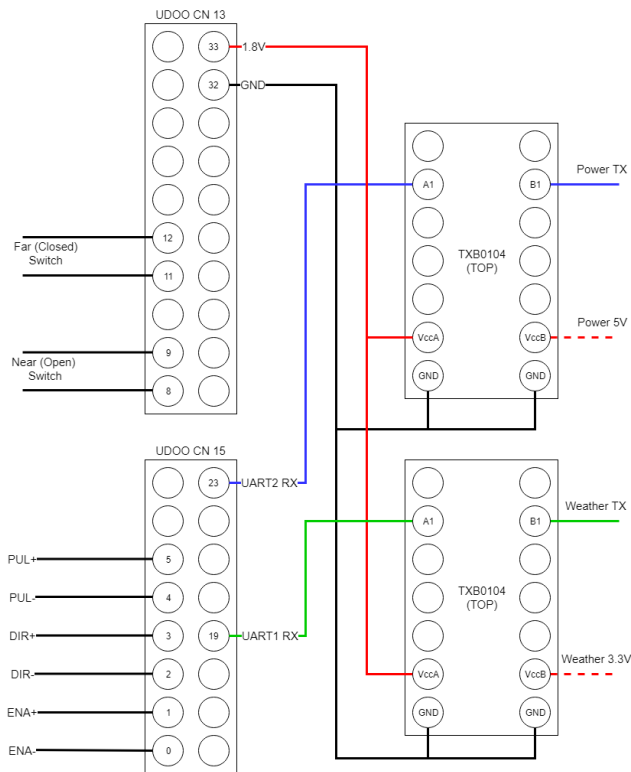


Fig. 77 Diagram showing all necessary wiring from the UDOO to weather detection module, power module, limit switches and stepper motor controller.

5. Full Risk Accounting

The criteria used in evaluating each identified risk are shown in Figures 78 and 79.

What Is the Likelihood the Risk Will Happen?			
Level		Your Approach and Processes...	
Likelihood	1	Not Likely:	...Will effectively avoid or mitigate this risk based on standard practices
	2	Low Likelihood:	...Have usually mitigated this type of risk with minimal oversight in similar cases
	3	Likely:	...May mitigate this risk, but workarounds will be required
	4	Highly Likely:	...Cannot mitigate this risk, but a different approach might
	5	Near Certainty:	...Cannot mitigate this type of risk; no known processes or workarounds are available

Fig. 78 Criteria for evaluating risk likelihood

Given the risk is realized, what would be the magnitude of the impact?				
Level	Technical	Schedule	Cost	
Consequence	1	Minimal or no impact	Minimal or no impact	Minimal or no impact
	2	Minor perf shortfall, same approach retained	Additional activities required; able to meet key dates	Budget increase or unit production cost increase <1%
	3	Mod perf shortfall, but workarounds available	Minor schedule slip; will miss need date	Budget increase or unit production cost increase <5%
	4	Unacceptable, but workarounds available	Program critical path affected	Budget increase or unit production cost increase <10%
	5	Unacceptable; no alternatives exist	Cannot achieve key program milestone	Budget increase or production cost increase >10%

Fig. 79 Criteria for evaluating risk recoverability

The highest severity risks which were not realised are discussed in detail here.

Risk: Starlink Streaks

ID: SLS

Category: Technical

Risk Statement: If additional streaks are present in the images taken, they have the potential to result in false-positive orbit updates, rendering the associated observations useless.

Likelihood: 5 **Recoverability:** 4 **Severity:** 20

GHOST was designed under the assumption that additional streaks of notable size were not likely to be present in the long exposure images created. With the advent of the SpaceX Starlink program, which intends to populate LEO with constellations of satellites for use in providing satellite internet, more objects capable of generating significant streaks are likely to be present in the sky at any given time.

Mitigation: Implementation of the Hough Transform image processor makes SHADE more robust to failure due to additional streaks, thus avoiding the risk rather than mitigating it.

Likelihood: 5 **Recoverability:** 1 **Severity:** 5

Risk: Target Orbit Instability

ID: TOI

Category: Technical

Risk Statement: If any targets have orbits with especially unstable characteristics, the uncertainty in their position will grow with time, reducing the likelihood of successful imaging attempts later on in the mission.

Likelihood: 4 **Recoverability:** 4 **Severity:** 16

WRAITH noted decay in orbit prediction accuracy as a possible risk for increasing the duration of their deployments, even though they did not pursue mission extension. Although mission extension allows for more attempted observations if one fails, the subsequent observations would be even more likely to fail as the orbit prediction becomes less accurate. Furthermore, planning for observations of different objects for the majority of the mission requires that some objects be imaged much later on, which gives less time for remedial observations and poses much greater risk to baseline observation success likelihood.

Mitigation: The study conducted on the instability of different orbits and the degree to which each characteristic affects the stability gives additional information to the scheduler to properly account for and prioritise objects with orbital characteristics which indicate instability.

Likelihood: 1 **Recoverability:** 2 **Severity:** 2

Risk: Sub-Optimal Charge

ID: SOC

Category: Technical

Risk Statement: If sub-optimal charging conditions are present during the day, the battery may not fully charge which then affects SHADE's ability to fully utilise the subsequent night for observations.

Likelihood: 5 **Recoverability:** 3 **Severity:** 15

Our expectation is not that the system will experience optimal charging conditions for even the majority of its missions. Some of the design inherently accounts for this in that optimal charging conditions will charge the battery twice as quickly than necessary. Given the variability in power output

capability of the panels based on the conditions, designing with less than optimal performance in mind allows for more flexible operation of SHADE more often.

Mitigation: Monitoring the battery’s state of charge will allow for SHADE to estimate the number of observations it can perform in a night and prioritise objects according to the available capacity. The modifications to the scheduler which now generates a schedule at the beginning of every night allows for more flexibility in the observation schedule than adhering to the initially generated schedule.

Likelihood: 5 Recoverability: 1 Severity: 5

All identified risks have been tabulated and are shown side-by-side to demonstrate the change in their component severity scores before and after the mitigation methods have been applied.

Technical Risks - Pre Mitigation					Technical Risks - Post Mitigation				
Risk	Risk ID	Likelihood	Recoverability	Severity	Risk	Risk ID	Likelihood	Recoverability	Severity
Starlink Streak	SLS	5	4	20	Starlink Streak	SLS	5	1	5
Diurnal Heating	DIH	5	4	20	Diurnal Heating	DIH	5	1	5
Target Orbit Instability	TOI	4	4	16	Target Orbit Instability	TOI	4	1	4
Suboptimal Charge	SOC	5	3	15	Suboptimal Charge	SOC	5	1	5
Power Budget Accuracy	PBA	3	3	9	Power Budget Accuracy	PBA	1	3	3
Self-Diagnostics Accuracy	SDA	2	4	8	Self-Diagnostics Accuracy	SDA	1	2	2
Weather Detection Commanding	WDC	2	4	8	Weather Detection Commanding	WDC	1	4	4
COTS Moisture Management	CMM	2	4	8	COTS Moisture Management	CMM	1	4	4
Roof Closing Routine	RCR	1	5	5	Roof Closing Routine	RCR	1	5	5
GPS Signal Acquisition	GPS	1	5	5	GPS Signal Acquisition	GPS	1	5	5
Auto-Calibration Accuracy	ACA	1	5	5	Auto-Calibration Accuracy	ACA	1	2	2
Processor Heating	PRH	2	2	4	Processor Heating	PRH	2	2	4
Weather Detection Fault Thresholds	WFT	2	2	4	Weather Detection Fault Thresholds	WFT	1	2	2

Fig. 80 Comparison of technical risks pre and post mitigation

Management Risks - Pre Mitigation					Management Risks - Post Mitigation				
Risk	Risk ID	Likelihood	Recoverability	Severity	Risk	Risk ID	Likelihood	Recoverability	Severity
Single Point Failure	SPF	4	4	16	Single Point Failure	SPF	2	4	8
Schedule Slip	SLP	3	3	9	Schedule Slip	SLP	3	2	6
Schedule Driven Progress	SDP	2	4	8	Schedule Driven Progress	SDP	2	2	4
Intra-Team Communication	ITC	3	2	6	Intra-Team Communication	ITC	3	1	3
Resource Management	RMA	3	2	6	Resource Management	RMA	2	2	4

Fig. 81 Comparison of management risks pre and post mitigation

External Risks - Pre Mitigation					External Risks - Post Mitigation				
Risk	Risk ID	Likelihood	Recoverability	Severity	Risk	Risk ID	Likelihood	Recoverability	Severity
Operator Error	BOP	2	4	8	Operator Error	BOP	1	4	4
Lockdown	LDN	3	2	6	Lockdown	LDN	3	1	3
Theft	THF	1	5	5	Theft	THF	1	5	5
Obscured Solar Panel	SPO	1	5	5	Obscured Solar Panel	SPO	1	5	5
Wildlife Interference	WLD	1	2	2	Wildlife Interference	WLD	1	2	2

Fig. 82 Comparison of external risks pre and post mitigation

6. Conceptual Design

1. Power System

Authors: Robert Redfern, Vinay Simlot, Jacob Weiner

SHADE's power system has split functionality and was designed to meet FR 2, 7 and 8. The power functional block diagram in Figure 83 shows the duality of the battery and how the system will charge during the day and discharge during a nighttime deployment. It also lists the power dependencies and the voltage that each subsystem or sensor operates at.

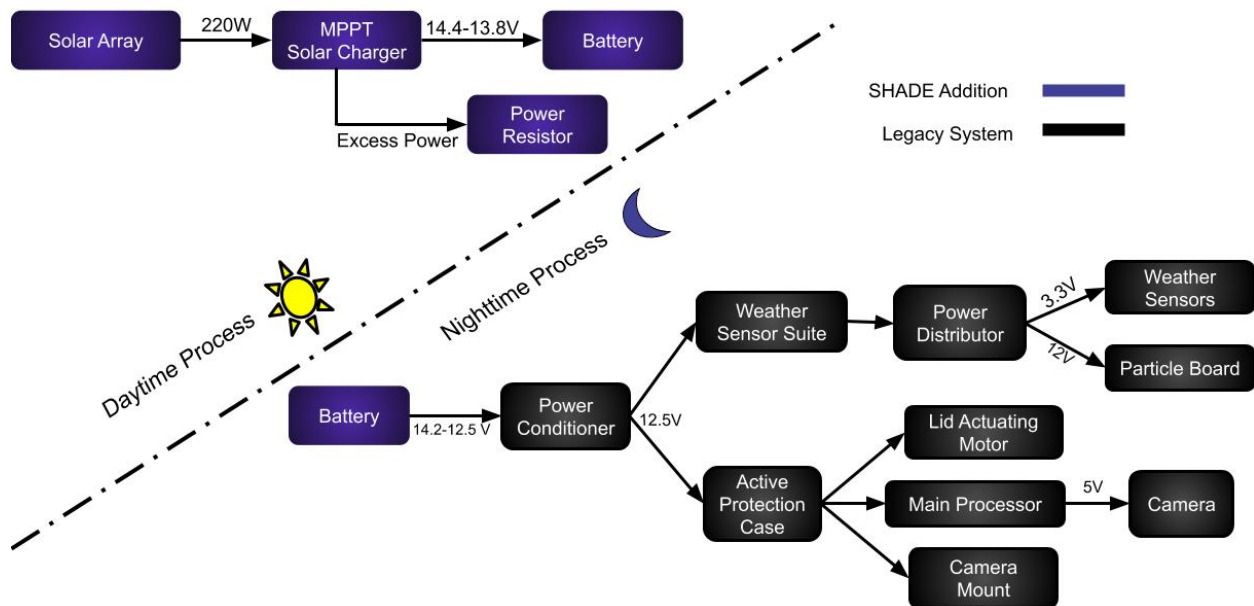


Fig. 83 Power System Functional Block Diagram

The core electrical components of SHADE remain largely unchanged from WRAITH and all receive clean, 12.5 VDC power from the power conditioner. The weather sensor suite and active protection box are both connected to the power conditioner via a junction box. The weather sensor suite receives power through an umbilical cable connected to a dual voltage power distribution board. The Particle board handles all cellular data communication and sends sensor data to the main UDOO processor. The Particle board

operates at 12.5 V while the sensors require a 3.3 V input from the power distribution board. Within the active protection box, the main processor, lid actuating motor and controller, as well as the camera mount all receive 12.5 V power from the electrical junction box. The camera is powered via a USB connection to the main processor and operates at 5 V.

SHADE’s power requirements are dependent on information from WRAITH. Due to the COVID-19 pandemic, WRAITH was not able to validate their own power requirements and the SHADE has not yet been undergone multi-day deployment testing to be able to determine the power requirements of system components and actual duty cycles. With this in mind, SHADE used a power budget developed by WRAITH, seen in Figure 84, and assumed this to be a worst case power usage scenario.

Power Budget			
Component	Peak Draw (A)	Duty Cycle (%)	Expected Draw (A)
Acutation Mount	2.00	40	0.80
Microcontroller	0.50	60	0.30
Main Processor	3.00	95	2.85
Camera	1.00	30	0.30
GPS	0.02	100	0.02
Motor/Controller	2.00	10	0.20
Lightning	3.50E-04	100	3.50E-04
Temp/RH/Baro	6.50E-04	20	1.30E-04
Precipitation	0.10	100	0.10
IR Therm	2.50E-03	100	2.50E-03
Anemometer	0.02	100	0.02
Motor	2.00	10	0.20
			x12 Hours
		Total Draw	55.12 Ah

Fig. 84 Power Budget

While a 12 hour, continuous imaging period is unlikely, the 55.14Ah power draw is still significant. In WRAITH’s previous testing the legacy 60Ah SLA batteries failed prior to the 12 hour mark of deployment. This drove SHADE to budget for a 30% overhead in total battery capacity. A 71.2Ah battery was then set as the minimum required capacity for SHADE to safely operate.

Battery: Designs Considered

Authors: Robert Redfern, Jacob Weiner

Since the battery is the crossover between the daytime and nighttime power systems, and is key to SHADE’s endurance, it was imperative that SHADE improved on the previous SLA battery pack. To do so, SHADE chose four different types of commercially available battery technologies to research and compare. Below is an analysis of Sealed Lead Acid, Lithium Iron Phosphate, Lithium Ion, and Lithium Polymer

batteries.

Sealed Lead Acid

The inherited power system used by WRAITH consisted of three Duracell DURDC12-20NB sealed lead acid batteries. Each battery is rated at 12 V with a nominal capacity of 20Ah. When connected in series, the total battery capacity is 720 Wh. Each battery weighs 13.3 lbs resulting in a power system mass of nearly 40 lbs. These three batteries can power SHADE for one night, but have an average cycle life of only 175. This means they will need to be replaced every 175 nights of deployment. Each battery costs approximately \$90, bringing the system cost to \$270.



Fig. 85 Duracell 12V SLA

Lithium Iron Phosphate (LiFePO4)

Lithium Iron Phosphate batteries are the most expensive power supply in the study at around \$750. To offset this they have the longest cycle life. They are mostly used in RV and marine applications due to their light weight, ability to quickly recharge, and long cycle life. This battery type was also the only one to receive independent certifications. One LiFePO4 battery weigh 20.5 lbs and have a nominal capacity of 75 Ah at 12 V or 900 Wh. This battery also does not require the use of an extra voltage regulator.



Fig. 86 Power Sonic 12V LiFePO4

Lithium Ion (Li-ion)

Li-Ion (Lithium ion 18650 based) Cost: \$675 Weight: 10 lbs Voltage: 25 Capacity: 32Ah/819Wh Cycle Life: 300-500 3rd Party Certifications: N/A Lithium ion batteries typically come in either 3.6 or 3.7 volt cells. As a result, 12 V battery packs do not exist. Furthermore, few commercial companies manufacture large capacity battery packs for the general consumer. As a result, many independent companies purchase the Li-ion cells and package them themselves. For this trade, the specific battery pack product uses LG LGDBHE21865 cells and the pack is not manufactured to any standards for safety or rated output that the group could find. That being said, the manufacturer estimates the 25 V battery pack to have a cycle life between 300 and 500 cycles and a nominal capacitance of 32 Ah or 819 Wh. The estimated weight is 10 lbs.

Lithium Polymer (LiPo)

Lithium Polymer batteries are a common choice for remote control enthusiasts and have some OTS solutions. Still, the group could not find a manufacture that had independent ratings for safety and output for a battery



Fig. 87 Example of Li-ion Battery Pack

that would be required by SHADE. LiPo batteries are also prone to ignite while charging and require a special charger to maintain individual cell voltages. For the purpose of this trade the LiPo battery chosen has a nominal voltage of 48V with a rated capacity of 22 Ah or 1056 Wh. The chosen pack has a weight overall of about 22 lbs with an estimated cycle life of 250 to 450 cycles.



Fig. 88 Lithium King 48V LiPo

Battery Summary

The figure below provides a table of each power supply option along with their respective Pros and Cons. Each system will be compared later in the corresponding trade study.

Power System Option	Pros	Cons
SLA Battery (Current)	Inexpensive (\$270) Carry over from WRAITH "Off the shelf"	3 Batteries Heavy weight (40lbs) Low cycle life (frequent replacement) Slow charging rate
Lithium Iron Phosphate Battery	1 Battery High cycle life Lighter weight Faster charging rate "Off the shelf"	Higher cost (\$750) Needs additional insulation Special charger
Lithium Ion	1 Battery Lighter weight Improved cycle life	Higher cost (\$675) Hard to find "off the shelf" solution Requires extra voltage regulator
Lithium Polymer	1 Battery Lighter weight "Off the shelf" Slightly improved cycle life	High risk for fire Requires extra voltage regulator Medium cost (\$400)

Fig. 89 Battery Pro Con Table

Battery Trade Study

To further determine which battery would best suit SHADE, a trade study was conducted. Figure 90 describes the metrics chosen and which functional requirements they are designed to meet.

Metric	Weight	Driving Requirement	Rational
Weight	0.30	FR 7 DR 7.1	To meet OSHA safety recommendations, the weight of the battery(s) must be factored into the selection process. This weight limit is fundamental to SHADE and is prioritized appropriately.
Cost	0.10	Budget	Balancing a budget is important but the battery(s) implementation is more so. As a result it receives minimal weight by comparison.
Cycle Life	0.10	FR 2 DR 2.2.1	It is expected that SHADE will endure multiple deployments over its lifetime. As a result, the team must consider the frequency of battery replacement and deployment duration.
Cost/Cycle Life	0.25	Budget	This metric is important when considering SHADE's final use. It is expected that SHADE will endure multiple deployments potentially spanning several days. A single night deployment equates to one cycle. For long term use, the operator will have to continuously replace batteries with a low cycle life. As a result, this section has taken a priority in weighting.
Reliability	0.25	FR 2 DR 2.1 DR 2.2	SHADE is expected to survive in a variety of weather conditions. Entering in and out of safe mode requires electrical power and the power solution must be able to, at a minimum enter SHADE into safe mode. The power system must also be safe for the operator when charging and in transit.

Fig. 90 Battery Choice Metrics and Rationale

Figure 92 shows the range of values associated with each metric. Reliability is quantified by independent verification and certifications of the selected batteries. These include but are not limited to UL, ISO, and similar standardizing bodies. Also included is whether or not an off the shelf solution exists for the product. In some cases, these might be small volume independent manufacturers as opposed to commercial companies.

Power Supply Metric Values

Metric	1	2	3	4	5
Weight [lbs]	> 35	30-35	25-30	20-25	< 20
Cost [\$USD]	> 1000	700-1000	500-700	300-500	< 300
Cycle Life [#]	< 200	200-500	500-1000	1000-1500	> 2000
Cost/Cycle Life [\$/#]	< 2	1.5-2	1-1.5	0.5-1	< 0.5
Reliability*	Immediate likelihood of failure	High likelihood of failure	Moderate likelihood of failure	Minimal chance of failure	Failure is improbable

Fig. 91 Battery Metrics Values

Figure 92 shows the results of the trade study and is followed by an in depth rationale of how each battery

was graded.

Power Supply Trade Study Results

Metric	Weight	SLA	LiFePO4	Li-ion	Li-Po
Total Weight [lbs]	0.30	1	4	5	4
Cost [\$USD]	0.10	5	2	3	4
Cycle Life [#]	0.10	1	5	4	2
Cost/Cycle Life [\$/#]	0.25	2	5	2	3
Reliability*	0.25	5	4	2	2
Total	1.0	2.65	4.15	3.20	3.05

Fig. 92 Battery Trade Study Results

Sealed Lead Acid (SLA)

- Weight - 1: The SLA system is comprised of three batteries of 13.3 lbs each. This generates a total power supply mass of approximately 40 lbs. This is system with the heaviest weight.
- Cost - 5: Each battery costs approximately \$90 USD. The system as a whole would therefore cost \$270. This is the least expensive battery option.
- Cycle Life - 1: These SLA batteries have a cycle life of 150-200. For this trade study the average was taken (175 cycles). This means the SLA batteries would need to be replaced every 175 deployments on average.
- Cost/Cycle Life - 2: Dividing the total cost by the average cycle life the batteries would cost \$1.54 per cycle.
- Reliability - 5: SLA batteries are very common and are known for their low fire risk. They are also easy to find off the shelf so supply would not be an issue. For these reasons SLA batteries receive the highest reliability rating.

Lithium Iron Phosphate (LiFePO4)

- Weight - 4: A single LiFePO4 battery would be sufficient to power the SHADE system. This one battery weighs 20.5 lbs, generating an almost 20 lbs reduction in overall mass.
- Cost - 2: This battery retails for approximately \$750 making it the most costly battery in this study. However it would still only account for 15% of the project budget.
- Cycle Life - 5: LiFePO4 batteries have an excellent cycle life of 2000. This is the highest in the trade study and would improve the longevity of the power supply.
- Cost/Cycle Life - 5: Dividing cost by cycle life each deployment would cost \$0.375 USD. This proves that even though the initial cost of the battery is high, the longevity it provides actually makes it more

affordable long term.

- Reliability - 4: LiFePO₄ batteries come with UL, IEC, UN, and ISO certifications. This documents them as reliable fast charging batteries with a low chance of failure.

Lithium Ion (Li-Ion)

- Weight - 5: SHADE would be able to operate on a 10 lbs Li-Ion battery, making it the lightest of all power supply options considered.
- Cost - 3: Li-Ion batteries are somewhat expensive due to their energy density. The required battery would cost \$675 USD, just below its LiFePO₄ counterpart.
- Cycle Life - 4: With a cycle life of 300-400, Li-ion batteries would almost double the cycle life of the current system.
- Cost/Cycle Life - 2: Due to the large increased in initial price, the cost per cycle life is estimated at \$1.92 per cycle.
- Reliability - 2: Li-ion batteries do have an increased fire risk. While the modularity of SHADE would shelter other components from fire damage, the reliability of the system itself is lower.

Lithium Polymer (Li-Po)

- Weight - 4: The required Li-Po battery would weigh 22 lbs when implemented. This would lower system mass and be beneficial to SHADE's functional requirements.
- Cost - 4: With a price of \$400, a single Li-Po based system would not increase buy in costs significantly, with the current system at \$270.
- Cycle Life - 2: With an average cycle life of 350, there is not a significant increase over the current system.
- Cost/Cycle Life - 3: With a higher cost and a small increase in cycle life, Li-Po battery based power would represent only a slight savings at \$1.14 per cycle.
- Reliability - 2: Li-Po batteries suffer some of the same fire risks that Li-Ion batteries do. This coupled with fewer 3rd party certifications means the probability of failure is higher than that of other power supplies.

Battery: Design Choice

Based on the trade study in Figure 92, a single LiFePO₄ battery was shown to be the best battery for SHADE. While there is a significant initial cost associated with LiFePO₄ batteries, they have the lowest cost per cycle life. The specific battery selected was a PowerSonic PSL-SC-12750-G24 that is rated for 75Ah at 12.5 volts. It weighs 20.5 lbs, reducing the current three battery system down weight by 20 lbs. This reduction helps limit the individual module weight and the number of modules required to maintain a 50 lbs weight limit.

Solar Panel: Designs Considered

Three types of solar cells currently exist on the consumer market: monocrystalline, polycrystalline and

thin-film solar cells. Monocrystalline and polycrystalline solar cells are both made from silicon. Polycrystalline solar cells are made by melting fragments of silicon to form wafers on the cells. Monocrystalline cells are made from cutting silicon bars into wafers and forming those wafers into a cell. The monocrystalline construction generally yields higher efficiencies. Thin-film solar cells yield the lowest efficiencies while having the highest cost, usually made from Gallium Arsenide or Cadmium Telluride. The pros and cons are listed in Figure 93.

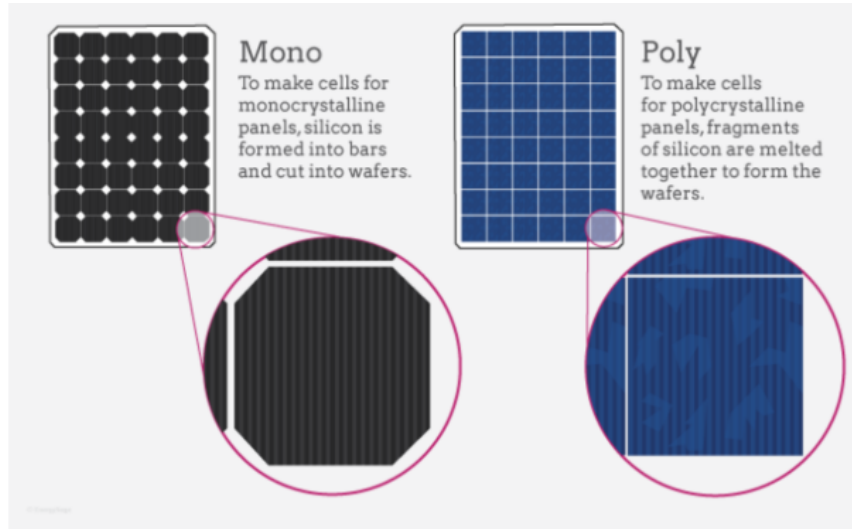


Fig. 93 Monocrystalline vs Polycrystalline cells

Solar Cell Trade Study

The solar cells were compared in a trade study (Figure 94) using the metrics in Figure 95.

Solar Technology Metric Values

Metric	1	2	3	4	5
Power Efficiency [%]	<10	10-12	12-17	17-20	>20
Thermal Coefficient [% / °C]	Larger than -0.8	-0.8 to -0.5	-0.5 to -0.4	-0.4 to -0.3	-0.3 and smaller
Cost (cell dependent)	Most Expensive		Moderately Expensive		Least Expensive

Fig. 94 Solar cell technology metrics

Solar Technology Trade Study Results

Metric	Weight	Monocrystalline	Polycrystalline	Thin Film
Power Efficiency	0.40	5	3	2
Thermal Resistance	0.40	3	3	4
Cost	0.20	2	3	4
Total	1.0	3.6	3.0	3.2

Fig. 95 Solar cell technology trade study

Monocrystalline

- Power Efficiency - 5: Monocrystalline solar cells are able to convert more solar energy into electrical energy than the other technologies currently available (about 20-23%). As a result, a solar array would need fewer individual cells to meet the power requirements of the battery charger.
- Thermal Coefficient - 3: Heat degrades solar cell performance regardless of technology. On average, monocrystalline cells lose performance at a rate of $-0.5\%^{\circ}\text{C}$. This value differs from manufacture to manufacturer.
- Cost - 2: Monocrystalline cells are less expensive per watt since they are becoming industry standard.

Polycrystalline

- Power Efficiency - 3: On average, polycrystalline solar cells have a power efficiency of 15-17%.
- Thermal Coefficient - 3: Polycrystalline cells will lose power performance at an average rate of $-0.5\%^{\circ}\text{C}$.
- Cost - 3: Because polycrystalline solar cells are an older technology, they are generally less expensive than other solar cells.

Thin Film

- Power Efficiency - 2: Thin film solar technologies only average around 11% efficiency.
- Thermal Coefficient - 4: At $-.35\%^{\circ}\text{C}$, thin film solar is the most affected by temperature changes.
- Cost - 4: Most applications for thin film solar are highly specialized. As a result, they are often more expensive than other commercial applications.

Solar Cell: Design Choice

Based on the solar cell trade study, monocrystalline solar cells were selected for SHADE's solar panels. The SunPower MAXEON Gen III monocrystalline solar cells were selected. The MAXEON Gen III cells have an efficiency of 23.1% and a power output of 3.54 W per cell. A SmartSolar charge controller was

selected to take input power from the solar panels, and charge SHADE's batteries. The charge controller will adjust the load to maximize the power output from the solar panels to charge the battery. The controller will divert power automatically when it exceeds the maximum power for the charger.

Silicon solar cells lose efficiency as the temperature increases. The MAXEON Gen III cells have a temperature coefficient of $-0.29\%/^{\circ}\text{C}$ when the temperature of the cells is above 25°C . The loss of efficiency necessitated thermal controls. Four cooling technologies have been explored for photovoltaics: water circulation, phase change materials, forced air circulation, and heat sinks. Water circulation would require large water tanks or water that would have to be replaced regularly, neither would fulfill the functional requirements. Phase change material technologies are still nascent and not commonly available. Forced air circulation for solar panels requires air to move between 2-5 m/s to have any impact, which would require fans the size of large ceiling fans. Heat sinks for solar panels are usually aluminum pieces attached to the underside of the panel, increasing the exposed surface area to facilitate convection.

2. Modularity

Author: Marlin Jacobson

Another critical project element of SHADE is modularity, which includes the weather detection, passive protection, and active protection systems. SHADE's modularity describes the degree to which its system components are separated and reorganized into transportation and deployment groups. SHADE implements this modular design to reduce the amount of weight the operator is required to carry in one trip from the vehicle to SHADE's deployment site. This critical project element satisfies **FR 2** by enabling the system to function autonomously during deployment and **FR 3** by autonomously entering and exiting a safe mode to protect itself from adverse weather using each modularity component.

The first core component of modularity is the modularization of the system as a whole for ease of transportation to the deployment site. This novel modularization satisfies **FR 7** by limiting the total system deployment time to 30 minutes and **FR 8** by limiting the amount of weight the operator is required to carry to 50 lbs or less in one trip from the vehicle to SHADE's deployment site. The second core component of modularity is the modification of the active protection system from WRAITH's project, which also satisfies **RFs 7 and 8**. This modification will be explained further in the Active Protection system section. The following options investigate and provide reasoning for the design choice of the modularity transportation groupings.

Transport Grouping Modules: Designs Considered

In order to determine the most feasible module grouping for transportation from the vehicle to SHADE's deployment site, a pros and cons list (Figure 96) was used.

Modularity Option	Pros	Cons
Option 1: <ul style="list-style-type: none"> ● Actuation Mount and Telephoto Lens/Camera ● Processor and Weather Protection Box ● Environmental Suite ● Solar Panel ● Battery Pack 	Camera and Mount will already be connected Weather Protection Box will be light	Awkward casing for transport will be needed for the camera and mount Power system will need to be connected during setup
Option 2: <ul style="list-style-type: none"> ● Actuation Mount and Telephoto Lens/Camera ● Processor, Battery Pack, and Weather Protection Box ● Environmental Suite ● Solar Panel 	Camera and Mount will already be connected Power system will already be in place Least amount of trips needed	Weather Protection Box will be heavy Awkward casing for transport will be needed for the camera and mount
Option 3: <ul style="list-style-type: none"> ● Actuation Mount ● Telephoto Lens/Camera ● Processor, Battery Pack, and Weather Protection Box ● Environmental Suite ● Solar Panel 	Power system will already be in place Easier to transport for actuation mount and camera	Weather Protection Box will be heavy Camera and Mount will need to be assembled
Option 4: <ul style="list-style-type: none"> ● Actuation Mount ● Telephoto Lens/Camera ● Processor and Weather Protection Box ● Environmental Suite ● Battery Pack ● Solar Panel 	Weather Protection Box will be light Easier to transport for actuation mount and camera	Power system will need to be connected during setup Camera and Mount will need to be assembled More trips between site and vehicle

Fig. 96 Modularity Options Pros and Cons

After analyzing the pros and cons list as a team and reviewing the design of each component, the group determined that a trade study was unnecessary to decide upon the appropriate transport module groupings. Instead, the group determined that the groupings would be driven by the new and modified designs of the active protection and power systems. Initially, Option 2 was chosen because it offered the smallest number of trips needed between the vehicle and deployment site. Four trips would help to maintain the total deployment time at 30 minutes or less while keeping the weight of each module at a minimum. During this part of the design process, however, the finished designs and weights of each component were unknown; therefore, the team was aware that the transport module groupings could change from Option 2.

Transport Grouping Modules: Design Choice

After greater development of the power and active protection systems, the team determined that two changes to the Option 2 module groupings was required. First, rather than combining the battery pack with

the active protection (weather) box, the group determined that the battery pack shall be transported in the same trip as the environmental suite. This change was made due to greater than initially predicted dimensions of the active protection system and battery pack weight. Overall, it was determined that carrying the active protection system box, which includes the processor and power distributor, in one trip and carrying the battery pack and environmental suite together in another trip was the most feasible option for the user. The second change to the Modularity Option 2 was the addition of a fifth trip if needed by the user. After further development of the solar panel design, it was determined that two solar panels were needed for the system. The user, therefore, may make two trips for the deployment of the solar panels. Figure 97 summarizes the design choice for the transport module groupings.



Fig. 97 Transport Grouping Modules Design Choice

3. Passive Protection

Authors: Marlin Jacobson, Davis Peirce

When there are adverse environmental conditions, SHADE must be able to physically protect itself. This protection may be against rain, snow, hail, extreme heat, extreme cold, or vibrations. To ensure a redundant and weatherproof system, each module of SHADE shall be protected from both vibrations during transport and the environment during deployment and operation. SHADE's passive protection will function to protect the system and its electrical components at all times and ensure it can survive during nominal to moderate environmental conditions. These conditions may include moisture buildup, heating, or cooling within the active protection box, power system, or environmental suite. The methods of passive protection considered include various COTS boxes. Designing and implementing modifications to each COTS box was anticipated, such as adding holes for wires, waterproofing, and any additional vibration protection required, in order to integrate each module with the others. The four COTS cases investigated are a general plastic storage Sterilite container with added insulation, the Pelican Air Case with Pick N' Pluck Foam, the Polycase WH-18 Hinged NEMA Enclosure with added insulation, and the Plano Sportsman's Trunk with added insulation.

Passive Protection: Designs Considered

Polycase WH-18 Hinged NEMA Enclosure

The Polycase WH-18 Hinged NEMA Enclosure is an ABS COTS box that comes in various sizes. The primary advantage that a Polycase WH-18 provides is the flexibility and ability for customization. The box may be customized via CNC machining, cutting any required holes for cables, threads for screws or attachments, venting, or other cutouts. The WH-18 is made of ABS plastic. With a relatively small size and a lack of built-in foam or other vibration protection, the Polycase option would not be suitable for housing the camera and GHOST hardware, but it could be used to house other electrical subsystems. Polycase also sells cable seals and glands.



Fig. 98 Polycase WH-18 Hinged NEMA Enclosure

Pelican Air Case with Pick N' Pluck Foam

The Pelican Air Case is a highly durable and highly protective, HPX² Polymer (proprietary polypropylene blend) COTS case that comes in various sizes and is used for storage and transportation of various materials. This case has an automatic purge valve that keeps water and dust out while balancing the air pressure inside and easily-modifiable polyurethane foam for insulation and vibration protection. The case is also sealed using a EPDM O-Ring, which provides substantial weather and thermal protection. Its advantages include high durability and substantial protection against vibrations, shock, and the environment without any modifications. Disadvantages of this case are that it may be difficult to add external modifications or holes for wiring along with the cost.



Fig. 99 Pelican Air Case

Sterilite Industrial Storage Bin

The Sterilite Industrial Storage Bin, which comes in various sizes, would enable a wide range of modifications to be made, which may include adding holes for wires and heat dissipation, various sizes of insulation for weather and vibration protection inside, and other weather-proofing materials. This COTS case is made of plastic, has channeled walls to provide strength and resistance to crushing from all sides, has a

fully-removable lid with two latch-style handles, key holes for tie-down during transportation, a tightly-fit lid for water protection, and a deeply recessed lid that enables secure stacking with other boxes for storage. Advantages of this case are that it is lightweight and strong, it can be easily modified, and is inexpensive. Downsides of this case are that many modifications would be needed for each module to provide vibration protection and that it does not provide high level protection off the shelf against severe weather and thermal conditions.



Fig. 100 Sterilite Industrial Storage Bin

Plano Small Sportsman's Trunk

The Plano Small Sportsman's Trunk is a plastic COTS box that comes in various sizes. It is of a size where it could hold any individual module during transportation and deployment, including the camera and GHOST hardware. It is lockable and has extensions so the box may be tied down during transportation. Notably, Plano does not list specifications on the type of plastic used or any material properties of the box. The Plano trunk would require manual modifications for cables and vibration protection as well as sealing and waterproofing.



Fig. 101 Plano Small Sportsman's Trunk

Passive Protection Summary

Figure 102 provides the advantages and disadvantages of each of the COTS casing options that will be used for SHADE's passive protection system. The items listed below were also considered for the Passive Protection Trade Study; thus, these pros and cons will be further analyzed in the following section.

Casing Options	Pros	Cons
Polycase WH-22 Hinged NEMA Enclosure	Guaranteed waterproof. Durable off the shelf. Clear lid enables view inside. Metal padlocking hinges. Inexpensive. Lightweight. Some thermal protection.	Does not include insulation. Requires screws and manual assembly.
Pelican Air Case with Pick N' Pluck Foam Insulation	Guaranteed waterproof. Extremely durable off the shelf. Includes foam insulation. Easily customizable foam padding. Lightweight. Provides better thermal protection	Expensive. Less feasibility to add holes for wiring.
Sterilite Industrial Storage Bin	Inexpensive. Lightweight. Easily modified for wiring and holes. Easily stackable with multiple cases.	Cannot guarantee level of weatherproof. Low strength of plastic lid latches. Does not include foam insulation. Low thermal protection. No O-Ring seal.
Plano Small Sportsman's Trunk	Inexpensive. Lightweight. Durable. Easily modified for wiring and holes.	Does not include foam insulation. Little thermal protection.

Fig. 102 Passive Protection Option Pros and Cons

Passive Protection Trade Study

A trade study on the passive protection COTS box options was performed using the metrics below. The metrics in this case are cost, durability, ease of modification, weight, environmental protection, and vibrational protection. The weights and rationales of each metric are given in Figure 103.

Metric	Weight	Driving Requirement	Rationale
Cost	0.1	Budget	The passive protection COTS casing must adhere to the constraints of the budget; however, this metric obtains the lowest weight because the other constraints immediately impact the system's operation.
Durability	0.2	FR 7, DR 7.1.1	The passive protection COTS casing must withstand an indefinite number of off-road transports, deployments, and operations with low risk and maintenance.
Ease of Modification	0.3	FR 7, DR 7.1.3	The passive protection COTS casing will need to be modified to meet protection requirements for waterproofing and vibration protection, as well as the requirement for toolless assembly. This is an essential factor to ensure that the environmental and vibration hazards are met.
Weight	0.1	FR 7, DR 7.1	Several modules will utilize passive protection for both environmental and vibration protection during deployment, so the weight of the casing should be factored into the weight of the module.
Environmental Protection	0.2	FR 7, DR 7.1.3	The passive protection must be able to protect the module components against unforeseen circumstances such as water, hail, temperature fluctuations, or other adverse weather effects.
Vibration Protection	0.1	FR 7, DR 7.1.2	The passive protection must be able to withstand vibrations and impulses as a result of travelling. Some modules, namely the GHOST hardware, are likely to be especially sensitive, but the other modules are less likely to sustain damage during transport.

Fig. 103 Passive Protection Metric Rationale and Descriptions

This trade study considers four COTS box options for SHADE's passive protection system: the Sterilite Industrial Storage Bin, the Pelican Air Case with Pick N' Pluck Foam, the Polycase WH-22 Hinged NEMA Enclosure, and the Plano Sportsman's Trunk. The table of metric values (Figure 103) was used to assign a scoring value to each option with one being the worst case and five as the most ideal. Using the values and weights assigned for each metric, the highest scoring case will be the chosen option for SHADE. The following sections outline the scores and rationales for each case considered. The final results of the study are presented in Figure 104.

Passive Protection Metric Values

Metric	1	2	3	4	5
Cost (per unit)	>\$50	\$40-\$50	\$30-\$40	\$20-\$30	<\$20
Durability	Not durable		Moderately durable		Extremely durable
Ease of Modification	Impossible	Difficult	Moderate	Simple	Trivial
Weight	>12 lbs	10-12 lbs	7-10 lbs	5-7 lbs	<5 lbs
Environmental Protection	Not water resistant, no thermal protection	Water resistant, little to no thermal protection	Water resistant, minimal thermal protection	Water resistant, moderate thermal protection	Waterproof, greatest thermal protection
Vibration Protection	None		Moderate		Extreme

Fig. 104 Passive Protection Metric Values

Passive Protection Trade Study Results

Metric	Weight	Polycase	Pelican	Sterilite	Plano
Cost	0.1	1	1	5	5
Durability	0.2	5	5	3	4
Ease of Modification	0.3	4	2	5	3
Weight	0.1	5	3	5	4
Environmental Protection	0.2	4	5	2	2
Vibration Protection	0.1	2	5	1	1
	1.0	3.8	3.5	3.6	3.1

Fig. 105 Passive Protection Case Study

Polycase WH-22 Hinged NEMA Enclosure

- Cost - 1: The WH-22 has a base price of \$60.55 per unit for the outdoor model. This would be further increased if customizations were added.
- Durability - 5: The WH-22 is made out of polycarbonate with well-documented material properties including tensile and flexural stress and strain as well as Izod impact tests.
- Ease of Modification - 4: Polycase offers the ability to order the boxes pre-machined, cutting down on work for the user but at a higher price.

- Weight - 5: The WH-22 weighs 3.61 lbs, although this may increase if vibration protection is added.
- Environmental Protection - 4: The WH-22 is designed to NEMA 1, 2, 4, and 4X, providing protection against ingress of dust, dirt, water, and snow. However, it is not guaranteed to be waterproof.
- Vibration Protection - 2: The polycarbonate provides some amount of protection against impulse, but it is still deficient in both the impulse and cyclical loading areas.

Pelican Air Case with Pick N' Pluck Foam

- Cost - 1: The case has a cost of \$236.95.
- Durability - 5: The Pelican case is made of a proprietary polypropylene blend. Its high strength and durability have been proven through extensive load and shock testing.
- Ease of Modification - 5: This case has been engineered to be waterproof up to 20 meters, resistant to substantial loading, and is made of a material with unknown properties. Modifications to this case will greatly reduce its other protective abilities.
- Weight - 5: The case weighs 8.78 lbs.
- Environmental Protection - 5: This case is waterproof up to 20 meters underwater, has an automatic pressure equalizer and provides protection in extreme hot and cold temperatures.
- Vibration Protection - 5: This case is extremely protective against impulses and comes with foam insulation for optimal protection.

Sterilite Industrial Storage Bin

- Cost - 5: The bin has a cost of \$9.89.
- Durability - 3: No information is provided for the case's type of plastic; however, customer reviews of this product express that it has some durability under loading and in rain.
- Ease of Modification - 5: This case has few parts involved and is made from plastic. Modifications to add holes, insulation, internal padding, and added weather protection will be feasible.
- Weight - 5: The case weighs 4.83 lbs.
- Environmental Protection - 2: This case offers some protection against rain but no protection against extreme temperatures or weather conditions.
- Vibration Protection - 1: The trunk offers little to no vibration protection and would require modification.

Plano Small Sportsman's Trunk

- Cost - 5: The trunk has a cost of \$19.99.
- Durability - 4: There is no information available about the material properties of the trunk nor what type of material it is, but Plano is a leader in the industry and is well known for the quality of their product.
- Ease of Modification - 3: Due to a lack of information, this is a conservative estimate based on the reputation of Plano boxes.
- Weight: - 4: No information was available on the weight of the trunk, so a reasonable estimate was chosen.
- Environmental Protection - 2: The trunk offers little in way of environmental protection and would require extensive modification.
- Vibration Protection - 1: The trunk offers little to no vibration protection and would require modification.

Passive Protection: Design Choice

As seen in Figure 105, Polycase COTS boxes scored the highest and, thus, have been modified and used for SHADE. Although they are relatively expensive, cost is not the driving factor for this design. Instead, the low weight, high durability, and ease of modification metrics compensated for it. The ability to purchase customized boxes with cable holes already cut may be desirable if multiple units of SHADE are constructed after the end of the project. Furthermore, depending on the size of modules, smaller COTS boxes may be used, which will reduce cost further. Polycase boxes, however, are lacking in vibration protection; therefore, they will need to be modified with insulating material for modules sensitive to vibration with further design. Finally, it is worth noting that all options scored within the range of three to four, indicating that any option would be fitting for this design.

4. Active Protection

Authors: Marlin Jacobson, Elliott Tung

The active protection module will act to protect SHADE's tracking hardware from inclement weather, heat, and the environment. This system uses WRAITH's active protection "Moonroof" idea as a baseline for the design of the new system. WRAITH's active protection system worked well to protect the tracking system using an automated, sliding roof that would close if inclement environmental conditions were detected. Their system, however, is too heavy to meet SHADE's requirements; therefore, has been redesigned using a new, light-weight material for SHADE. SHADE's lightweight active protection system satisfies **FR 7** by enabling the user to carry and set up the system efficiently in under 30 minutes. **FRs 3 and 8** will be satisfied because the system will function autonomously throughout its mission and close when adverse environmental conditions are detected. The options investigated for the active protection system's new materials include 316 Stainless Steel, Magnesium Alloy (AZ31), and Polycarbonate Plastic.

Active Protection: Designs Considered

6061-T6 Aluminum

This aluminum is used in the inherited WRAITH design. Since WRAITH did not conduct a trade study on other materials, this will serve as a baseline for the alternate materials. The aluminum has a density of 2.7 g/cm^3 , a thermal conductivity of 167 W/mK , and a emissivity of 0.1. The cost for a 1/4" thick 12"x12" sheet is \$27.



Fig. 106 WRAITH Weather Protection Box with 6061-T6 Aluminum

Type 316 Stainless Steel

Although the Stainless Steel is extremely heavy, the benefits for using this material is its extreme durability and great thermal protection. It has a density of 7.99 g/cm^3 , a thermal conductivity of 14.6 W/mK , and a emissivity of 0.28. The cost for a 1/4" thick 12"x12" sheet is \$141. Although this option does not seem to be a good choice for the weather protection box, it was considered due to the fact that the box will be scaled down in size and therefore the weight and cost may be reconsidered.



Fig. 107 Type 316 Stainless Steel Sheet

Magnesium Alloy (AZ31)

The magnesium alloy was considered because it is one of lightest metal alloys found in industry. The alloy has a density of 1.77 g/cm^3 , a thermal conductivity of 96 W/mK , and a emissivity of 0.07. The cost for a 1/4" thick 12"x12" sheet is \$207 and is the most expensive option. Due to the fact that it is also easy to manufacture and still extremely light weight for a metal alloy this is a front runner among the material options.



Fig. 108 Magnesium Alloy (AZ31) Sheet

Polycarbonate Plastic

Polycarbonate is the only plastic material considered in this trade study due to its high impact strength compared to other plastics. In addition it does not degrade in sunlight which can be a factor if the SHADE system is not picked up right after its night deployment. The polycarbonate has a density of 1.15 g/cm^3 , a thermal conductivity of 0.21 W/mK , and an emissivity of 0.9. The downside of using polycarbonate is that it is translucent in nature, but this can be changed with a layer of paint. In addition polycarbonate plastic sheets come in a minimum thickness of 1/2" which might increase the weight of the system slightly. The cost for a 1/2" thick 12"x12" sheet is \$85.



Fig. 109 Polycarbonate Plastic Sheet

Figure 110 shows the Pros and Cons for each type of material for the weather protection box. These materials are also analyzed in the following section under the Materials Trade Study.

Material Option	Pros	Cons
6061-T6 Aluminum (Current)	Inexpensive Easy to Manufacture Sturdy/Durable	Heavy weight Does not offer insulation
Type 316 Stainless Steel	Easy to Manufacture Very Sturdy/Durable Well Insulated	Expensive Extremely heavy
Magnesium Alloy (AZ31)	Easy to Manufacture Sturdy/Durable Fairly light weight	Very Expensive Poor insulation
Polycarbonate Plastic	Light weight Well Insulated Can be painted to cover translucency Cheap	Not as durable as the metal alloys Harder to Manufacture Translucent

Fig. 110 Material Options Pros and Cons

Under the inherited design, WRAITH required two persons to deploy and set-up the system. SHADE has modularized components during transportation and setup in order for a one person deployment team to be feasible. Under OSHA guidelines, each individual component must not weigh over 50 lbs. Given that there are trade studies seeking to identify a more effective power system to reduce weight and passive protection

cases used for transportation, the main focus is to reduce the weight of the active protection enclosure. In addition to reducing the size of the box, SHADE has used a different material to reduce the weight. The trade study will consist of finding a lighter and more insulated material while retaining the structural rigidity that was offered previously.

Metric	Weight	Driving Requirement	Rationale
Weight	0.50	FR 7 DR 7.1	To meet OSHA safety recommendations, the weight of the weather protection box must be factored into the selection process. This weight limit is fundamental to SHADE and is prioritized appropriately.
Cost	0.10	Budget	Balancing a budget is important but material use is more so. Even though some materials are more expensive, the total cost of materials will still be relatively cheap
Thermal Conductivity	0.15	FR 3 DR 3.1 FR 8 DR 8.1	SHADE will need to be able to survive adverse weather conditions during deployment. This metric will determine the material's conductivity
Emissivity	0.05	FR 3 DR 3.1 FR 8 DR 8.1	This metric will also help determine SHADE's ability to survive in adverse weather conditions. In addition to conductivity, the material's black body radiation will also be measured using emissivity.
Reliability	0.20	FR 3 DR 3.1 FR 7 DR 7.1.1	SHADE will need to be durable enough for frequent offroad transport and will need to withstand the elements of multiple deployments. It is important to select a material to use for the weather protection box that will be able to survive and protect the sensitive systems inside over multiple deployments

Fig. 111 Material Metric Rationale and Descriptions

Materials Metric Values

Metric	1	2	3	4	5
Density (g/cm ³)	>= 3	2.4 - 2.99	1.8 - 2.39	1.2 - 1.79	< 1.2
Thermal Conductivity (W/m-K)	> 100	75 - 100	50 - 74.9	25 - 49.9	< 25
Emissivity	0.8 - 1	0.6 - 0.79	0.4 - 0.59	0.2 - 0.39	0 - 0.19
Cost 0.125”(t)/sqft (\$)	> 90	90 - 70	70 - 50	30 - 50	< 30
Reliability	Immediate likelihood of failure	High likelihood of failure	Moderate likelihood of failure	Minimal chance of failure	Failure is improbable

Fig. 112 Materials Metric Values

Materials Trade Study Results

Metric	Weight	6061-T6 Aluminum	Type 316 Stainless Steel	Magnesium Alloy (AZ31)	Polycarbonate Plastic
Density	0.4	2	1	4	5
Thermal Conductivity	0.15	1	5	2	5
Emissivity	0.05	5	4	5	1
Cost	0.1	5	1	1	4
Reliability	0.2	5	5	5	4
	1.0	2.9	2.55	3.65	4.5

Fig. 113 Materials Trade Study Results

6061-T6 Aluminum

- Density - 2: The aluminum has a density of $2.7g/cm^3$.
- Thermal Conductivity - 1: The aluminum has a thermal conductivity of $167W/mK$.
- Emissivity - 5: The aluminum has an emissivity of 0.1.
- Cost: - 5: The aluminum costs approximately \$27 per square foot for a quarter inch sheet.
- Reliability - 5: An aluminium box is easy to manufacture and will be able to survive the constant off-road transport and deployments without suffering structural damage.

Type 316 Stainless Steel

- Density - 1: The stainless steel has a density of $7.99g/cm^3$.
- Thermal Conductivity - 5: The stainless steel has a thermal conductivity of $14.6W/mK$.
- Emissivity - 4: The stainless steel has an emissivity of 0.28.
- Cost: - 1: The aluminum costs approximately \$141 per square foot for a quarter inch sheet.
- Reliability - 5: The stainless steel is extremely durable and is often used in surgical and aerospace tools.

Magnesium Alloy (AZ31)

- Density - 4: The magnesium alloy has a density of $1.77g/cm^3$.
- Thermal Conductivity - 2: The magnesium alloy has a thermal conductivity of $96W/mK$.
- Emissivity - 5: The magnesium alloy has an emissivity of 0.07.
- Cost: - 1: The aluminum costs approximately \$33 per square foot for a quarter inch sheet.
- Reliability - 5: Polycarbonate plastic is often used in outdoor settings but can be more susceptible to cracks compared to metal alloys.

Polycarbonate Plastic

- Density - 5: Polycarbonate plastic has a density of $1.15g/cm^3$.
- Thermal Conductivity - 5: Polycarbonate plastic has a thermal conductivity of $0.21W/mK$.
- Emissivity - 1: Polycarbonate plastic has an emissivity of 0.9.
- Cost: - 4: Polycarbonate plastic costs approximately dollars per square foot for a quarter inch sheet.
- Reliability - 4: The magnesium alloy is extremely durable and is resistant to corrosion.

Active Protection: Design Choice

As a result of the material trade study seen in Figure 113, the polycarbonate plastic scored the highest by a considerable margin. The density of the material, which was the highest weighted metric, is extremely lightweight, which would greatly decrease the total weight of the box as a whole. In addition, its thermal conductivity and reliability scored fairly high, which will be beneficial towards keeping a thermally insulated system as well as maintaining a structurally-sound enclosure.

5. System Verification: Open Enclosure Force and Moment Models

Author: Marlin Jacobson

In order to ensure the stability and durability of the Active Protection System enclosure during operation, two force and moment models were created. First, a hardware tipping prevention model was developed to ensure that the enclosure will not tip over while the enclosure's roof is open, which was discussed earlier in Tipping. To ensure that the enclosure's roof sliders will not break while the roof is open, a similar analysis was performed. The slider tracks together can withstand up to 600 lbf distributed across them while fully extended. This maximum value was used to determine the maximum allowable moment on the slider and, therefore, its factor of safety. Based on this model, the slider's factor of safety is 173.9, which means adding additional weight on the sliders specifically will not cause the system to break.

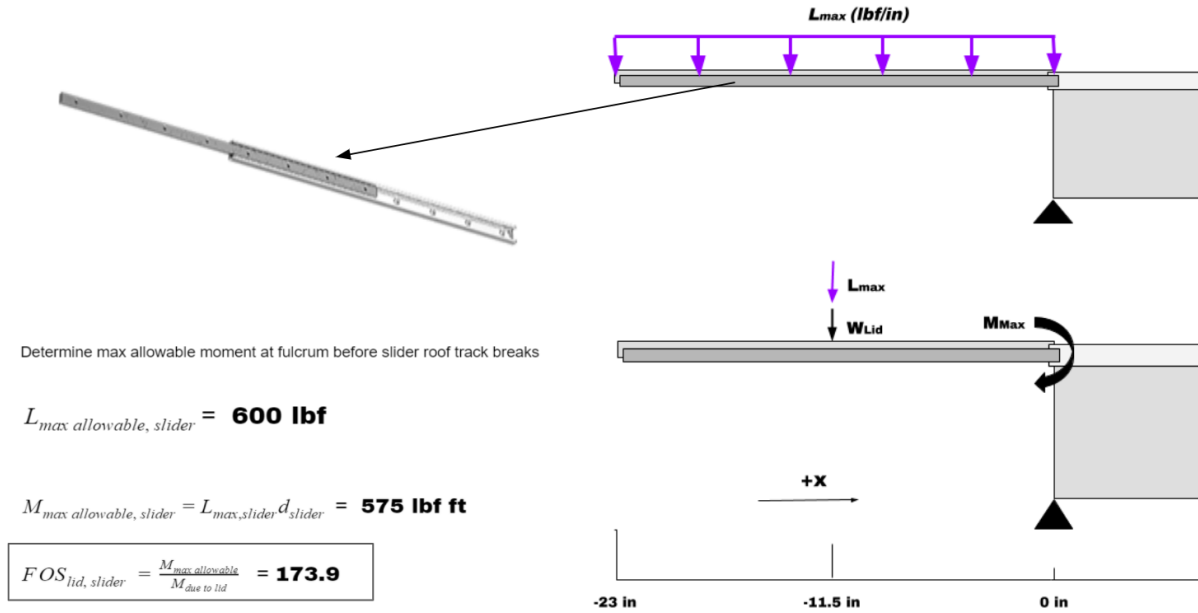


Fig. 114 Hardware Failure Prevention Model

The factors of safety of both the Tipping Prevention and Hardware Failure Prevention models were compared to one another. The models show that the open roof’s factor of safety is much smaller than that of the roof sliders; therefore, the enclosure will tip over before breaking if a load greater than 13 lbs is applied to the end of the open roof.

6. System Verification: Closed Enclosure Force and Moment Models

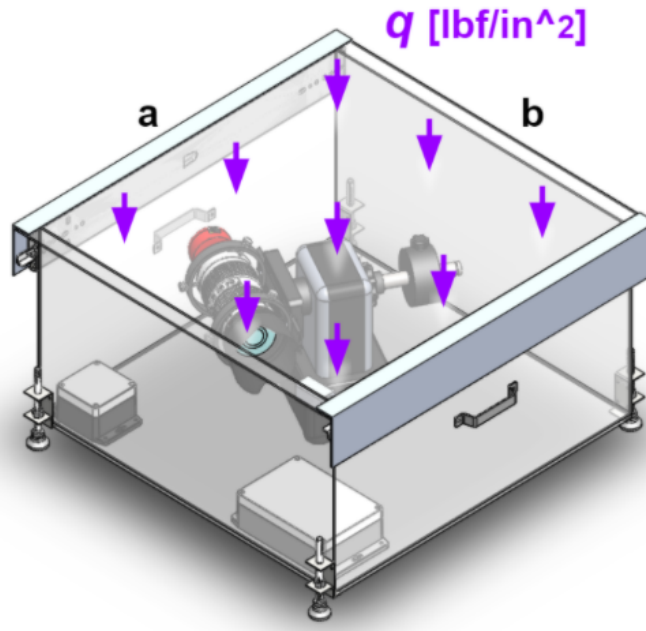
Author: Marlin Jacobson

Two additional force and moment models were created to ensure the enclosure’s ability to withstand high loads while the system’s roof is closed and the system is not in use. While polycarbonate is a durable material, it is important to verify that the roof can withstand high loads while closed due to its low thickness (0.25"). Two models were created: a maximum allowable distributed load model and a maximum center load model. Both were created to ensure the enclosure could protect the internal components against environmental conditions like hail, heavy snow, or an animal stepping on the system. These maximum loads were derived using a boundary condition of the maximum allowable deflection of the roof’s center. Moreover, if the enclosure’s roof deflects greater than two inches downward, the tracking hardware and camera may be damaged. Using a combination of a maximum allowable downward deflection of one inch and polycarbonate’s modulus of elasticity, therefore, the maximum allowable loads were computed. The maximum distributed load model is shown in Figure 115. It indicates that the enclosure can withstand a maximum of 172 lbf distributed across the roof, and this loading is driven by the maximum allowable stress of the material.

Maximum Load Distributed

Symbols used:

- q = Load per unit area (N/m², lbs/in²)
- v = Poisson's ratio (assumed to be 0.3)
- E = Young's modulus, (N/m², lbs/in²)
- t = plate thickness, (m, in)
- a = plate length, (m, in)
- b = plate width, (m, in)
- σ_{max} = maximum stress, (N/m², lbs/in²)
- y_{max} = maximum deflection, (m, in)
- R = Reaction force (N/m, lbs/in)
- β = Constant derived from table a/b
- α = Constant derived from table a/b
- γ = Constant derived from table a/b



- t = 0.25 in
- a = 25.05 in
- b = 24.5 in
- E = 260 ksi
- σ_{max} = 16 ksi
- v = 0.32
- γ = 0.42
- α = 0.0444
- β = 0.2874

y_{max} = -1 in
 This deflection value will drive the maximum load allowed on the surface.

Uniform Loading over the Entire Plate:

Stress at Center

$$\sigma_{max} = \sigma_b = \frac{\beta q b^2}{t^2} = 16 \text{ ksi}$$

Deflection at Center

$$y_{max} = \frac{-\alpha q b^4}{Et^3} = -1 \text{ in}$$

The equations were solved for q to determine maximum load per unit area.

$$q_{max_\sigma} = 0.3 \text{ lbf/in}^2$$

$$P_{max_\sigma} = 172 \text{ lbf}$$

$$q_{max_y} = 6.3 \text{ lbf/in}^2$$

$$P_{max_y} = 3627 \text{ lbf}$$

$$q_{max_\sigma} < q_{max_y}$$

Fig. 115 Maximum Distributed Load Model

Figure 116 presents the maximum center load model, which indicates that the maximum allowable load applied in a 0.5" radius on the center of the roof is 58.1 lbf. This value implies that, if a small animal steps on the closed system, the enclosure will prevent the tracking hardware from breaking.

Maximum Load At Center

Symbols used:

W = Total applied load or force (N, lbs)

ν = Poisson's ratio (assumed to be 0.3)

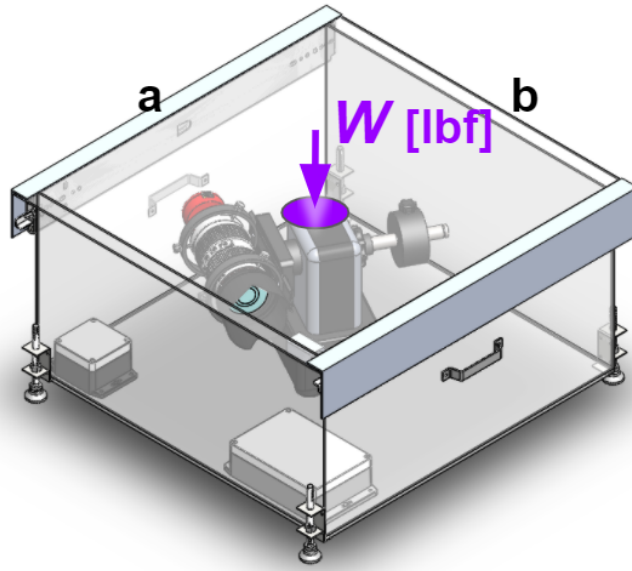
t = plate thickness, (m, in)

a = plate length, (m, in)

b = plate width, (m, in)

r_o = Radius, (m, in)

σ_{max} = maximum stress, (N/m², lbs/in²)



$t = 0.25$ in
 $a = 25.05$ in
 $b = 24.5$ in
 $E = 260$ ksi
 $\sigma_{max} = 16$ ksi
 $\nu = 0.32$
 $\gamma = 0.42$
 $\alpha = 0.1267$
 $\beta = 0.435$
 $R_o = 0.5$ in

Stress at Center

$$\sigma_{max} = \frac{3W}{2\pi t^2} \left[(1 + \nu) \ln \frac{2b}{\pi r_o} + \beta \right]$$

Deflection:

$$y_{max} = \frac{-\alpha W b^2}{E t^3}$$

The equations were solved for W to determine maximum load at center.

$y_{max} = -1$ in

This deflection value will drive the maximum load allowed on the surface.

$$W_{max_\sigma} = 387.1 \text{ lbf}$$

$$W_{max_y} = 58.1 \text{ lbf}$$

$$W_{max_\sigma} > W_{max_y}$$

Fig. 116 Maximum Load at Center Model

Overall, all force and moment models verify that the Active Protection System will protect the tracking hardware from inclement weather, environmental conditions, and animals.

7. Full Work Breakdown Structure

1. SHADE
 - 1.1. Legacy System Testing
 - 1.1.1. GHOST System
 - 1.1.1.1. Power
 - 1.1.1.1.1. Power Conditioner
 - 1.1.1.1.2. Power Distribution Board
 - 1.1.1.1.3. Power to Processor Integration
 - 1.1.1.2. Scheduler
 - 1.1.1.2.1. SGP4 Propagator
 - 1.1.1.2.2. Weighting System
 - 1.1.1.3. Imaging
 - 1.1.1.3.1. Camera & Lens
 - 1.1.1.3.2. iOptron Base
 - 1.1.1.3.3. Image Processor
 - 1.1.1.3.4. Orbit Determination
 - 1.1.1.4. Component Integration and Subsystem Tests
 - 1.1.1.4.1. Power Integration
 - 1.1.1.4.2. Scheduler Integration
 - 1.1.1.4.3. Processing Integration
 - 1.1.1.4.4. Full System Integration
 - 1.1.1.4.5. Full System Test
 - 1.1.1.4.6. Full System Validation
 - 1.1.2. WRAITH System
 - 1.1.2.1. Active Protection
 - 1.1.2.1.1. Motor Controller
 - 1.1.2.1.2. Stepper Motor
 - 1.1.2.1.3. Limit Switch
 - 1.1.2.2. Dynamic Scheduler
 - 1.1.2.2.1. Missed Observation Routine
 - 1.1.2.2.2. Dynamic Scheduler
 - 1.1.2.3. Weather Detection
 - 1.1.2.3.1. Lightning Detector
 - 1.1.2.3.2. Anemometer
 - 1.1.2.3.3. Thermometer
 - 1.1.2.3.4. Precipitation Sensor
 - 1.1.2.3.5. Resistive Heater
 - 1.1.2.4. Component Integration and Subsystem Tests
 - 1.1.2.4.1. Active Protection Integration
 - 1.1.2.4.2. Dynamic Scheduler Integration with GHOST Scheduler
 - 1.1.2.4.3. Weather Detection Integration
 - 1.1.2.4.4. Full System Integration to GHOST
 - 1.1.2.4.5. Full System Test
 - 1.1.2.4.6. Full System Validation

- 1.2. Management/Admin
 - 1.2.1. Scheduling
 - 1.2.1.1. Legacy Testing Schedule
 - 1.2.1.2. Design/Development Schedule
 - 1.2.1.3. Procurement Schedule
 - 1.2.1.4. Novel Tests Schedule
 - 1.2.2. Budgeting
 - 1.2.2.1. Financial
 - 1.2.2.2. Temporal
 - 1.2.2.2.1. Deployment & Recovery Time Budget
 - 1.2.2.2.2. Observational Time Budget
 - 1.2.2.3. Power Consumption Budget
 - 1.2.3. Requirements Analysis
 - 1.2.3.1. Legacy Requirements Modification/Allocation
 - 1.2.3.2. Novel Design Requirements
 - 1.2.3.2.1. Power System
 - 1.2.3.2.2. Protection Systems
 - 1.2.3.2.3. Deployment & Recovery
 - 1.2.3.2.4. Mission Duration
 - 1.2.3.3. Compliance Tracking
 - 1.2.4. Risk Management
 - 1.2.4.1. Planning
 - 1.2.4.2. Identification
 - 1.2.4.3. Analysis
 - 1.2.4.4. Handling
 - 1.2.4.5. Monitoring

- 1.3. Design
 - 1.3.1. Preliminary Design
 - 1.3.1.1. Requirements Allocation
 - 1.3.1.2. Trade Studies
 - 1.3.1.2.1. Modularity
 - 1.3.1.2.2. Active Protection Box Material
 - 1.3.1.2.3. Fasteners
 - 1.3.1.2.4. Passive Protection COTS Boxes
 - 1.3.1.2.5. Batteries
 - 1.3.1.2.6. Calibration Methods
 - 1.3.1.2.7. Solar Panel Technologies
 - 1.3.1.3. Evaluation
 - 1.3.1.3.1. Solar Power Generation Feasibility
 - 1.3.1.3.2. Battery Feasibility
 - 1.3.1.3.3. Solar Panel Thermal Regulation Feasibility
 - 1.3.1.3.4. Orbit Propagation Feasibility
 - 1.3.1.3.5. Active Protection Box Material Feasibility
 - 1.3.1.3.6. Active Protection Box Thermal Feasibility
 - 1.3.1.4. PDR Presentation
 - 1.3.2. Detailed Design
 - 1.3.2.1. Module & Subsystem Synthesis
 - 1.3.2.1.1. Roof Actuation - Active Protection Box Integration
 - 1.3.2.1.2. Solar Power to Power Distribution Integration
 - 1.3.2.1.3. Calibration to Scheduling Integration
 - 1.3.2.2. Prototype Modelling
 - 1.3.2.2.1. Active Protection Box
 - 1.3.2.2.2. Solar Panels
 - 1.3.2.2.3. Solar Panel Stand
 - 1.3.2.2.4. Solar Panel Cooling
 - 1.3.2.2.5. Power Module
 - 1.3.2.3. CDR Presentation

- 1.4. Manufacturing
 - 1.4.1. Active Protection
 - 1.4.1.1. Polycarbonate Machining
 - 1.4.1.2. Module Interface Machining
 - 1.4.1.3. Roof Rail Assembly
 - 1.4.1.4. Weather Proofing
 - 1.4.2. Passive Protection
 - 1.4.2.1. COTS Box Apertures
 - 1.4.2.2. Weather Proofing
 - 1.4.3. Power System
 - 1.4.3.1. Solar Panel Construction
 - 1.4.3.2. Cooling System Fixtures
 - 1.4.3.3. Panel Stand Construction
 - 1.4.4. Module Connections
 - 1.4.4.1. Weather Detection Umbilical
 - 1.4.4.2. Solar Panel Umbilical
 - 1.4.4.3. Imaging Module Connectors

- 1.5. Software Development
 - 1.5.1. Scheduler Modifications
 - 1.5.1.1. Orbit Propagation Integration
 - 1.5.1.2. Observation Weighting & Prioritisation
 - 1.5.1.3. Observation Scheduling
 - 1.5.1.4. Missed Object Handling
 - 1.5.1.5. Hardware Commanding
 - 1.5.2. Automated Setup
 - 1.5.2.1. Hardware Self-Check Routine
 - 1.5.2.2. Automated TLE Conversion
 - 1.5.2.3. Data Path Verification
 - 1.5.2.4. Power State Verification
 - 1.5.2.5. Environmental Sensor Suite Integration
 - 1.5.3. Hough Transform Image Processor
 - 1.5.3.1. Orbit Determination Integration
 - 1.5.3.2. Scheduler Integration
 - 1.5.3.3. Automatic Calibration

- 1.6. Testing (Novel Developments and Modifications)
 - 1.6.1. Hardware
 - 1.6.1.1. Power System
 - 1.6.1.1.1. Battery & Distribution
 - 1.6.1.1.1.1. Battery Duration Test
 - 1.6.1.1.1.2. Low-Power Shutdown Test
 - 1.6.1.1.1.3. Full Discharge Power System Test
 - 1.6.1.1.1.4. Power State Verification Test
 - 1.6.1.1.2. Solar Panels
 - 1.6.1.1.2.1. Solar Panel Interface Test
 - 1.6.1.1.2.2. Single Solar Panel Charging Test
 - 1.6.1.1.2.3. Full Panel Thermal Test
 - 1.6.1.2. Active Protection
 - 1.6.1.2.1. Thermal Tests
 - 1.6.1.2.2. Structural Load Tests
 - 1.6.1.2.3. Lid Actuation Test
 - 1.6.1.2.4. Weather Detection Safety Override Tests
 - 1.6.1.3. Passive Protection
 - 1.6.1.3.1. Thermal Tests
 - 1.6.1.4. Deployment & Recovery
 - 1.6.1.4.1. 30 Minute Portability Test
 - 1.6.2. Software
 - 1.6.2.1. Scheduler Modifications
 - 1.6.2.1.1. Orbit Propagation Tests
 - 1.6.2.1.2. Weighting & Prioritisation Tests
 - 1.6.2.1.3. Multi-Day Scheduling Test
 - 1.6.2.1.4. Hardware Commanding Sequence Test
 - 1.6.2.2. Automated Setup
 - 1.6.2.2.1. Hardware Fault Identification Tests
 - 1.6.2.2.2. TLE Conversion Tests
 - 1.6.2.2.3. Data Path Fault Handling
 - 1.6.2.2.4. Automated Calibration
 - 1.6.2.3. Hough Transform Image Processor
 - 1.6.2.3.1. Streak Error Handling
 - 1.6.2.3.1.1. Angular Difference
 - 1.6.2.3.1.2. Differential Brightness
 - 1.6.2.3.1.3. Extra Streaks
 - 1.6.2.3.1.4. Deformed Streaks
 - 1.6.2.3.1.5. Partial Streaks
 - 1.6.3. Full System Tests
 - 1.6.3.1. 30 Minute Deployment Test
 - 1.6.3.1.1. SHADE Operation Manual Procedure Testing
 - 1.6.3.2. One Night Deployment
 - 1.6.3.3. Multi-Night Deployment